

Deciphering the Belle II data on $B \rightarrow K\nu\bar{\nu}$ decay in the (dark) SMEFT with minimal flavour violation

Biao-Feng Hou,^a Xin-Qiang Li,^{a,b} Meng Shen,^a Ya-Dong Yang^{a,c} and Xing-Bo Yuan^a

^a*Institute of Particle Physics and Key Laboratory of Quark and Lepton Physics (MOE), Central China Normal University, Wuhan, Hubei 430079, China*

^b*Center for High Energy Physics, Peking University, Beijing 100871, China*

^c*Institute of Particle and Nuclear Physics, Henan Normal University, Xinxiang 453007, China*

E-mail: resonhou@zcknu.edu.cn, xqli@ccnu.edu.cn,
shenmeng@mails.ccnu.edu.cn, yangyd@ccnu.edu.cn, y@ccnu.edu.cn

ABSTRACT: Recently, the Belle II collaboration announced the first measurement of the branching ratio $\mathcal{B}(B^+ \rightarrow K^+\nu\bar{\nu})$, which is found to be about 2.7σ higher than the Standard Model (SM) prediction. We decipher the data with two new physics scenarios: the underlying quark-level $b \rightarrow s\nu\bar{\nu}$ transition is, besides the SM contribution, further affected by heavy new mediators that are much heavier than the electroweak scale, or amended by an additional decay channel with undetected light final states like dark matter or axion-like particles. These two scenarios can be most conveniently analyzed in the SM effective field theory (SMEFT) and the dark SMEFT (DSMEFT) framework, respectively. We consider the flavour structures of the resulting effective operators to be either generic or satisfy the minimal flavour violation (MFV) hypothesis, both for the quark and lepton sectors. In the first scenario, once the MFV assumption is made, only one SM-like low-energy effective operator induced by the SMEFT dimension-six operators can account for the Belle II excess, whose parameter space is, however, excluded by the Belle upper bound of the branching ratio $\mathcal{B}(B^0 \rightarrow K^{*0}\nu\bar{\nu})$. In the second scenario, it is found that the Belle II excess can be accommodated by 22 of the DSMEFT operators involving one or two scalar, fermionic, or vector dark matters as well as axion-like particles. These operators also receive dominant constraints from the $B^0 \rightarrow K^{*0} + \text{inv}$ and $B_s \rightarrow \text{inv}$ decays. Once the MFV hypothesis is assumed, the number of viable operators is reduced to 14, and the $B^+ \rightarrow \pi^+ + \text{inv}$ and $K^+ \rightarrow \pi^+ + \text{inv}$ decays start to put further constraints on them. Within the parameter space allowed by all the current experimental data, the q^2 distributions of the $B \rightarrow K^{(*)} + \text{inv}$ decays are then studied for each viable operator. We find that the resulting prediction of the operator $\mathcal{Q}_{q\chi} = (\bar{q}_p\gamma_\mu q_r)(\bar{\chi}\gamma^\mu\chi)$ with a fermionic dark matter mass $m_\chi \approx 700 \text{ MeV}$ can closely match the Belle II event distribution in the bins $2 \leq q^2 \leq 7 \text{ GeV}^2$. In addition, we, for the first time, calculate systematically the longitudinal polarization fraction F_L of K^* in the $B \rightarrow K^* + \text{inv}$ decays within the DLEFT. By combining the decay spectra and F_L , almost all the DSMEFT operators are found to be distinguishable from each other. Finally, the future prospects at Belle II, CEPC and FCC-ee are also discussed for some of these FCNC processes.

Contents

| | | |
|----------|--|-----------|
| 1 | Introduction | 1 |
| 2 | Minimal Flavour Violation | 4 |
| 2.1 | Quark sector | 4 |
| 2.2 | Lepton sector | 7 |
| 3 | $M_1 \rightarrow M_2 + \nu\bar{\nu}$ | 9 |
| 3.1 | SMEFT | 9 |
| 3.2 | Observables | 10 |
| 3.2.1 | $b \rightarrow s(d)\nu\bar{\nu}$ decay | 10 |
| 3.2.2 | $b \rightarrow s\ell\ell$ decay | 12 |
| 3.2.3 | $s \rightarrow d\nu\bar{\nu}$ decay | 13 |
| 4 | $M_1 \rightarrow M_2 + \text{DM}$ | 13 |
| 4.1 | DSMEFT | 13 |
| 4.2 | DLEFT | 16 |
| 4.3 | Observables | 18 |
| 5 | Numerical analysis | 19 |
| 5.1 | $M_1 \rightarrow M_2 + \nu\bar{\nu}$ | 19 |
| 5.2 | $M_1 \rightarrow M_2 + \text{DM}$ | 22 |
| 5.2.1 | General flavour structure | 24 |
| 5.2.2 | MFV | 30 |
| 6 | Conclusion | 37 |
| A | Hadronic matrix elements | 39 |
| A.1 | Decay constants | 39 |
| A.2 | Transition form factors | 40 |

1 Introduction

The flavour-changing neutral current (FCNC) processes are highly suppressed by the Glashow-Iliopoulos-Maiani (GIM) mechanism in the Standard Model (SM) [1], making them sensitive probes of new physics (NP) beyond the SM. In particular, the $B \rightarrow K^{(*)}\nu\bar{\nu}$ decays are one of the cleanest channels within the SM and most suitable for indirect NP searches [2–4] (see also refs. [5–10] for recent studies on these

as well as other related decays in the context of NP, but before the recent Belle II announcement [11]).

Recently, using the dataset with an integrated luminosity of 362 fb^{-1} , the Belle II collaboration reported the first evidence of the $B^+ \rightarrow K^+ + \nu\bar{\nu}$ decay with a branching ratio [11]

$$\mathcal{B}(B^+ \rightarrow K^+ \nu\bar{\nu})_{\text{Belle II}} = [23 \pm 5(\text{stat})_{-4}^{+5}(\text{syst})] \times 10^{-6}, \quad (1.1)$$

which is obtained by combining the inclusive and hadronic tagging results. Interestingly, this measurement shows about 2.7σ higher than the SM prediction $(4.16 \pm 0.57) \times 10^{-6}$, which is based on the calculations in refs. [2–4] but with updated input parameters. In the future, the Belle II with just 5 ab^{-1} integrated luminosity is expected to measure this decay with $20 \sim 30\%$ uncertainty relative to the SM value [12, 13], and could therefore confirm or exclude such an excess. Nevertheless, it has already motivated numerous studies of possible NP explanations [14–30].

As an interesting feature, the Belle II result, once the 2σ range in eq. (1.1) is considered, would be higher than the SM prediction by a factor of $3 \sim 8$. Such a large excess motivates us to ask the following questions: why has such a large NP effect not shown up or will it be found in other $b \rightarrow s$ processes, such as the $B \rightarrow K^* \nu\bar{\nu}$ and $B_s \rightarrow \nu\bar{\nu}$ decays [31, 32]? In this paper, we aim to answer these questions by performing a detailed model-independent analysis of possible NP effects on these and related FCNC processes in the Effective Field Theory (EFT) framework.

The $B^+ \rightarrow K^+ \nu\bar{\nu}$ excess reported by Belle II could be explained by introducing heavy NP particles that are much heavier than the electroweak scale and hence contribute to the $b \rightarrow s \nu\bar{\nu}$ transition as virtual mediators. In this case, the Standard Model Effective Field Theory (SMEFT) provides a well-suited model-independent framework to study such kinds of NP effects [33, 34]. Here, all the NP effects are encoded in the Wilson coefficients of the higher-dimensional operators that are invariant under the SM gauge group. Below the electroweak scale, the heavy SM particles like the massive bosons and the top quark also decouple, and the dynamics is then described by the Low-energy Effective Field Theory (LEFT) [35, 36], which consists of, besides the QCD and QED Lagrangians for light SM fermions, a set of higher-dimensional operators compatible with the QCD and QED gauge symmetries. The Wilson coefficients of these higher-dimensional operators encode all the physics related to the heavy SM and NP degrees of freedom. Starting with the SMEFT, one can also fix these low-energy Wilson coefficients by perform a matching between these two EFTs at the electroweak scale [36–38]. Such a procedure has been extensively applied to various B -meson and kaon decays [35, 36]. In this paper, we will interpret the Belle II excess in terms of the SMEFT operators and consider the LEFT as the low-energy limit of SMEFT to calculate the relevant B -meson and kaon decays.

The Belle II excess could also be accommodated by amending the $B^+ \rightarrow K^+ \nu\bar{\nu}$ decay by an additional decay channel with undetected light final states like dark

matter (DM) or axion-like particles (ALP). To mimic the signal, these new light states must couple to the SM quark sector and be sufficiently long-lived to escape the detector. The potential candidates are new light particles that are singlet under the SM gauge group. In order to study the interactions of such new states with the SM quark sector model-independently, it is also convenient to work in an EFT framework, such as the DM EFT [39, 40] without any stabilizing symmetry on the DM fields.¹ In this respect, the SMEFT can be extended by including the scalar, fermionic or vector DM fields, resulting in the so-called Dark SMEFT (DSMEFT) [41–46]. In the DSMEFT, the new operators involving the DM fields are invariant under the SM $SU(3)_C \otimes SU(2)_L \otimes U(1)_Y$ gauge group and the electroweak symmetry is broken by the usual Higgs mechanism. The general non-redundant operator basis can be found in ref. [45] up to dim=6, and in ref. [46] up to dim=8. In order to describe the low-energy processes below the electroweak scale, such as $d_i \rightarrow d_j + \text{DM}$ decays, a general framework is the generalization of the LEFT to include the scalar, fermionic and vector DM fields, referred to as the Dark LEFT (DLEFT) [45]. In the DLEFT, the DM particles should be lighter than the electroweak scale and the effective operators are invariant under the $SU(3)_C \otimes U(1)_{\text{em}}$ gauge group. A complete basis of the DLEFT operators can be found in refs. [45, 47] for $\text{dim} \leq 6$, and in ref. [48] for $\text{dim} \leq 7$. In this work, starting from the DSMEFT and considering the DLEFT as the low-energy limit of DSMEFT, we investigate the parameter space of each DSMEFT operator required to explain the Belle II excess, together under the constraints from the other $b \rightarrow s + \text{inv}$ decays. The future prospects at Belle II, CEPC and FCC-ee will also be discussed for some of these FCNC processes. In addition, for completeness, our analyses also include the ALP case [49–52] in the EFT framework [53–58].

The above two NP scenarios proposed to account for the Belle II excess could also affect the quark-level $b \rightarrow d$ and $s \rightarrow d$ processes. In order to correlate the $b \rightarrow s$ to the $b \rightarrow d$ and $s \rightarrow d$ transitions, we have to specify the underlying flavour structures of the EFT considered [59, 60]. To this end, we assume the minimal flavour violation (MFV) hypothesis [61–63] and implement it into the SMEFT and DSMEFT frameworks. According to the hypothesis, all the flavour violating currents are controlled by the SM Yukawa couplings, so that all the FCNC interactions in the quark sector are naturally suppressed by the CKM factors. Therefore, any potential large FCNCs in the SMEFT and DSMEFT can be avoided. Considering the current experimental data on the $b \rightarrow s + \text{inv}$, $b \rightarrow d + \text{inv}$ and $s \rightarrow d + \text{inv}$ processes, such as the $B \rightarrow \pi + \text{inv}$ and $K \rightarrow \pi + \text{inv}$ decays, we derive the constraints on each operator in the SMEFT and DSMEFT with the MFV hypothesis. Implications of the resulting parameter space of each viable operator for the differential distributions of these decays are also investigated in detail, which can be tested at the Belle II with

¹In this work, we do not impose any symmetry to stabilize the DM fields in the EFT framework. Thus, the DM fields we are considering are actually just new singlets under the SM gauge group.

more statistics. In addition, in order to distinguish the various DSMEFT operators, we, for the first time, calculate systematically the polarization fraction F_L of K^* in the $B \rightarrow K^* + \text{inv}$ decays within the DELFT.

The remainder of this paper is organized as follows. In section 2, we introduce the MFV hypothesis. In sections 3 and 4, we investigate the various $d_i \rightarrow d_j \nu \bar{\nu}$ and $d_i \rightarrow d_j + \text{DM}$ decays in the SMEFT and DSMEFT, respectively. In these EFT frameworks, the flavour structures of the effective operators are taken to be either of the most general form or satisfy the MFV hypothesis. We present our detailed numerical analyses and discussions in section 5. Our conclusion is finally made in section 6. The hadronic matrix elements involved throughout this work, such as the transition form factors and decay constants, are summarized in appendix A.

2 Minimal Flavour Violation

In this section, we discuss the idea of MFV hypothesis and its application in the SMEFT and DSMEFT.

2.1 Quark sector

In the interaction eigenbasis, the SM Yukawa interactions in the quark sector are described by the Lagrangian

$$-\mathcal{L}_Y = \bar{q} Y_d H d + \bar{q} Y_u \tilde{H} u + \text{h.c.}, \quad (2.1)$$

where $\tilde{H} \equiv i\sigma_2 H^*$ with H being the SM Higgs doublet. The fields q and u, d denote the left-handed quark doublet and the right-handed quark singlets in the SM, respectively. The Yukawa coupling matrices $Y_{u,d}$ are 3×3 complex matrices in flavour space. In the SM, these Yukawa interactions violate the global flavour symmetry [61, 64]

$$G_{\text{QF}} = SU(3)_q \otimes SU(3)_u \otimes SU(3)_d. \quad (2.2)$$

We can formally recover this flavour symmetry by promoting the Yukawa matrices $Y_{u,d}$ to spurion fields [63]. The Yukawa spurions should transform under G_{QF} as

$$Y_u \sim (\mathbf{3}, \bar{\mathbf{3}}, \mathbf{1}), \quad Y_d \sim (\mathbf{3}, \mathbf{1}, \bar{\mathbf{3}}). \quad (2.3)$$

Then, we can construct two useful basic building blocks $\mathbf{A} \equiv Y_u Y_u^\dagger$ and $\mathbf{B} \equiv Y_d Y_d^\dagger$, which transform as $(\mathbf{1} \oplus \mathbf{8}, \mathbf{1}, \mathbf{1})$ under the flavour group G_{QF} . As will be seen later, these building blocks are useful to parameterize the quark flavour transitions in effective theories.

In the SMEFT and DSMEFT, there are four types of quark currents relevant for the down-type FCNC transitions, which read

$$\bar{q} \gamma^\mu C q, \quad \bar{d} \gamma^\mu C d, \quad \bar{q} C d, \quad \bar{q} \sigma^{\mu\nu} C d, \quad (2.4)$$

where \mathcal{C} denotes the Wilson coefficient of the operator \mathcal{Q} and is a 3×3 matrix in quark flavour space. Here and in the following, we suppress the operator index i , i.e., \mathcal{C} denoting \mathcal{C}_i . In the MFV hypothesis, it is assumed that at low energy the Yukawa couplings are the only source of flavour violation in the SM and beyond [63]. Technically, this hypothesis implies that the quark currents in eq. (2.4) should be invariant under the flavour group G_{QF} . Therefore, the Wilson coefficient \mathcal{C} can be written in the following form:

$$\mathcal{C}^{\text{MFV}} = \begin{cases} f(\mathbf{A}, \mathbf{B}) & \text{for } \bar{q}\gamma^\mu \mathcal{C}q, \\ f(\mathbf{A}, \mathbf{B})Y_d & \text{for } \bar{q}\mathcal{C}d, \bar{q}\sigma^{\mu\nu}\mathcal{C}d, \\ \epsilon_0\mathbb{1} + Y_d^\dagger g(\mathbf{A}, \mathbf{B})Y_d & \text{for } \bar{d}\gamma^\mu \mathcal{C}d, \end{cases} \quad (2.5)$$

where ϵ_0 is a real constant. The functions $f(\mathbf{A}, \mathbf{B})$ and $g(\mathbf{A}, \mathbf{B})$ are infinite series of the building blocks \mathbf{A} and \mathbf{B} , e.g., explicitly $f(\mathbf{A}, \mathbf{B}) \equiv \xi_{ijk\dots} \mathbf{A}^i \mathbf{B}^j \mathbf{A}^k \dots$ with real coefficients $\xi_{ijk\dots}$ to ensure no new sources of CP violation beyond the Yukawa couplings. By application of the Cayley-Hamilton identity, the infinite series in $f(\mathbf{A}, \mathbf{B})$ and $g(\mathbf{A}, \mathbf{B})$ can be resummed into a finite number of terms. Taking $f(\mathbf{A}, \mathbf{B})$ as an example, its explicit summed expression can be written as [65–67]

$$f(\mathbf{A}, \mathbf{B}) = \epsilon_0\mathbb{1} + \epsilon_1\mathbf{A} + \epsilon_3\mathbf{A}^2 + \epsilon_5\mathbf{A}\mathbf{B} + \epsilon_7\mathbf{A}\mathbf{B}\mathbf{A} + \epsilon_{10}\mathbf{A}\mathbf{B}^2 + \epsilon_{12}\mathbf{A}^2\mathbf{B}^2 + \epsilon_{14}\mathbf{B}^2\mathbf{A}\mathbf{B} + \epsilon_{15}\mathbf{A}\mathbf{B}^2\mathbf{A}^2 \\ + \epsilon_2\mathbf{B} + \epsilon_4\mathbf{B}^2 + \epsilon_6\mathbf{B}\mathbf{A} + \epsilon_9\mathbf{B}\mathbf{A}\mathbf{B} + \epsilon_8\mathbf{B}\mathbf{A}^2 + \epsilon_{13}\mathbf{B}^2\mathbf{A}^2 + \epsilon_{11}\mathbf{A}\mathbf{B}\mathbf{A}^2 + \epsilon_{16}\mathbf{B}^2\mathbf{A}^2\mathbf{B}.$$

During the resummation, higher-order polynomials of \mathbf{A} and \mathbf{B} contribute to the coefficients ϵ_i , and make them complex generally. However, it is found that the imaginary parts of the coefficients are tiny (e.g., $\text{Im}\epsilon_i \propto |\text{Tr}(\mathbf{A}^2\mathbf{B}\mathbf{A}\mathbf{B}^2)| \ll 1$) and can be therefore neglected in the numerical analysis [65, 66, 68–70]. In the following, we assume the coefficients ϵ_i are of the same orders of magnitude. Therefore, only the terms built by \mathbf{A} are kept, while all the terms involving \mathbf{B} are neglected, as the spurion \mathbf{B} is suppressed by $\mathcal{O}(\hat{\lambda}_d^2)$, where $\hat{\lambda}_d$ denotes the diagonal Yukawa coupling matrix for down-type quarks defined by eq. (2.8). Finally, we obtain the approximation [71]

$$f(\mathbf{A}, \mathbf{B}) \approx \epsilon_0\mathbb{1} + \epsilon_1\mathbf{A} + \epsilon_2\mathbf{A}^2, \quad (2.6)$$

where the coefficients $\epsilon_{0,1,2}$ are free real parameters. Similarly, being suppressed by $\mathcal{O}(\hat{\lambda}_d^2)$, the approximation $Y_d^\dagger g(\mathbf{A}, \mathbf{B})Y_d \approx 0$ can be taken.

In the MFV framework discussed above, the quark currents are all given in the interaction eigenbasis. In order to rotate to the fermion mass eigenbasis, the following transforms should be performed:

$$u_L \rightarrow U_u u_L, \quad u_R \rightarrow W_u u_R, \quad d_L \rightarrow U_d d_L, \quad d_R \rightarrow W_d d_R, \quad (2.7)$$

where $U_{u,d}$ and $W_{u,d}$ are 3×3 unitary matrices introduced to diagonalize the Yukawa matrices

$$U_d^\dagger Y_d W_d = \hat{\lambda}_d, \quad U_u^\dagger Y_u W_u = \hat{\lambda}_u. \quad (2.8)$$

Therefore, the CKM matrix is given by $V = U_u^\dagger U_d$. In the following, we turn to the fermion mass eigenbasis and derive explicit expressions of the MFV couplings.

The current $\bar{q}\gamma^\mu \mathcal{C}q$ involves the following down-type quark interactions in the mass eigenbasis:

$$\bar{d}_L U_d^\dagger \gamma_\mu \mathcal{C}^{\text{MFV}} U_d d_L \approx \bar{d}_L \gamma^\mu V^\dagger (\epsilon_0 + \epsilon_1 \hat{\lambda}_u^2 + \epsilon_2 \hat{\lambda}_u^4) V d_L, \quad (2.9)$$

where d_L denotes now the left-handed down-type quark in the mass eigenbasis, and $\hat{\lambda}_u$ denotes the diagonal Yukawa coupling matrix for up-type quarks, whose diagonal elements are given by $\lambda_{u_i} = \sqrt{2}m_{u_i}/v$ with the vacuum expectation value $v = 246$ GeV. It is noted that, due to the large hierarchy among the diagonal elements λ_{u_i} , the matrices $\epsilon_1 \hat{\lambda}_u^2$ and $\epsilon_2 \hat{\lambda}_u^4$ have almost the same structures. Therefore, one can obtain the following approximation [72]:

$$V^\dagger (\epsilon_1 \hat{\lambda}_u^2 + \epsilon_2 \hat{\lambda}_u^4) V \approx V^\dagger (\epsilon_1 \hat{\lambda}_u^2) V \equiv \epsilon_1 \Delta_q, \quad (2.10)$$

which is equivalent to taking the approximation $\lambda_t^4 - \lambda_{u,c}^4 \approx \lambda_t^2 (\lambda_t^2 - \lambda_{u,c}^2)$ and redefining $\epsilon_1 + \epsilon_2 \lambda_t^2 \rightarrow \epsilon_1$.² For the observables investigated in this paper, we have verified that the numerical differences caused by this approximation are negligible. Finally, by defining the basic FCNC couplings

$$\Delta_q = V^\dagger \hat{\lambda}_u^2 V, \quad (2.11)$$

we arrive at

$$\bar{d}_L U_d^\dagger \gamma_\mu \mathcal{C}^{\text{MFV}} U_d d_L \approx \bar{d}_L \gamma^\mu (\epsilon_0 \mathbb{1} + \epsilon_1 \Delta_q) d_L. \quad (2.12)$$

Similarly, from the current $\bar{q}\mathcal{C}d$, the following scalar interactions among the down-type quarks are obtained in the mass eigenbasis:

$$\bar{d}_L U_d^\dagger \mathcal{C}^{\text{MFV}} W_d d_R \approx \bar{d}_L V^\dagger (\epsilon_0 \mathbb{1} + \epsilon_1 \hat{\lambda}_u^2 + \epsilon_2 \hat{\lambda}_u^4) V \hat{\lambda}_d d_R \approx \bar{d}_L (\epsilon_0 \hat{\lambda}_d + \epsilon_1 \Delta_q \hat{\lambda}_d) d_R, \quad (2.13)$$

where d_R is the right-handed down-type quark in the mass eigenbasis, and the diagonal elements of the diagonal Yukawa coupling matrix for down-type quarks are given by $\lambda_d^i = \sqrt{2}m_{d_i}/v$. Here the approximation in eq. (2.10) has been used. In addition, due to the same flavour structure as of the scalar interactions, the tensor interactions $\bar{d}_L U_d^\dagger \sigma^{\mu\nu} \mathcal{C}^{\text{MFV}} W_d d_R$ resulting from the current $\bar{q}\sigma^{\mu\nu} \mathcal{C}^{\text{MFV}} d$ have the same MFV coupling as in eq. (2.13).

For the vector interactions originating from the current $\bar{d}\gamma^\mu \mathcal{C}d$, the MFV coupling in the mass eigenbasis is given by

$$\bar{d}_R W_d^\dagger \gamma^\mu \mathcal{C}^{\text{MFV}} W_d d_R \approx \bar{d}_R \gamma^\mu (\epsilon_0 \mathbb{1}) d_R. \quad (2.14)$$

²Using the unitarity of the CKM matrix, one can obtain $[V^\dagger (\epsilon_1 \hat{\lambda}_u^2 + \epsilon_2 \hat{\lambda}_u^4) V]_{ij} = \lambda_t^2 (\epsilon_1 + \epsilon_2 \lambda_t^2) \delta_{ij} - (\lambda_t^2 - \lambda_u^2) [\epsilon_1 + \epsilon_2 (\lambda_t^2 + \lambda_u^2)] V_{ui}^* V_{uj} - (\lambda_t^2 - \lambda_c^2) [\epsilon_1 + \epsilon_2 (\lambda_t^2 + \lambda_c^2)] V_{ci}^* V_{cj} \approx \lambda_t^2 (\epsilon_1 + \epsilon_2 \lambda_t^2) \delta_{ij} - (\lambda_t^2 - \lambda_u^2) [\epsilon_1 + \epsilon_2 \lambda_t^2] V_{ui}^* V_{uj} - (\lambda_t^2 - \lambda_c^2) [\epsilon_1 + \epsilon_2 \lambda_t^2] V_{ci}^* V_{cj} = (\epsilon_1 + \epsilon_2 \lambda_t^2) [V^\dagger \hat{\lambda}_u^2 V]_{ij}$, where the approximation $\lambda_t^2 + \lambda_{u,c}^2 \approx \lambda_t^2$ have been used.

This implies that the vector interactions among the right-handed down-type quarks are approximately flavour diagonal and universal. Thus, the FCNC vector interactions among the right-handed down-type quarks are forbidden in the MFV scenario.

As a summary, the MFV couplings for various down-type quark currents are given in the mass eigenbasis by

$$\mathcal{C}_i^{\text{MFV}} = \begin{cases} \epsilon_0^i \mathbf{1} + \epsilon_1^i \Delta_q & \text{for } \bar{d}_L \gamma^\mu \mathcal{C}_i d_L, \\ \epsilon_0^i \hat{\lambda}_d + \epsilon_1^i \Delta_q \hat{\lambda}_d & \text{for } \bar{d}_L \mathcal{C}_i d_R, \bar{d}_L \sigma^{\mu\nu} \mathcal{C}_i d_R, \\ \epsilon_0^i \mathbf{1} & \text{for } \bar{d}_R \gamma^\mu \mathcal{C}_i d_R. \end{cases} \quad (2.15)$$

It is then clear that only two types of MFV couplings, Δ_q and $\Delta_q \hat{\lambda}_d$, can generate FCNC interactions among the down-type quarks and their numerical values are given, respectively, by

$$\Delta_q = \begin{pmatrix} 0.8 & -3.3 - 1.5i & 79.3 + 35.4i \\ -3.3 + 1.5i & 16.6 & -397.5 + 8.1i \\ 79.3 - 35.4i & -397.5 - 8.1i & 9839.0 \end{pmatrix} \times 10^{-4}, \quad (2.16)$$

and

$$\Delta_q \hat{\lambda}_d = \begin{pmatrix} 0.0021 & -0.18 - 0.08i & 191.3 + 85.4i \\ -0.009 + 0.004i & 0.88 & -958.7 + 19.6i \\ 0.21 - 0.10i & -21.1 - 0.4i & 23728.1 \end{pmatrix} \times 10^{-6}. \quad (2.17)$$

One can see that a large hierarchy exists among the down-type FCNC interactions, i.e., $\mathcal{C}_{bs}^{\text{MFV}} \gg \mathcal{C}_{bd}^{\text{MFV}} \gg \mathcal{C}_{sd}^{\text{MFV}}$. It is also seen that the flavour-conserving couplings $\mathcal{C}_{bb}^{\text{MFV}}$ is more than one order of magnitude larger than all the other couplings.

2.2 Lepton sector

One can also apply the MFV hypothesis to the lepton sector. However, since the mechanism of neutrino mass generation is still unknown, there are different approaches to formulate the leptonic MFV [73–79]. Here, we consider the realization of leptonic MFV within the so-called minimal field content [73, 74], in which the neutrino masses are generated by the Weinberg operator. In this case, the Yukawa interactions in the lepton sector can be written as

$$-\Delta\mathcal{L} = \bar{e} Y_e H^\dagger l + \frac{1}{2\Lambda_{\text{LN}}} (\bar{l}^c \tau_2 H) Y_\nu (H^T \tau_2 l) + \text{h.c.}, \quad (2.18)$$

where l denotes the left-handed lepton doublet with the charge conjugated field given by $l^c = -i\gamma_2 l^*$, and e is the right-handed charged lepton singlet. Λ_{LN} denotes the breaking scale of the lepton number symmetry $U(1)_{\text{LN}}$. Y_e and Y_ν stand for the 3×3 Yukawa coupling matrices in flavour space. In the absence of these Yukawa couplings, the lepton sector respects the flavour symmetry

$$G_{\text{LF}} = SU(3)_l \otimes SU(3)_e. \quad (2.19)$$

Analogous to the quark sector, this flavour symmetry can be restored by promoting the Yukawa couplings $Y_{e,\nu}$ to spurion fields. Then, the relevant building blocks are $\mathbf{A}_\ell = Y_\nu^\dagger Y_\nu$ and $\mathbf{B}_\ell = Y_e^\dagger Y_e$, which transform as $(\mathbf{1} \oplus \mathbf{8}, \mathbf{1})$ under the lepton flavour group G_{LF} .

For the three SMEFT operators, $\mathcal{Q}_{lq}^{(1,3)}$ and \mathcal{Q}_{ld} , relevant to the $B^+ \rightarrow K^+ \nu \bar{\nu}$ decay, they contain the lepton current

$$\bar{l} \gamma^\mu \mathcal{C} l, \quad (2.20)$$

where \mathcal{C} denotes the Wilson coefficient of the operator \mathcal{Q} and is a 3×3 matrix in lepton flavour space. In the MFV hypothesis, analogous to the quark current, the Wilson coefficient \mathcal{C} should take the form $\mathcal{C}_{\text{MFV}} = h(\mathbf{A}_\ell, \mathbf{B}_\ell)$, where $h(\mathbf{A}_\ell, \mathbf{B}_\ell)$ is a finite polynomial of \mathbf{A}_ℓ and \mathbf{B}_ℓ . After neglecting all the terms involving \mathbf{B}_ℓ , which are suppressed by the small lepton Yukawa couplings Y_e , we obtain

$$\mathcal{C}_{\text{MFV}} \approx \kappa_0 + \kappa_1 \mathbf{A}_\ell + \kappa_2 \mathbf{A}_\ell^2, \quad (2.21)$$

where the coefficients $\kappa_{0,1,2}$ are free real parameters. In the numerical analysis, we keep only the leading lepton flavour violation term \mathbf{A}_ℓ for simplicity, i.e., $\kappa_2 = 0$. Turning to the lepton mass eigenbasis, the current $\bar{l} \gamma^\mu \mathcal{C} l$ gives in the MFV hypothesis the following interactions:

$$\bar{e}_L \gamma^\mu (\kappa_0 \mathbf{1} + \kappa_0 \Delta_\ell) e_L + \bar{\nu}_L \gamma^\mu (\kappa_0 \mathbf{1} + \kappa_0 \hat{\lambda}_\nu^2) \nu_L, \quad (2.22)$$

where the basic LFV coupling Δ_ℓ can be obtained from \mathbf{A}_ℓ and takes the form

$$\Delta_\ell = U \hat{\lambda}_\nu^2 U^\dagger, \quad (2.23)$$

where U is the PMNS matrix. Here e_L and ν_L denote the left-handed charged lepton and neutrino in the mass eigenbasis, respectively. $\hat{\lambda}_\nu \equiv 2m_\nu \Lambda_{\text{LN}}/v^2$ stands for the diagonal effective neutrino Yukawa coupling and m_ν the diagonal neutrino mass matrix. As can be seen from eq. (2.22), the lepton vector current does not induce neutral LFV in the leptonic MFV with minimal field content.³

As discussed above, the charged LFV interactions are governed by the MFV coupling Δ_ℓ . Numerically, we obtain

$$\Delta_\ell^{\text{NO}} = \begin{pmatrix} -0.19 - 0.01i & -0.25 - 0.02i & 0.31 - 0.04i \\ 0.12 + 0.01i & 0.28 - 0.00i & 0.29 + 0.04i \\ -0.37 - 0.01i & 0.21 - 0.05i & -0.03 + 0.01i \end{pmatrix}, \quad (2.24)$$

³This is, however, not true for the most generic leptonic MFV. For example, in the leptonic MFV with type-I seesaw mechanism, the basic LFV coupling $\Delta_\ell = U \hat{\lambda}_\nu U^\dagger$ should be replaced by $U \hat{\lambda}_\nu^{1/2} O O^\dagger \hat{\lambda}_\nu^{1/2} U^\dagger$, where O is a general complex orthogonal matrix satisfying $O O^T = \mathbf{1}$ [71]. Therefore, any non-diagonal matrix $O O^\dagger$ can induce neutral LFV.

for normal ordering (NO), and

$$\Delta_\ell^{\text{IO}} = \begin{pmatrix} 0.21 + 0.09i & -0.34 + 0.05i & 0.03 + 0.11i \\ 0.31 + 0.12i & 0.19 + 0.00i & -0.15 - 0.14i \\ 0.12 - 0.02i & 0.04 - 0.19i & 0.34 - 0.10i \end{pmatrix}, \quad (2.25)$$

for inverted ordering (IO) of neutrino masses. Here $\Lambda_{\text{LN}} = 10^{14}$ GeV and the lightest neutrino mass $m_{\nu_1} = 0.2$ eV have been taken. One can see that the magnitudes of all the matrix elements of Δ_ℓ are of similar size except for $(\Delta_\ell^{\text{NO}})_{33}$, which has much smaller magnitude than the other couplings.

Let us finally make a comment on the DSMEFT with MFV. In general, similar to the SM fermions, the DM particles can also appear in a form of multiple generations. In this case, the SM flavour symmetry could be extended to include the global symmetry associated with the DM multiplet and the MFV hypothesis can be generalized to the DM sector [80–84]. In this paper, we focus on a minimal DM sector, which contains only one or two DM generations, and leave a detailed study of the DM with MFV for future work.

3 $M_1 \rightarrow M_2 + \nu\bar{\nu}$

In this section, we first summarize the SMEFT framework with the most general flavour structure as well as in the MFV hypothesis. Then, the NP effects on various rare FCNC decays are discussed.

3.1 SMEFT

If new particles are much heavier than the electroweak scale and the electroweak symmetry breaking is realized linearly, their effects can be parameterized by a series of higher dimensional gauge-invariant operators in the SMEFT (see refs. [33, 34] for recent reviews). The SMEFT Lagrangian at dim-6 takes the form [85, 86]

$$\mathcal{L}_{\text{SMEFT}} = \sum_i \frac{\mathcal{C}_i}{\Lambda^2} \mathcal{Q}_i, \quad (3.1)$$

where Λ denotes the NP scale. The dim-6 effective operators \mathcal{Q}_i are built out of the SM fields and respect the SM gauge symmetry $SU(3)_C \otimes SU(2)_L \otimes U(1)_Y$, with \mathcal{C}_i the corresponding dimensionless Wilson coefficients.

For the $b \rightarrow s\nu\bar{\nu}$ transition, the relevant operators are given by

$$\begin{aligned} \mathcal{Q}_{lq}^{(1)} &= (\bar{l}_p \gamma^\mu l_r) (\bar{q}_s \gamma_\mu q_t), & \mathcal{Q}_{Hq}^{(1)} &= (H^\dagger i \overleftrightarrow{D}_\mu H) (\bar{q}_p \gamma^\mu q_r), \\ \mathcal{Q}_{lq}^{(3)} &= (\bar{l}_p \gamma^\mu \tau^I l_r) (\bar{q}_s \tau^I \gamma_\mu q_t), & \mathcal{Q}_{Hq}^{(3)} &= (H^\dagger i \overleftrightarrow{D}_\mu^I H) (\bar{q}_p \tau^I \gamma^\mu q_r), \\ \mathcal{Q}_{ld} &= (\bar{l}_p \gamma^\mu l_r) (\bar{d}_s \gamma_\mu d_t), & \mathcal{Q}_{Hd} &= (H^\dagger i \overleftrightarrow{D}_\mu H) (\bar{d}_p \gamma^\mu d_r), \end{aligned} \quad (3.2)$$

where $D_\mu = \partial_\mu + ig_s T^a G_\mu^a + ig_2 t^I W_\mu^I + ig_1 Y B_\mu$ denotes the covariant derivative under the SM gauge symmetry. Here $T^a = \lambda^a/2$ and $t^I = \tau^I/2$ are the $SU(3)$ and $SU(2)$ generators, where λ^a and τ^I stand for the Gell-Mann and Pauli matrices, respectively. l and q denote the left-handed lepton and quark doublets respectively, while d is the right-handed down-type quark singlet, all being given in the mass eigenbasis. The generation indices of the SM fields are characterized by p, r, s, t .

The operators $\mathcal{Q}_{Hq}^{(1)}$, $\mathcal{Q}_{Hq}^{(3)}$ and \mathcal{Q}_{Hd} can induce a tree-level $\bar{s}\gamma^\mu b Z_\mu$ coupling, and thus contribute to the $b \rightarrow s\nu\bar{\nu}$ transition. However, the same $\bar{s}\gamma^\mu b Z_\mu$ interaction also affects the $b \rightarrow s\ell^+\ell^-$ processes [2, 3]. Due to the $SU(2)_L$ gauge invariance, its contributions to these two processes are of equal magnitudes and lepton flavour universal. Thus, it is impossible to explain the Belle II data on the branching ratio $\mathcal{B}(B^+ \rightarrow K^+\nu\bar{\nu})$ while satisfying the stringent constraints from the precisely measured $b \rightarrow s\ell^+\ell^-$ observables, e.g., the branching ratio $\mathcal{B}(B_s \rightarrow \mu^+\mu^-)$. Explicitly, it is found that $\mathcal{B}(B^+ \rightarrow K^+\nu\bar{\nu})$ can only be enhanced by about 20% after considering other relevant experimental constraints [16]. Therefore, we will not consider these operators and focus on the remaining three four-fermion operators in the following.

In the MFV hypothesis, by using eqs. (2.12), (2.14) and (2.22), the relevant four-fermion operators take the following forms:

$$\begin{aligned} \mathcal{C}_{ld}\mathcal{Q}_{ld} &= \left[\bar{e}_L \gamma_\mu (\kappa_0 \mathbf{1} + \kappa_1 \Delta_\ell) e_L + \bar{\nu}_L \gamma_\mu (\kappa_0 \mathbf{1} + \kappa_1 \hat{\lambda}_\nu^2) \nu_L \right] \left[\bar{d}_R \gamma^\mu (\epsilon_0 \mathbf{1}) d_R \right], \quad (3.3) \\ \mathcal{C}_{lq}^{(1,3)} \mathcal{Q}_{lq}^{(1,3)} &\supset \left[\bar{e}_L \gamma_\mu (\kappa_0 \mathbf{1} + \kappa_1 \Delta_\ell) e_L \pm \bar{\nu}_L \gamma_\mu (\kappa_0 \mathbf{1} + \kappa_1 \hat{\lambda}_\nu^2) \nu_L \right] \left[\bar{d}_L \gamma^\mu (\epsilon_0 \mathbf{1} + \epsilon_1 \Delta_q) d_L \right], \end{aligned}$$

in the mass eigenbasis. Here we have suppressed the operator indices for the MFV parameters $\epsilon_{0,1}$ and $\kappa_{0,1}$ are suppressed. It is noted that \mathcal{Q}_{ld} does not involve any quark FCNC interactions, and thus has no contribution to the $b \rightarrow s\nu\bar{\nu}$ transition.

3.2 Observables

3.2.1 $b \rightarrow s(d)\nu\bar{\nu}$ decay

The $B \rightarrow K^{(*)}\nu\bar{\nu}$ decays are induced by the $b \rightarrow s\nu_i\bar{\nu}_j$ transitions. In the most general case, the effective weak Hamiltonian contains only two operators and can be written as [2, 3]

$$\mathcal{H}_{\text{eff}}^{b \rightarrow s\nu\nu} = -\frac{4G_F}{\sqrt{2}} \frac{\alpha_e}{4\pi} V_{tb} V_{ts}^* \sum_{i,j=e,\mu,\tau} (C_L^{\nu_i\nu_j} \mathcal{O}_L^{\nu_i\nu_j} + C_R^{\nu_i\nu_j} \mathcal{O}_R^{\nu_i\nu_j}) + \text{h.c.}, \quad (3.4)$$

with the effective operators defined by

$$\mathcal{O}_L^{\nu_i\nu_j} = (\bar{s}\gamma_\mu P_L b) (\bar{\nu}_i \gamma^\mu P_L \nu_j), \quad \mathcal{O}_R^{\nu_i\nu_j} = (\bar{s}\gamma_\mu P_R b) (\bar{\nu}_i \gamma^\mu P_L \nu_j). \quad (3.5)$$

In the SM, $C_R^{\nu_i\nu_j}$ is negligible and $C_L^{\nu_i\nu_j} = C_L^{\text{SM}} \delta_{ij}$ with $C_L^{\text{SM}} = -12.64 \pm 0.14$ [3] after including the NLO QCD corrections [87–89] and the two-loop electroweak contributions [90]. In the SMEFT, by comparing eqs. (3.1) and (3.4), one can derive that

the NP contributions to these two operators are given, respectively, by

$$C_{L,\text{NP}}^{\nu_i\nu_j} = c_\nu([\mathcal{C}_{lq}^{(1)}]_{ij23} - [\mathcal{C}_{lq}^{(3)}]_{ij23}), \quad C_{R,\text{NP}}^{\nu_i\nu_j} = c_\nu[\mathcal{C}_{ld}]_{ij23}, \quad (3.6)$$

with the normalization factor $c_\nu \equiv (2\pi/(\alpha_e V_{tb}V_{ts}^*)) \cdot (v^2/\Lambda^2)$. In the MFV framework, by using eq. (3.3), we find that

$$\begin{aligned} C_{L,\text{MFV}}^{\nu_i\nu_j} &= c_\nu \Delta_q^{23} [\epsilon_1^{(1)} (\kappa_0^{(1)} + \kappa_1^{(1)} \lambda_{\nu_i}^2) - ((1) \rightarrow (3))] \delta_{ij}, \\ C_{R,\text{MFV}}^{\nu_i\nu_j} &= 0, \end{aligned} \quad (3.7)$$

where $\epsilon_1^{(n)}$ and $\kappa_{0,1}^{(n)}$ denote the MFV parameters associated with the operator $\mathcal{Q}_{lq}^{(n)}$, with $n = 1, 3$. Thus, one can see that the transition $b \rightarrow s\nu\bar{\nu}$ in the MFV hypothesis is only induced by the effective operator $\mathcal{O}_L^{\nu_i\nu_j}$, which also conserves the lepton flavour. In addition, it is straightforward to obtain the operators and Wilson coefficients for the $b \rightarrow d\nu_i\bar{\nu}_j$ transitions by changing the corresponding flavour indices.

Starting with the effective weak Hamiltonian in eq. (3.4), we can write the dineutrino invariant mass spectrum of the $B \rightarrow K^*\nu\bar{\nu}$ decay as [2, 3]

$$\frac{d\Gamma(B \rightarrow K^*\nu\bar{\nu})}{ds_B} = m_B^2 \sum_{i,j=e,\mu,\tau} \left(|A_{\perp}^{ij}(s_B)|^2 + |A_{\parallel}^{ij}(s_B)|^2 + |A_0^{ij}(s_B)|^2 \right), \quad (3.8)$$

where $s_B = q^2/m_B^2$, and q^2 denotes the dineutrino invariant mass squared in the B -meson rest frame. The three polarization amplitudes $A_{\perp,\parallel,0}^{ij}$ are functions of the $B \rightarrow K^*$ transition form factors and the Wilson coefficients, and take the form

$$\begin{aligned} A_{\perp}^{ij}(s_B) &= 2\sqrt{2}N \lambda^{1/2}(1, \tilde{m}_{K^*}^2, s_B) (C_L^{\nu_i\nu_j} + C_R^{\nu_i\nu_j}) \frac{V(s_B)}{1 + \tilde{m}_{K^*}}, \\ A_{\parallel}^{ij}(s_B) &= -2\sqrt{2}N (1 + \tilde{m}_{K^*}) (C_L^{\nu_i\nu_j} - C_R^{\nu_i\nu_j}) A_1(s_B), \\ A_0^{ij}(s_B) &= -\frac{N(C_L^{\nu_i\nu_j} - C_R^{\nu_i\nu_j})}{\tilde{m}_{K^*}\sqrt{s_B}} \left[(1 - \tilde{m}_{K^*}^2 - s_B)(1 + \tilde{m}_{K^*})A_1(s_B) \right. \\ &\quad \left. - \lambda(1, \tilde{m}_{K^*}^2, s_B) \frac{A_2(s_B)}{1 + \tilde{m}_{K^*}} \right], \end{aligned} \quad (3.9)$$

with $\tilde{m}_{K^*} = m_{K^*}/m_B$ and $N = 1/2 V_{tb}V_{ts}^* [G_F^2 \alpha_e^2 m_B^3 s_B \lambda^{1/2}(1, \tilde{m}_{K^*}^2, s_B)/(3 \cdot 2^{10} \pi^5)]^{1/2}$. Similarly, the dineutrino invariant mass distribution of the $B \rightarrow K\nu\bar{\nu}$ decay can be written as [2, 3, 91]

$$\begin{aligned} \frac{d\Gamma(B \rightarrow K\nu\bar{\nu})}{ds_B} &= \frac{G_F^2 \alpha_e^2}{3 \cdot 2^{10} \pi^5} |V_{tb}V_{ts}^*|^2 m_B^5 \lambda^{3/2}(1, \tilde{m}_K^2, s_B) [f_+^{B \rightarrow K}(s_B)]^2 \\ &\quad \times \sum_{i,j=e,\mu,\tau} |C_L^{\nu_i\nu_j} + C_R^{\nu_i\nu_j}|^2. \end{aligned} \quad (3.10)$$

For convenience, all the relevant form factors present in the above expressions are given in appendix A.2. In addition, it is straightforward to obtain the distributions

of other $b \rightarrow s(d)\nu\bar{\nu}$ decays, such as $B \rightarrow \pi\nu\bar{\nu}$ and $B_s \rightarrow \phi\nu\bar{\nu}$, from the above expressions with some replacements. Finally, one should notice that for charged B -meson decays, there is a long-distance contribution arising from the tree-level weak annihilation mediated by the on-shell τ lepton [92]. For example, the $B^+ \rightarrow \tau^+(\rightarrow K^+\bar{\nu})\nu$ process provides an additional $\mathcal{O}(10\%)$ contribution to the $B^+ \rightarrow K^+\nu\bar{\nu}$ decay, and constitutes a background in the experimental extraction of the branching ratio [11]. Here we do not include the tree-level contribution, which has already been subtracted away during the experimental data analysis [11].

3.2.2 $b \rightarrow s\ell\ell$ decay

The quark-level $b \rightarrow s\ell^+\ell^-$ transitions, such as the rare $B_s \rightarrow \ell^+\ell^-$, $B \rightarrow K^{(*)}\ell^+\ell^-$ and $B_s \rightarrow \phi\ell^+\ell^-$ decays, can provide promising probes of various NP effects (see refs. [93, 94] for a recent review). For a general $b \rightarrow s\ell_i^-\ell_j^+$ transition, the effective weak Hamiltonian can be written as [35]

$$\mathcal{H}_{\text{eff}}^{b \rightarrow s\ell\ell} = -\frac{4G_F}{\sqrt{2}} \frac{e^2}{16\pi^2} V_{tb}V_{ts}^* \sum_k C_k \mathcal{O}_k + \text{h.c.}, \quad (3.11)$$

where the most relevant operators are $\mathcal{O}_9^{(\prime)}$ and $\mathcal{O}_{10}^{(\prime)}$. They are defined, respectively, by

$$\begin{aligned} \mathcal{O}_9^{ij} &= (\bar{s}\gamma_\mu P_L b) (\bar{\ell}_i \gamma^\mu \ell_j), & \mathcal{O}_{10}^{ij} &= (\bar{s}\gamma_\mu P_L b) (\bar{\ell}_i \gamma^\mu \gamma_5 \ell_j), \\ \mathcal{O}'_9^{ij} &= (\bar{s}\gamma_\mu P_R b) (\bar{\ell}_i \gamma^\mu \ell_j), & \mathcal{O}'_{10}^{ij} &= (\bar{s}\gamma_\mu P_R b) (\bar{\ell}_i \gamma^\mu \gamma_5 \ell_j). \end{aligned} \quad (3.12)$$

In the SMEFT, the NP contributions to their Wilson coefficients are given by

$$\begin{aligned} C_{9,\text{NP}}^{ij} &= +c_\ell ([\mathcal{C}_{lq}^{(1)}]_{ij23} + [\mathcal{C}_{lq}^{(3)}]_{ij23}), & C'_{9,\text{NP}}{}^{ij} &= +c_\ell [\mathcal{C}_{ld}]_{ij23}, \\ C_{10,\text{NP}}^{ij} &= -c_\ell ([\mathcal{C}_{lq}^{(1)}]_{ij23} + [\mathcal{C}_{lq}^{(3)}]_{ij23}), & C'_{10,\text{NP}}{}^{ij} &= -c_\ell [\mathcal{C}_{ld}]_{ij23}, \end{aligned} \quad (3.13)$$

with the normalization constant $c_\ell \equiv (\pi/(\alpha_e V_{tb}V_{ts}^*)) \cdot (v^2/\Lambda^2)$. In the MFV framework, from eq. (3.3), we can further obtain

$$\begin{aligned} C_{9,\text{MFV}}^{ij} &= -C_{10,\text{MFV}}^{ij} = c_\ell \Delta_q^{23} [\epsilon_1^{(1)} (\kappa_0^{(1)} \delta^{ij} + \kappa_1^{(1)} \Delta_\ell^{ij}) + ((1) \rightarrow (3))], \\ C'_{9,\text{MFV}}{}^{ij} &= C'_{10,\text{MFV}}{}^{ij} = 0, \end{aligned} \quad (3.14)$$

where $\epsilon_1^{(n)}$ and $\kappa_{0,1}^{(n)}$ denote the MFV parameters for the operator $\mathcal{Q}_{lq}^{(n)}$ ($n = 1, 3$). For the $B \rightarrow \pi\ell_i\ell_j$, $B \rightarrow K^{(*)}\ell_i\ell_j$ and $B_s \rightarrow \ell_i\ell_j$ decays, which are all induced by the quark-level $b \rightarrow s(d)\ell_i\ell_j$ transitions and will be included in our numerical analysis. These decays have been studied in refs. [72, 95–98] and the explicit expressions of their branching ratios can be found in, e.g., refs. [72, 97, 98].

3.2.3 $s \rightarrow d\nu\bar{\nu}$ decay

Both the $K^+ \rightarrow \pi^+\nu\bar{\nu}$ and $K_L \rightarrow \pi^0\nu\bar{\nu}$ decays are induced by the $s \rightarrow d\nu_i\bar{\nu}_j$ transition. The corresponding effective weak Hamiltonian, including the effective operators and their Wilson coefficients, can be obtained from the ones of the $b \rightarrow s\nu\bar{\nu}$ transition in section 3.2.1 by replacing the related flavour indices. In addition, for the $K^+ \rightarrow \pi^+\nu\bar{\nu}$ decay, a non-negligible charm contribution must be taken into account [88, 89].

In absence of the operator $O_R^{\nu_i\nu_j}$, the branching ratio of the $K^+ \rightarrow \pi^+\nu\bar{\nu}$ decay is given by [99–101]

$$\mathcal{B}(K^+ \rightarrow \pi^+\nu\bar{\nu}) = \kappa_+(1 + \Delta_{\text{EM}}) \sum_{i,j=e,\mu,\tau} \frac{1}{3} \left[\left(\sin^2 \theta_W \frac{\text{Im}[\lambda_t C_L^{\nu_i\nu_j}]}{2\lambda^5} \right)^2 + \left(\frac{\text{Re}\lambda_c}{\lambda} P_c(X) \delta^{ij} - \sin^2 \theta_W \frac{\text{Re}[\lambda_t C_L^{\nu_i\nu_j}]}{2\lambda^5} \right)^2 \right], \quad (3.15)$$

where $\lambda_i = V_{is}^* V_{id}$, $\lambda = |V_{us}|$, and $\sin^2 \theta_W = 0.23116$ is the weak mixing angle. The parameter $\kappa_+ = (5.173 \pm 0.025) \times 10^{-11} (\lambda/0.225)^8$ contains, besides some other factors, the hadronic matrix element of the weak current $\bar{s}\gamma_\mu P_L d$ that can be extracted from the $K_{\ell 3}$ data with the help of isospin symmetry [102]. $\Delta_{\text{EM}} = -0.003$ accounts for the isospin-breaking electromagnetic corrections [100, 101]. $P_c(X) = 0.404 \pm 0.024$ comprises the short- and long-distance charm contributions [102–105].

The rare decay $K_L \rightarrow \pi^0\nu\bar{\nu}$ proceeds almost entirely through direct CP violation in the SM [106, 107], and the charm contribution can be fully neglected [99]. The branching ratio of this decay can be written as [99, 108]

$$\mathcal{B}(K_L \rightarrow \pi^0\nu\bar{\nu}) = \kappa_L(1 - \delta_\epsilon) \sum_{i,j=e,\mu,\tau} \frac{1}{3} \left(\frac{\sin^2 \theta_W}{2\lambda^5} \text{Im}[\lambda_t C_L^{\nu_i\nu_j}] \right)^2, \quad (3.16)$$

where $\kappa_L = (2.231 \pm 0.013) \times 10^{-10} (\lambda/0.225)^8$ encodes, besides some other factors, the hadronic matrix element that can be again extracted from the $K_{\ell 3}$ decay with the help of isospin symmetry [100, 109]. The parameter δ_ϵ encodes, on the other hand, the highly suppressed indirect CP-violating contribution [107].

4 $M_1 \rightarrow M_2 + \text{DM}$

In this section, we first recapitulate the theoretical framework of the DSMEFT and DLEFT, and then detail the calculation of $M_1 \rightarrow M_2 + \text{DM}$ decays.

4.1 DSMEFT

It is known that EFT can provide a systematic framework for parameterizing various effects induced by the DM particles. The DSMEFT is a generalization of

the SMEFT [85, 86] to include the DM particles, which can be either lighter or heavier than the electroweak scale and are gauge singlets under the SM gauge group [45, 46, 48]. It is also assumed that electroweak symmetry breaking must be implemented via the usual Higgs mechanism. Following the convention of ref. [45], the DSMEFT Lagrangian takes the form

$$\mathcal{L}_{\text{DSMEFT}} \supset \frac{1}{\Lambda} \sum_i \mathcal{C}_i \mathcal{Q}_i^{(5)} + \frac{1}{\Lambda^2} \sum_j \mathcal{C}_j \mathcal{Q}_j^{(6)}, \quad (4.1)$$

where Λ is the NP scale above which new degrees of freedom appear and interact with the SM and DM particles. The dim- d effective operators $\mathcal{Q}_i^{(d)}$ involve at least one DM field and respect the SM $SU(3)_C \otimes SU(2)_L \otimes U(1)_Y$ gauge symmetry. \mathcal{C}_i denote the corresponding dimensionless Wilson coefficients. We will define the DSMEFT at the electroweak scale μ_{EW} .

In the DSMEFT framework, three types of DM particles can be added: spin-0 scalar ϕ , spin-1/2 fermion χ and spin-1 vector X . Generally, each type of the DM particles can have multiple generations. For simplicity, the case of one generation DM will be assumed in this paper. For the operators vanishing in the case of one generation, however, two generations of DM particles will be considered. Furthermore, in order to affect the rare B -meson and kaon FCNC decays, only the operators that can induce tree-level FCNC interactions among the down-type quarks are included in our analysis. Finally, motivated by the large excess of $\mathcal{B}(B^+ \rightarrow K^+ + \nu\bar{\nu})$ reported by Belle II [11], we will focus on the dim-5 and dim-6 operators, which are less suppressed than the ones with $\text{dim} \geq 7$. Consequently, the DSMEFT operators we are considering must involve two down-type quarks and at least one DM field. Furthermore, in order to mimic the rare B -meson and kaon FCNC decays involving a dineutrino final state, the DM particles must be light enough to be produced in these decays. For each type of the DM particles, the relevant effective operators are given in the following.

For the scalar DM particles, there are four operators,

$$\begin{aligned} \mathcal{Q}_{d\phi} &= (\bar{q}_p d_r H) \phi + \text{h.c.}, & \mathcal{Q}_{d\phi^2} &= (\bar{q}_p d_r H) \phi^2 + \text{h.c.}, \\ \mathcal{Q}_{\phi q} &= (\bar{q}_p \gamma_\mu q_r) (i\phi_1 \overleftrightarrow{\partial}^\mu \phi_2), & \mathcal{Q}_{\phi d} &= (\bar{d}_p \gamma_\mu d_r) (i\phi_1 \overleftrightarrow{\partial}^\mu \phi_2), \end{aligned} \quad (4.2)$$

where $\phi_1 \overleftrightarrow{\partial}^\mu \phi_2 = \phi_1 (\partial^\mu \phi_2) - (\partial^\mu \phi_1) \phi_2$, and $\phi_{(i)}$ is the real scalar DM field with the generation index characterized by i . For the operators which are not hermitian, “+h.c.” should be added to them to indicate that the hermitian conjugated operators should be included in the DSMEFT Lagrangian eq. (4.1). In addition, constructions of the operators $\mathcal{Q}_{\phi q}$ and $\mathcal{Q}_{\phi d}$ requires at least two generations of scalar DM fields.

For the fermionic DM particles, there are only two operators,

$$\mathcal{Q}_{q\chi} = (\bar{q}_p \gamma_\mu q_r) (\bar{\chi} \gamma^\mu \chi), \quad \mathcal{Q}_{d\chi} = (\bar{d}_p \gamma_\mu d_r) (\bar{\chi} \gamma^\mu \chi), \quad (4.3)$$

where χ denotes the fermionic DM field. In this paper, all the observables considered are insensitive to the chirality of the fermionic DM. Without loss of generality, χ will be therefore chosen as the right-handed Dirac field.

For the vector DM particles, by using the field strength tensor as the building block, there is only one operator,

$$\mathcal{Q}_{dHX} = (\bar{q}_p \sigma_{\mu\nu} d_r) H X^{\mu\nu} + \text{h.c.}, \quad (4.4)$$

where $X_{\mu\nu} = \partial_\mu X_\nu - \partial_\nu X_\mu$, and X_μ denotes the real vector DM field. Taking X_μ an additional building block, the following operators also appear [46]:

$$\begin{aligned} \mathcal{Q}_{dX} &= (\bar{d}_p \gamma_\mu d_r) X^\mu, & \mathcal{Q}_{HdX} &= (H^\dagger H) (\bar{d}_p \gamma^\mu d_r) X_\mu, \\ \mathcal{Q}_{qX} &= (\bar{q}_p \gamma_\mu q_r) X^\mu, & \mathcal{Q}_{HqX}^{(1)} &= (H^\dagger H) (\bar{q}_p \gamma^\mu q_r) X_\mu, \\ \mathcal{Q}_{dX^2} &= (\bar{q}_p d_r H) X_\mu X^\mu + \text{h.c.}, & \mathcal{Q}_{HqX}^{(3)} &= (H^\dagger \tau^I H) (\bar{q}_p \tau^I \gamma^\mu q_r) X_\mu, \\ \mathcal{Q}_{qXX} &= (\bar{q}_p \gamma_\mu q_r) X^{\mu\nu} X_\nu, & \mathcal{Q}_{dXX} &= (\bar{d}_p \gamma_\mu d_r) X^{\mu\nu} X_\nu, \\ \mathcal{Q}_{q\tilde{X}X} &= (\bar{q}_p \gamma_\mu q_r) \tilde{X}^{\mu\nu} X_\nu, & \mathcal{Q}_{d\tilde{X}X} &= (\bar{d}_p \gamma_\mu d_r) \tilde{X}^{\mu\nu} X_\nu, \\ \mathcal{Q}_{DqX^2} &= i(\bar{q}_p \gamma^\mu D^\nu q_r) X_\mu X_\nu + \text{h.c.}, & \mathcal{Q}_{DdX^2} &= i(\bar{d}_p \gamma^\mu D^\nu d_r) X_\mu X_\nu + \text{h.c.}, \\ \mathcal{Q}_{dHX^2} &= (\bar{q}_p \sigma_{\mu\nu} d_r H) X_1^\mu X_2^\nu + \text{h.c.}, & & \end{aligned} \quad (4.5)$$

where $\tilde{X}^{\mu\nu} = \epsilon^{\mu\nu\rho\sigma} X_{\rho\sigma}/2$. It is noted that the rare B -meson and kaon decay rates induced by the operators involving the vector DM field X_μ are divergent in the $m_X \rightarrow 0$ limit. Such a divergence is caused by the longitudinal polarization of the vector field and related to the phenomenon that it is impossible to consistently define a massless limit for a vector field without an active gauge symmetry [42]. As in refs. [42, 47, 110], this singularity is treated by assuming some kind of Higgs mechanism in the dark sector. As a result, the Wilson coefficients of the operators in eq. (4.5) should be proportional to some powers of (m_X/Λ) and can be redefined as

$$\mathcal{C}_i = \tilde{\mathcal{C}}_i \cdot \begin{cases} (m_X/\Lambda)^2 & \text{for } \mathcal{Q}_i = \mathcal{Q}_{dX^2}, \mathcal{Q}_{DdX^2}, \mathcal{Q}_{DqX^2}, \mathcal{Q}_{dHX^2}, \\ (m_X/\Lambda) & \text{for } \mathcal{Q}_i = \text{others.} \end{cases} \quad (4.6)$$

These redefined Wilson coefficients $\tilde{\mathcal{C}}_i$ will be used in the following analysis.

We can also include the axion or axion-like particles (ALPs) [49–52] in the EFT approach [53–58]. They are pseudo Nambu-Goldstone bosons with non-trivial properties, and can emerge from spontaneous breaking of some global symmetries. Up to dim-5, there are only two operators,

$$\mathcal{Q}_{qa} = (\bar{q}_p \gamma_\mu q_r) \partial^\mu a, \quad \mathcal{Q}_{da} = (\bar{d}_p \gamma_\mu d_r) \partial^\mu a, \quad (4.7)$$

where a denotes the ALP field.

In the MFV hypothesis discussed in section 2, the Wilson coefficients of the DSMEFT operators should take special flavour structures. Explicitly, by using the quark currents in eqs. (2.12)-(2.14), we obtain

$$\mathcal{C}_i^{\text{MFV}} = \begin{cases} \epsilon_0^i \hat{\lambda}_d + \epsilon_1^i \Delta_q \hat{\lambda}_d & \text{for } \mathcal{Q}_i = \mathcal{Q}_{d\phi}, \mathcal{Q}_{d\phi^2}, \mathcal{Q}_{dHX}, \mathcal{Q}_{dHX^2}, \mathcal{Q}_{dX^2}, \\ \epsilon_0^i \mathbb{1} + \epsilon_1^i \Delta_q & \text{for } \mathcal{Q}_i = \mathcal{Q}_{\phi q}, \mathcal{Q}_{q\chi}, \mathcal{Q}_{qXX}, \mathcal{Q}_{q\bar{X}X}, \mathcal{Q}_{DqX^2}, \mathcal{Q}_{qX}, \mathcal{Q}_{HqX}^{(1,3)}, \mathcal{Q}_{qa}, \\ \epsilon_0^i \mathbb{1} & \text{for } \mathcal{Q}_i = \mathcal{Q}_{\phi d}, \mathcal{Q}_{d\chi}, \mathcal{Q}_{dXX}, \mathcal{Q}_{d\bar{X}X}, \mathcal{Q}_{DdX^2}, \mathcal{Q}_{dX}, \mathcal{Q}_{HdX}, \mathcal{Q}_{da}, \end{cases} \quad (4.8)$$

for the DSMEFT operators discussed above. Here the Wilson coefficient $\mathcal{C}_i^{\text{MFV}}$ are given for the down-type quark currents expressed in the mass eigenbasis, and they are 3×3 matrices in flavour space. Generally, the real parameters $\epsilon_{0,1}^i$ are different from each other for different operators \mathcal{Q}_i . We can see that the operators listed in the last line of the above equation do not generate tree-level FCNC interactions among the down-type quarks.

4.2 DLEFT

Below the electroweak scale, the NP effects induced by the DM particles can be described by the DLEFT [45]. This EFT is obtained by integrating out all the heavy particles with masses at or above the electroweak scale and can be considered as an extension of the LEFT [35, 36] by including besides the light SM fields also the light DM particles. The DLEFT respects the SM $SU(3)_C \otimes U(1)_{\text{em}}$ gauge symmetry, and does not contain the Higgs boson. Thus, it can be considered without reference to the DSMEFT for the light DM and light SM particles interacting at energies below the electroweak scale. Following the same convention as in ref. [45], we can write the DLEFT Lagrangian as

$$\mathcal{L}_{\text{DLEFT}} \supset \frac{1}{\Lambda} \sum_i L_i \mathcal{O}_i^{(5)} + \frac{1}{\Lambda^2} \sum_j L_j \mathcal{O}_j^{(6)}, \quad (4.9)$$

up to dim-6, where $\mathcal{O}_i^{(d)}$ denote the dim- d effective operators and L_i the corresponding Wilson coefficients.

Analogous to the DSMEFT case, we can write down all the relevant DLEFT operators involving the scalar, fermionic and vector DM fields. For the scalar DM, we have

$$\begin{aligned} \mathcal{O}_{d\phi} &= (\bar{d}_{Lp} d_{Rr}) \phi + \text{h.c.}, & \mathcal{O}_{\phi d}^L &= (\bar{d}_{Lp} \gamma_\mu d_{Lr}) (i\phi_1 \overleftrightarrow{\partial}^\mu \phi_2), \\ \mathcal{O}_{d\phi^2} &= (\bar{d}_{Lp} d_{Rr}) \phi^2 + \text{h.c.}, & \mathcal{O}_{\phi d}^R &= (\bar{d}_{Rp} \gamma_\mu d_{Rr}) (i\phi_1 \overleftrightarrow{\partial}^\mu \phi_2), \end{aligned} \quad (4.10)$$

where d_L and d_R denote the left-handed and right-handed down-type quarks, respectively. For the fermionic DM, the relevant operators are given by

$$\mathcal{O}_{d\chi}^{V,LR} = (\bar{d}_{Lp} \gamma_\mu d_{Lr}) (\bar{\chi}_a \gamma^\mu \chi_b), \quad \mathcal{O}_{d\chi}^{V,RR} = (\bar{d}_{Rp} \gamma_\mu d_{Rr}) (\bar{\chi}_a \gamma^\mu \chi_b),$$

$$\begin{aligned}
\mathcal{O}_{dX}^{S,LR} &= (\bar{d}_{Rp}d_{Lr})(\chi_a^T C \chi_b) + \text{h.c.}, & \mathcal{O}_{dX}^{S,RR} &= (\bar{d}_{Lp}d_{Rr})(\chi_a^T C \chi_b) + \text{h.c.}, \\
\mathcal{O}_{dX}^{T,RR} &= (\bar{d}_{Lp}\sigma^{\mu\nu}d_{Rr})(\chi_a^T C \sigma_{\mu\nu}\chi_b) + \text{h.c.}, & &
\end{aligned} \tag{4.11}$$

with the charge conjugate operator defined by $C = i\gamma^2\gamma^0$. For the vector DM, there is only one operator,

$$\mathcal{O}_{dX}^T = (\bar{d}_{Lp}\sigma_{\mu\nu}d_{Rr})X_a^{\mu\nu} + \text{h.c.}, \tag{4.12}$$

by using the field strength $X_{\mu\nu}$ as the building block. However, including X_μ as additional building block, the following operators are obtained:

$$\begin{aligned}
\mathcal{O}_{dX}^L &= (\bar{d}_{Lp}\gamma_\mu d_{Lr})X^\mu, & \mathcal{O}_{dX}^R &= (\bar{d}_{Rp}\gamma_\mu d_{Rr})X^\mu, \\
\mathcal{O}_{dXX}^L &= (\bar{d}_{Lp}\gamma_\mu d_{Lr})X^{\mu\nu}X_\nu, & \mathcal{O}_{dXX}^R &= (\bar{d}_{Rp}\gamma_\mu d_{Rr})X^{\mu\nu}X_\nu, \\
\mathcal{O}_{d\tilde{X}X}^L &= (\bar{d}_{Lp}\gamma_\mu d_{Lr})\tilde{X}^{\mu\nu}X_\nu, & \mathcal{O}_{d\tilde{X}X}^R &= (\bar{d}_{Rp}\gamma_\mu d_{Rr})\tilde{X}^{\mu\nu}X_\nu, \\
\mathcal{O}_{DdX^2}^L &= i(\bar{d}_{Lp}\gamma^\nu D^\mu d_{Lr})X_\mu X_\nu + \text{h.c.}, & \mathcal{O}_{DdX^2}^R &= i(\bar{d}_{Rp}\gamma^\nu D^\mu d_{Rr})X_\mu X_\nu + \text{h.c.}, \\
\mathcal{O}_{dX^2}^L &= (\bar{d}_{Lp}d_{Rr})X_\mu X^\mu + \text{h.c.}, & \mathcal{O}_{dX^2}^T &= (\bar{d}_{Lp}\sigma_{\mu\nu}d_{Rr})X_1^\mu X_2^\nu + \text{h.c.},
\end{aligned} \tag{4.13}$$

where $D_\mu = \partial_\mu + ig_s T^a G_\mu^a + ieQA_\mu$ denotes the covariant derivative of the $SU(3)_C \otimes U(1)_{\text{em}}$ gauge symmetry. Here we have chosen the basis where the combinations of $X_{\mu\nu}$ and X_μ are similar as in the DSMEFT operators of eq. (4.5). One can prove that this basis is equivalent to the one adopted in ref. [47]. In addition, there are two operators involving the ALP field, which take the form

$$\mathcal{O}_{da}^L = (\bar{d}_{Lp}\gamma_\mu d_{Lr})\partial^\mu a, \quad \mathcal{O}_{da}^R = (\bar{d}_{Rp}\gamma_\mu d_{Rr})\partial^\mu a. \tag{4.14}$$

Although the DLEFT can be considered without reference to the DSMEFT, the former should arise as the low-energy limit of the latter, if we start from the DSMEFT. At the electroweak scale μ_{EW} , the tree-level matching conditions between these two EFTs are summarized below:

- Scalar DM:

$$L_{\phi d}^L = \mathcal{C}_{\phi q}, \quad L_{\phi d}^R = \mathcal{C}_{\phi d}, \quad L_{d\phi^2} = \frac{v}{\sqrt{2}\Lambda}\mathcal{C}_{d\phi^2}, \quad L_{d\phi} = \frac{v}{\sqrt{2}\Lambda}\mathcal{C}_{d\phi}. \tag{4.15}$$

- Fermionic DM:

$$L_{dX}^{V,LR} = \mathcal{C}_{qX}, \quad L_{dX}^{V,RR} = \mathcal{C}_{dX}, \quad L_{dX}^{S,LR} = 0, \quad L_{dX}^{S,RR} = 0, \quad L_{dX}^{T,RR} = 0. \tag{4.16}$$

- Vector DM:

$$\begin{aligned}
L_{dX}^T &= \frac{v}{\sqrt{2}\Lambda}\mathcal{C}_{dHX}, \quad L_{dX}^L = \mathcal{C}_{qX} + \frac{v^2}{2\Lambda^2}(\mathcal{C}_{HqX}^{(1)} + \mathcal{C}_{HqX}^{(3)}), \quad L_{dX}^R = \mathcal{C}_{dX} + \frac{v^2}{2\Lambda^2}\mathcal{C}_{HdX}, \\
L_{dXX}^L &= \mathcal{C}_{qXX}, \quad L_{d\tilde{X}X}^L = \mathcal{C}_{q\tilde{X}X}, \quad L_{DdX^2}^L = \mathcal{C}_{DqX^2}, \quad L_{dX^2} = \frac{v}{\sqrt{2}\Lambda}\mathcal{C}_{dX^2}, \\
L_{dXX}^R &= \mathcal{C}_{dXX}, \quad L_{d\tilde{X}X}^R = \mathcal{C}_{d\tilde{X}X}, \quad L_{DdX^2}^R = \mathcal{C}_{DdX^2}, \quad L_{dX^2}^T = \frac{v}{\sqrt{2}\Lambda}\mathcal{C}_{dHX^2}.
\end{aligned} \tag{4.17}$$

- ALP:

$$L_{da}^L = \mathcal{C}_{qa}, \quad L_{da}^R = \mathcal{C}_{da}. \quad (4.18)$$

Here all the Wilson coefficients are given in the mass eigenbasis. In the MFV hypothesis, the Wilson coefficients in DSMEFT take the form of eq. (4.8).

Since the above matching conditions are given at the electroweak scale, i.e., $L_i \equiv L_i(\mu_{\text{EW}})$ and $\mathcal{C}_i \equiv \mathcal{C}_i(\mu_{\text{EW}})$, the renormalization group (RG) evolution should be performed in the DLEFT to obtain the corresponding Wilson coefficients at the typical scales of B -meson and kaon decays. In the DLEFT, as the DM particles are color singlet, we need only consider the QCD RG evolution of the quark current in each DLEFT operator. Furthermore, the different DLEFT operators do not mix under the QCD RG running. Accordingly, the RG equations take the form

$$\frac{dL_i(\mu)}{d \ln \mu} = \frac{\alpha_s}{4\pi} \gamma_i L_i(\mu), \quad (4.19)$$

where $L_i(\mu)$ denote the Wilson coefficients of the operators \mathcal{O}_i at the scale μ . γ_i denote the anomalous dimension matrices (ADM) for the operators \mathcal{O}_i . They can be obtained from the ADM of the semi-leptonic operators in the LEFT [35, 111]. For the DLEFT operators with a non-zero matching condition, the values of these ADM are given by

$$\gamma_i = \begin{cases} -6C_F & \text{for } \mathcal{O}_i = \mathcal{O}_{d\phi}, \mathcal{O}_{d\phi^2}, \mathcal{O}_{dX^2}, \\ +2C_F & \text{for } \mathcal{O}_i = \mathcal{O}_{dX}^T, \mathcal{O}_{dX^2}^T, \\ 0 & \text{for } \mathcal{O}_i = \mathcal{O}_{\phi d}^{L,R}, \mathcal{O}_{d\chi}^{V,LR}, \mathcal{O}_{d\chi}^{V,RR}, \mathcal{O}_{dX}^{L,R}, \mathcal{O}_{dXX}^{L,R}, \mathcal{O}_{d\tilde{X}\tilde{X}}^{L,R}, \mathcal{O}_{DdX^2}^{L,R}, \end{cases} \quad (4.20)$$

with $C_F = (N_c^2 - 1)/(2N_c)$ and $N_c = 3$. Numerically, we find

$$L_i(4.8 \text{ GeV}) = L_i(m_Z) \cdot \begin{cases} 1.37 & \text{for } \mathcal{O}_i = \mathcal{O}_{d\phi}, \mathcal{O}_{d\phi^2}, \mathcal{O}_{dX^2}, \\ 0.90 & \text{for } \mathcal{O}_i = \mathcal{O}_{dX}^T, \mathcal{O}_{dX^2}^T, \end{cases} \quad (4.21)$$

$$L_i(2.0 \text{ GeV}) = L_i(m_Z) \cdot \begin{cases} 1.59 & \text{for } \mathcal{O}_i = \mathcal{O}_{d\phi}, \mathcal{O}_{d\phi^2}, \mathcal{O}_{dX^2}, \\ 0.86 & \text{for } \mathcal{O}_i = \mathcal{O}_{dX}^T, \mathcal{O}_{dX^2}^T, \end{cases} \quad (4.22)$$

which can be used in the B -meson and kaon decays, respectively.

4.3 Observables

Within the DLEFT, by using the similar treatment as for the $d_i \rightarrow d_j \nu \bar{\nu}$ transitions discussed in section 3.2, one can calculate the various $d_i \rightarrow d_j + \text{DM}$ processes. Generally, the amplitudes of these decays can be factorized into the product of the Wilson coefficient and the hadronic matrix element of the corresponding effective operator that can be parameterized form factors or decay constants. In appendix A,

we summarize the relevant hadronic matrix elements used in this paper. For the explicit expressions of the decay rates, we refer the readers to refs. [42, 112–117] for the $d_i \rightarrow d_j + \phi (+\phi)$ decays, refs. [5, 42, 118, 119] for the $d_i \rightarrow d_j + \chi + \chi$ decay, refs. [42, 47, 116] for the $d_i \rightarrow d_j + X (+X)$ decays, and refs. [120–122] for the $d_i \rightarrow d_i + a$ decays. To the best of our knowledge, a complete computation of the longitudinal polarization fraction F_L of the vector meson V in $P \rightarrow V + \text{DM}$ decays within the DLEFT is still missing, although the cases with some effective operators have been studied previously, e.g., in refs. [2, 42]. In this work, we systematically calculate the polarization observables in the DLEFT. All the relevant analytical expressions have been implemented in our recently developed package `HadronToNP` [123], which will be used in the following numerical analysis.

5 Numerical analysis

In this section, we proceed to present our numerical results and discussions. In table 1, we list the main input parameters used in our numerical analysis. Table 2 summaries our SM predictions and the up-to-date experimental measurements of the relevant observables. We take $\Lambda_{\text{NP}} = 1 \text{ TeV}$ in the SMEFT and DSMEFT. In the following, we investigate two explanations to the recent Belle II measurement of $\mathcal{B}(B^+ \rightarrow K^+ \nu \bar{\nu})$ [11]. In section 5.1, we consider the $b \rightarrow s + \nu \bar{\nu}$ transition in the SMEFT. In section 5.2, the missing energy signals in the Belle II measurement are interpreted in the DSMEFT as contributions from DM particles.

5.1 $M_1 \rightarrow M_2 + \nu \bar{\nu}$

The recent Belle II measurement of the $B^+ \rightarrow K^+ + \text{inv}$ decay could be explained by NP contributions to the $b \rightarrow s \nu \bar{\nu}$ transition. In this case, the theoretical prediction of the related $M_1 \rightarrow M_2 + \text{inv}$ processes takes the form

$$\mathcal{B}_{\text{th}}(M_1 \rightarrow M_2 + \text{inv}) = \sum_{i,j=e,\mu,\tau} \mathcal{B}(M_1 \rightarrow M_2 \nu_i \bar{\nu}_j). \quad (5.1)$$

The NP contributions to these processes can be generally described in the framework of SMEFT. We refer to refs. [15, 16, 27, 131] for the recent relevant studies. In the following, we also focus on the SMEFT but with the MFV hypothesis.

In the SMEFT, as mentioned in section 3.2.1, one interesting implication of the MFV hypothesis is that the $d_i \rightarrow d_j \nu \bar{\nu}$ transitions are all governed by only one effective operator at low energy. As a consequence, the ratio of the branching fractions of any two $b \rightarrow s \nu \bar{\nu}$ decays should be independent of the NP contribution. Considering as an example the $B^+ \rightarrow K^+ \nu \bar{\nu}$ and $B^0 \rightarrow K^{*0} \nu \bar{\nu}$ decays, we obtain

$$\frac{\mathcal{B}(B^+ \rightarrow K^+ \nu \bar{\nu})}{\mathcal{B}(B^0 \rightarrow K^{*0} \nu \bar{\nu})} = \frac{\mathcal{B}(B^+ \rightarrow K^+ \nu \bar{\nu})_{\text{SM}}}{\mathcal{B}(B^0 \rightarrow K^{*0} \nu \bar{\nu})_{\text{SM}}} = 0.46 \pm 0.07, \quad (5.2)$$

| Input | Value | Unit | Reference |
|--------------------------------------|--|-----------------------------|-----------|
| m_t^{pole} | 172.69 ± 0.30 | GeV | [31] |
| $ V_{cb} (\text{semi-leptonic})$ | $41.15 \pm 0.34 \pm 0.45$ | 10^{-3} | [124] |
| $ V_{ub} (\text{semi-leptonic})$ | $3.88 \pm 0.08 \pm 0.21$ | 10^{-3} | [124] |
| $ V_{us} f_+^{K \rightarrow \pi}(0)$ | 0.2165 ± 0.0004 | | [124] |
| γ | $72.1_{-5.7}^{+5.4}$ | \circ | [124] |
| $f_+^{K \rightarrow \pi}(0)$ | $0.9675 \pm 0.0009 \pm 0.0023$ | | [124] |
| Δm_{21}^2 | $7.41_{-0.20}^{+0.21}$ ($7.41_{-0.20}^{+0.21}$) | $10^{-5} \cdot \text{eV}^2$ | [31] |
| Δm_{32}^2 | $2.437_{-0.027}^{+0.028}$ ($-2.498_{-0.025}^{+0.032}$) | $10^{-3} \cdot \text{eV}^2$ | [31] |
| θ_{12} | $33.41_{-0.72}^{+0.75}$ ($33.41_{-0.72}^{+0.75}$) | \circ | [31] |
| θ_{23} | $49.1_{-1.3}^{+1.0}$ ($49.5_{-1.2}^{+0.9}$) | \circ | [31] |
| θ_{13} | $8.54_{-0.12}^{+0.11}$ ($8.57_{-0.11}^{+0.12}$) | \circ | [31] |
| δ_{CP} | 197_{-25}^{+42} (286_{-32}^{+27}) | \circ | [31] |

Table 1: Main input parameters used in our numerical analysis. The values (in brackets) of the parameters in the lepton sector correspond to the NO (IO) of neutrino masses.

where summation over the neutrino flavours has been taken into account. In this ratio, all the relevant SMEFT operators, i.e. $\mathcal{Q}_{lq}^{(1)}$ and $\mathcal{Q}_{lq}^{(3)}$, have been included simultaneously.⁴ When deriving this ratio, it is noted that only the MFV hypothesis in the quark sector is required to eliminate the right-handed operator \mathcal{O}_R . Therefore, the ratio still holds even by assuming generic couplings in the lepton sector, i.e., without the leptonic MFV. In addition, as both the CKM and Wilson coefficients involved are cancelled in this ratio, the theoretical uncertainty is reduced compared to that of the individual branching ratios. If future experimental measurements find any deviation from the theoretical value, it could imply new sources of flavour violation beyond the Yukawa couplings. By using the above ratio, the Belle 90% CL bound $\mathcal{B}(B^0 \rightarrow K^{*0}\nu\bar{\nu}) < 18 \times 10^{-6}$ would imply that

$$\mathcal{B}(B^+ \rightarrow K^+\nu\bar{\nu})_{\text{MFV}} < 10.5 \times 10^{-6}, \quad (5.3)$$

which is obviously lower than the 90% CL lower bound of the Belle II measurement, $\mathcal{B}(B^+ \rightarrow K^+\nu\bar{\nu}) > 12.5 \times 10^{-6}$. Or inversely, the Belle II measurement $\mathcal{B}(B^+ \rightarrow K^+\nu\bar{\nu}) = (23_{-6}^{+7}) \times 10^{-6}$ would indicate that

$$\mathcal{B}(B^0 \rightarrow K^{*0}\nu\bar{\nu})_{\text{MFV}} = (50_{-16}^{+17}) \times 10^{-6}, \quad (5.4)$$

⁴The ratio still holds after including the operators $\mathcal{Q}_{Hq}^{(1,3)}$, although they are not considered in our analysis as mentioned in section 3.1.

| Observable | SM | Exp | Unit | Sensitivity |
|---|-----------------|------------------------------------|------------|-----------------------------|
| $\mathcal{B}(B^+ \rightarrow K^+ \nu \bar{\nu})$ | 4.16 ± 0.57 | $23 \pm 5_{-4}^{+5}$ [125] | 10^{-6} | 19% [13] |
| $\mathcal{B}(B^0 \rightarrow K^0 \nu \bar{\nu})$ | 3.85 ± 0.52 | < 26 [126] | 10^{-6} | 87% [13] |
| $\mathcal{B}(B^+ \rightarrow K^{*+} \nu \bar{\nu})$ | 9.70 ± 0.94 | < 61 [126] | 10^{-6} | 75% [13] |
| $\mathcal{B}(B^0 \rightarrow K^{*0} \nu \bar{\nu})$ | 9.00 ± 0.87 | < 18 [126] | 10^{-6} | 40% [13] |
| $\mathcal{B}(B_s \rightarrow \phi \nu \bar{\nu})$ | 9.93 ± 0.72 | < 5400 [127] | 10^{-6} | 2% [128] |
| $\mathcal{B}(B^+ \rightarrow \pi^+ \nu \bar{\nu})$ | 1.40 ± 0.18 | < 140 [126] | 10^{-7} | |
| $\mathcal{B}(B^0 \rightarrow \pi^0 \nu \bar{\nu})$ | 6.52 ± 0.85 | < 900 [126] | 10^{-8} | |
| $\mathcal{B}(B^+ \rightarrow \rho^+ \nu \bar{\nu})$ | 4.06 ± 0.79 | < 300 [126] | 10^{-7} | |
| $\mathcal{B}(B^0 \rightarrow \rho^0 \nu \bar{\nu})$ | 1.89 ± 0.36 | < 400 [126] | 10^{-7} | |
| $\mathcal{B}(K^+ \rightarrow \pi^+ \nu \bar{\nu})$ | 8.42 ± 0.61 | $10.6_{-3.4}^{+4.0} \pm 0.9$ [129] | 10^{-11} | |
| $\mathcal{B}(K_L \rightarrow \pi^0 \nu \bar{\nu})$ | 3.41 ± 0.45 | < 300 [130] | 10^{-11} | |
| $\mathcal{B}(B_s \rightarrow \nu \bar{\nu})$ | ≈ 0 | < 5.9 [32] | 10^{-4} | $< 1.1 \times 10^{-5}$ [12] |
| $\mathcal{B}(B^0 \rightarrow \nu \bar{\nu})$ | ≈ 0 | < 1.4 [32] | 10^{-4} | $< 5.0 \times 10^{-6}$ [12] |

Table 2: Our SM predictions and the experimental measurements of the relevant observables. Upper limits are all given at 90% confidence level (CL). The last column shows the expected sensitivities at the Belle II (5 ab^{-1}) or at the CEPC (Tera- Z phase). The sensitivities at the FCC-ee are very similar to that at the CEPC, and hence are not given here.

which is incompatible with the Belle 90% CL bound $\mathcal{B}(B^0 \rightarrow K^{*0} \nu \bar{\nu}) < 18 \times 10^{-6}$. As a conclusion, the recent Belle II measurement of the $B^+ \rightarrow K^+ \nu \bar{\nu}$ decay cannot be explained in the SMEFT with MFV hypothesis. However, the MFV prediction of $\mathcal{B}(B^0 \rightarrow K^{*0} \nu \bar{\nu})$ is well within the reach of Belle II at 5 ab^{-1} (cf. table 2), which can be used as a further test of the MFV hypothesis considered here.

Similarly, the ratio of the branching fractions of a $b \rightarrow s \nu \bar{\nu}$ and a $b \rightarrow d \nu \bar{\nu}$ decay is also independent of the NP contribution in the SMEFT with MFV hypothesis. As an illustration, let us consider the $B^+ \rightarrow K^+ \nu \bar{\nu}$ and $B^+ \rightarrow \pi^+ \nu \bar{\nu}$ decays, and obtain

$$\frac{\mathcal{B}(B^+ \rightarrow K^+ \nu \bar{\nu})}{\mathcal{B}(B^+ \rightarrow \pi^+ \nu \bar{\nu})} = \frac{\mathcal{B}(B^+ \rightarrow K^+ \nu \bar{\nu})_{\text{SM}}}{\mathcal{B}(B^+ \rightarrow \pi^+ \nu \bar{\nu})_{\text{SM}}} = 29.7 \pm 5.6, \quad (5.5)$$

where summation over the neutrino flavours has been included. Taking as input the Belle II measurement in eq. (1.1), this ratio implies that

$$\mathcal{B}(B^+ \rightarrow \pi^+ \nu \bar{\nu})_{\text{MFV}} = (7.8_{-2.6}^{+2.8}) \times 10^{-7}, \quad (5.6)$$

which shows a 2.3σ deviation from the SM prediction $\mathcal{B}(B^+ \rightarrow \pi^+\nu\bar{\nu})_{\text{SM}} = (1.40 \pm 0.18) \times 10^{-7}$, but is still compatible with the current 90% CL experimental bound $\mathcal{B}(B^+ \rightarrow \pi^+\nu\bar{\nu}) < 140 \times 10^{-7}$. Of course, similar ratios can also be constructed for other processes to test the framework used here.

In the MFV framework, all the quark FCNC or the LFV processes are related with each other. Explicitly, for the operators $\mathcal{Q}_{lq}^{(i)}$ ($i = 1, 3$), all the quark FCNC transitions are governed by the two parameter products $\epsilon_1^{(i)}\kappa_0^{(i)}$ and $\epsilon_1^{(i)}\kappa_1^{(i)}$. In order to constrain them, we consider several quark (and lepton) FCNC processes, including the $B \rightarrow K^{(*)}\nu\bar{\nu}$, $B \rightarrow K^{(*)}e\mu$, $B \rightarrow \pi e\mu$, $B_s \rightarrow e\mu$, $B_s \rightarrow \mu^+\mu^-$ as well as $K \rightarrow \pi\nu\bar{\nu}$ decays. Besides the input parameters listed in table 1, the lepton number breaking scale $\Lambda_{\text{LN}} = 10^{14}$ GeV and the lightest neutrino mass $m_{\nu_1} = 0.2$ eV are used in the leptonic MFV. Numerically, we find that the dominant constraints come from the $B^+ \rightarrow K^+\nu\bar{\nu}$, $B^0 \rightarrow K^{*0}\nu\bar{\nu}$, $B^0 \rightarrow K^{*0}e^-\mu^+$ and $B_s \rightarrow \mu^+\mu^-$ decays. The allowed parameter regions of $\epsilon_1^{(i)}\kappa_0^{(i)}$ and $\epsilon_1^{(i)}\kappa_1^{(i)}$ are shown in figure 1. We can see that there is a small gap between the allowed regions of the $B^+ \rightarrow K^+\nu\bar{\nu}$ and $B^0 \rightarrow K^{*0}\nu\bar{\nu}$ decays. This reflects the discrepancy between the MFV prediction in eq. (5.4) and the current Belle bound on $\mathcal{B}(B^0 \rightarrow K^{*0}\nu\bar{\nu})$.

Since the uncertainty of the recent Belle II measurement is still quite large, we use instead all the processes except the $B^+ \rightarrow K^+\nu\bar{\nu}$ decay to derive the allowed parameter space. As shown in figure 1, the upper bounds on the magnitudes of the products $\epsilon_1^{(i)}\kappa_0^{(i)}$ and $\epsilon_1^{(i)}\kappa_1^{(i)}$ for the two operators $\mathcal{Q}_{lq}^{(1,3)}$ are all around 0.05 in the cases of NO and IO of neutrino masses, which are much smaller than the parameter regions required to explain the $B^+ \rightarrow K^+\nu\bar{\nu}$ excess. Using the allowed parameter regions for $\mathcal{Q}_{lq}^{(i)}$, we can derive the following numerical predictions:

$$\begin{aligned} 3.4(3.5) \times 10^{-6} &< \mathcal{B}(B^+ \rightarrow K^+\nu\bar{\nu})_{\text{MFV}} < 5.0(4.9) \times 10^{-6}, \\ 7.4(7.5) \times 10^{-6} &< \mathcal{B}(B^0 \rightarrow K^{*0}\nu\bar{\nu})_{\text{MFV}} < 10.8(10.6) \times 10^{-6}, \\ 1.1(1.2) \times 10^{-7} &< \mathcal{B}(B^+ \rightarrow \pi^+\nu\bar{\nu})_{\text{MFV}} < 1.7(1.7) \times 10^{-7}, \end{aligned} \quad (5.7)$$

which correspond the NO (IO) of neutrino masses. The numerical results show less than 0.5% difference between $\mathcal{Q}_{lq}^{(1)}$ and $\mathcal{Q}_{lq}^{(3)}$, implying that both of these two operators coincide with each other under the above bounds. From these bounds, we can see that the NP contributions to the $B \rightarrow K\nu\bar{\nu}$ and $B \rightarrow \pi\nu\bar{\nu}$ decays should be less than $\sim 20\%$ of their SM predictions. It is noted that the leptonic MFV has been used to derive the allowed parameter space and the above bounds. Therefore, the bound on $\mathcal{B}(B^+ \rightarrow K^+\nu\bar{\nu})$ is more stringent than the one in eq. (5.3) derived without the leptonic MFV.

5.2 $M_1 \rightarrow M_2 + \text{DM}$

The large excess of $\mathcal{B}(B^+ \rightarrow K^+\nu\bar{\nu})$ reported by Belle II can also be explained by light NP particles that contribute to the signal as $B^+ \rightarrow K^+ + \text{missing energy}$. In

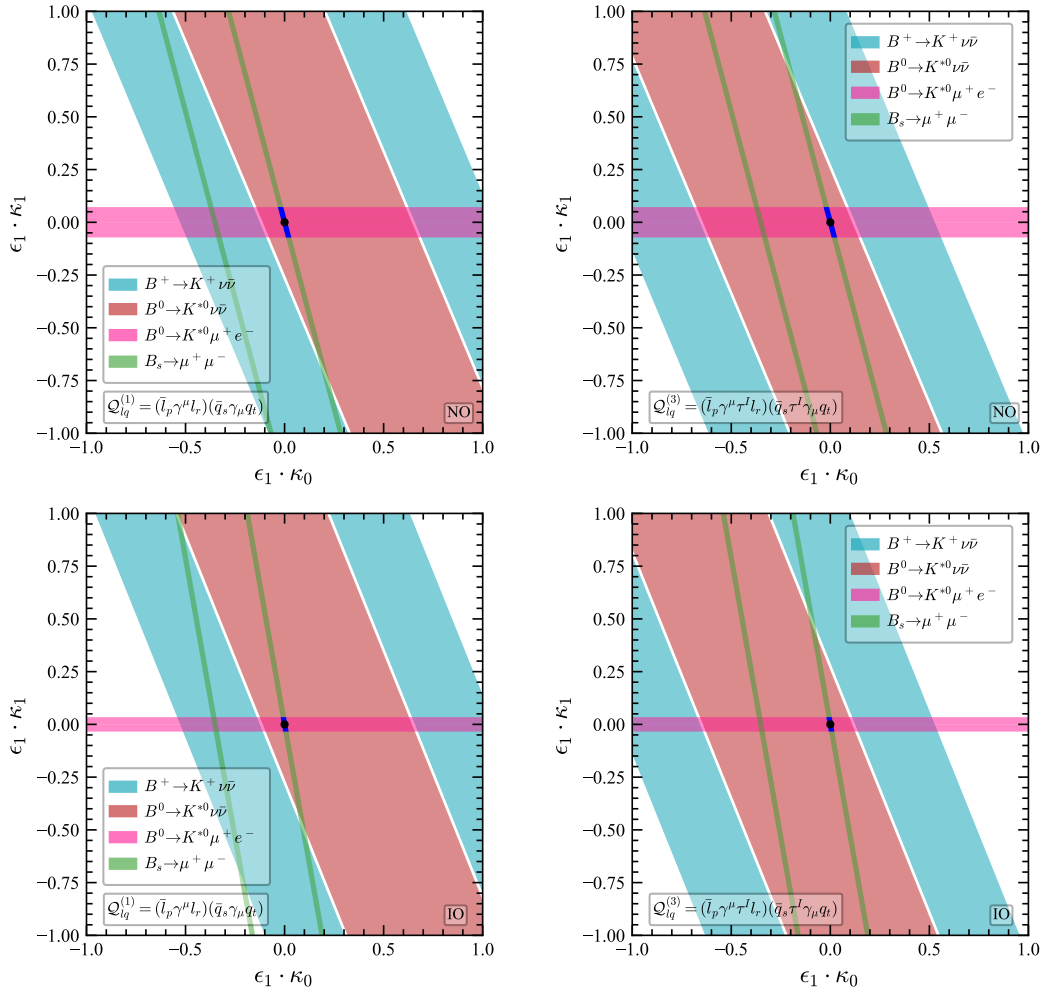


Figure 1: Constraints on the MFV parameter products $(\epsilon_1^{(i)} \kappa_0^{(i)}, \epsilon_1^{(i)} \kappa_1^{(i)})$ for $\mathcal{Q}_i = \mathcal{Q}_{lq}^{(1)}$ (left) and $\mathcal{Q}_i = \mathcal{Q}_{lq}^{(3)}$ (right) in the cases of NO (upper) and IO (lower) of neutrino masses. The allowed regions by the measurement of $\mathcal{B}(B^+ \rightarrow K^+ \nu \bar{\nu})$ are at 2σ level, while the regions by $\mathcal{B}(B^0 \rightarrow K^{*0} \nu \bar{\nu})$, $\mathcal{B}(B^0 \rightarrow K^{*0} \mu^+ e^-)$ and $\mathcal{B}(B_s \rightarrow \mu^+ \mu^-)$ at 90% CL. The allowed regions by all the last three observables are shown in blue. The black points $(0, 0)$ denote the SM case.

this case, the theoretical predictions of the $M_1 \rightarrow M_2 + \text{inv}$ decay can be written as

$$\mathcal{B}_{\text{th}}(M_1 \rightarrow M_2 + \text{inv}) = \mathcal{B}_{\text{SM}}(M_1 \rightarrow M_2 + \nu \bar{\nu}) + \mathcal{B}_{\text{NP}}(M_1 \rightarrow M_2 + \text{DM}). \quad (5.8)$$

As discussed in section 4, the effects of light NP particles in the second term can be generally described in the EFT framework. In the following, we investigate this explanation in the DSMEFT framework, in which the Wilson coefficients are taken to be the most general form or satisfy the MFV hypothesis.

5.2.1 General flavour structure

In the DSMEFT with general flavour structure, only the $b \rightarrow s + \text{inv}$ processes are directly related to the $B^+ \rightarrow K^+ + \text{inv}$ decays, which include $B^0 \rightarrow K^0 + \text{inv}$, $B^{0,+} \rightarrow K^{*0,+} + \text{inv}$, $B_s \rightarrow \phi + \text{inv}$ and $B_s \rightarrow \text{inv}$ decays. In the following, we investigate constraints on the DSMEFT operators from the experimental data on these decays as summarized in table 2, and discuss future prospects at Belle II, CEPC and FCC-ee. As discussed in section 4.1, seven DSMEFT operators are not hermitian. In order to compare with the MFV analysis in the next subsection, contributions from the hermitian conjugation of these operators are neglected in the numerical analysis in this subsection, i.e., $\mathcal{C}_{ji} = 0$ is taken for $d_i \rightarrow d_j$ processes.⁵ For example, contributions to the $b \rightarrow s\phi\phi$ processes from the operator $\mathcal{Q}_{d\phi^2}$ are calculated by taking $[\mathcal{C}_{d\phi^2}]_{23} \neq 0$ and $[\mathcal{C}_{d\phi^2}]_{32} = 0$. Two exceptions are the operators \mathcal{Q}_{DqX^2} and \mathcal{Q}_{DdX^2} . Consider the former as an example, we take $[\mathcal{C}_{DqX^2}]_{ji} = [\mathcal{C}_{DqX^2}]_{ij}^*$ for the $d_i \rightarrow d_j$ processes to compare with the MFV analysis, where its MFV coupling matrix in eq. (2.16) also implies a hermitian \mathcal{C}_{DqX^2} . In this case, the hadronic matrix elements of the weak currents can be parameterized in terms of the transition form factors of the vector current as discussed in appendix A.2.

For the scalar DM, there are three operators ($\mathcal{Q}_{d\phi^2}$, $\mathcal{Q}_{\phi q}$ and $\mathcal{Q}_{\phi d}$, cf. eq. (4.2)) contributing to the three-body $d_i \rightarrow d_j\phi\phi$ and one operator ($\mathcal{Q}_{d\phi}$, cf. eq. (4.2)) to the two-body $d_i \rightarrow d_j\phi$ decay. Allowed regions of the Wilson coefficients for these four operators are shown in figure 2. From this figure, we make the following observations:

- The $B^0 \rightarrow K^{*0} + \text{inv}$ decay provides the strongest constraints on the parameter regions allowed by the Belle II measurement of the $B^+ \rightarrow K^+ + \text{inv}$ decay. Especially, for the operators $\mathcal{Q}_{\phi q}$ and $\mathcal{Q}_{\phi d}$, the regions of $m_{\phi_2} \lesssim 2.0 \text{ GeV}$ ($m_{\phi_1} < m_{\phi_2}$ is assumed without loss of generality) are excluded by the decay. For the operator $\mathcal{Q}_{d\phi}$, on the other hand, large part of the parameter region with $m_\phi \lesssim 3.8 \text{ GeV}$ is excluded.
- Another stronger constraint arises from the $B_s \rightarrow \text{inv}$ decay, which benefits from the large phase space. As a result, it excludes the parameter region for large DM mass, e.g., the region with $m_\phi \gtrsim 2.3 \text{ GeV}$ is excluded for the operator $\mathcal{Q}_{d\phi^2}$. For the operators $\mathcal{Q}_{\phi q}$ and $\mathcal{Q}_{\phi d}$, however, the $B_s \rightarrow \phi_1\phi_2$ amplitude vanishes in the case of $m_{\phi_1} = m_{\phi_2}$ due to the derivative term $\phi_1 \overleftrightarrow{\partial}^\mu \phi_2$ in the operators. Therefore, only the parameter regions with $m_{\phi_1} \neq m_{\phi_2}$ receive constraint from the $B_s \rightarrow \text{inv}$ decay.
- Compared to the $B^0 \rightarrow K^{*0} + \text{inv}$ and $B_s \rightarrow \text{inv}$ decays, the $B^0 \rightarrow K^0 + \text{inv}$, $B^+ \rightarrow K^{*+} + \text{inv}$ and $B_s \rightarrow \phi + \text{inv}$ decays provide almost no further constraints.

⁵Let us consider $\mathcal{Q}_{d\phi^2}$ as an example. For the $b \rightarrow s\phi\phi$ process, $[\mathcal{C}_{d\phi^2}]_{23} \neq 0$ and $[\mathcal{C}_{d\phi^2}]_{32} = 0$ are taken in the general DSMEFT analysis. In the MFV hypothesis, the coupling matrix eq. (2.17) implies that $[\mathcal{C}_{d\phi^2}]_{23} \gg [\mathcal{C}_{d\phi^2}]_{32}$, which results in the approximation $[\mathcal{C}_{d\phi^2}]_{32} \approx 0$.

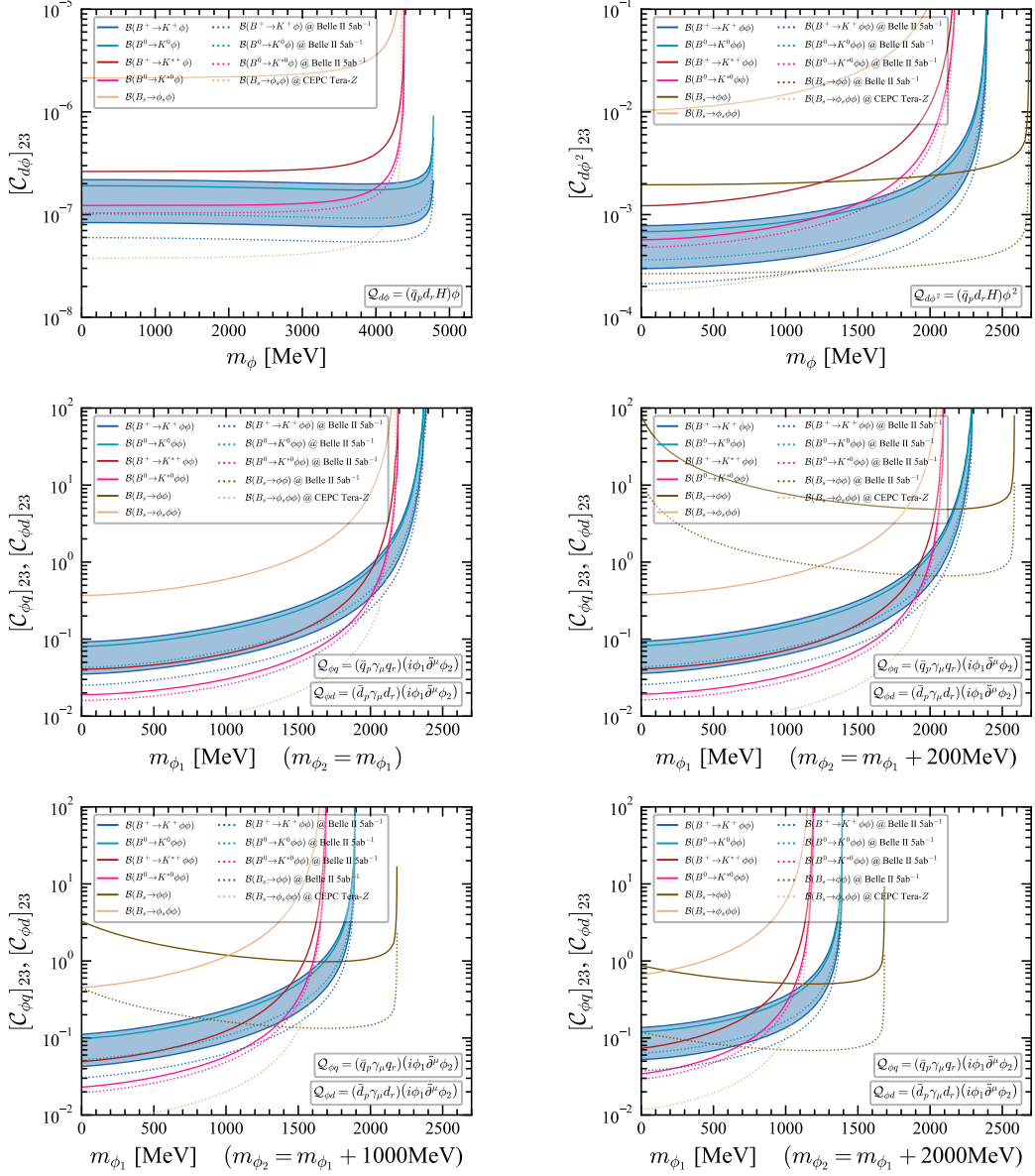


Figure 2: Constraints on the Wilson coefficients of the operators involving scalar DM as a function of the scalar mass m_ϕ . The blue band denotes the 2σ allowed region by the recent Belle II measurement of the $B^+ \rightarrow K^+ + \text{inv}$ decay. The upper bounds from other measurements are shown by the solid lines, while the expected sensitivities at Belle II and CEPC by the dotted lines. The sensitivities at FCC-ee are very similar to that at CEPC and hence are not shown. For the operators $\mathcal{Q}_{\phi q}$ and $\mathcal{Q}_{\phi d}$, we have considered four different cases for the DM masses, as indicated in the last four plots.

The upper bounds from these three decays are comparable to or weaker than the upper limits of the 2σ allowed region required to explain the $B^+ \rightarrow K^+ + \text{inv}$

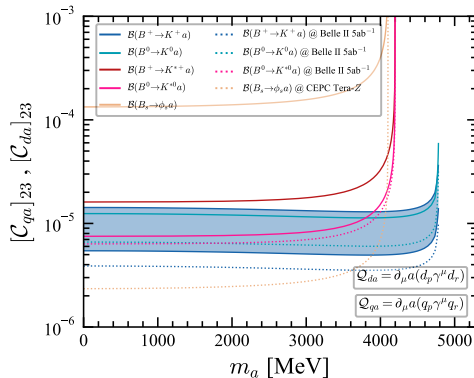


Figure 3: Same as in figure 2, but for the operators involving ALP.

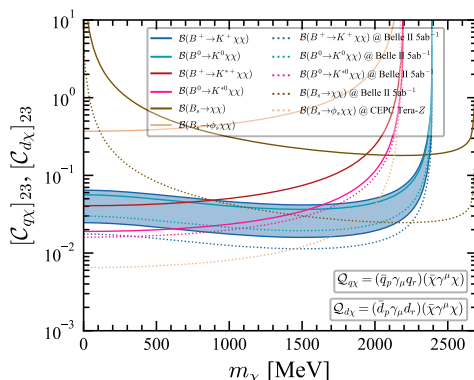


Figure 4: Same as in figure 2, but for the operators involving fermionic DM.

excess.

- All the processes put very weak constraints on the parameter regions with $m_\phi \lesssim 2.3 \text{ GeV}$ for the operator $\mathcal{Q}_{d\phi^2}$.

In addition, constraints on the operators involving ALP are shown in figure 3, which are very similar to the ones for the operator $\mathcal{Q}_{d\phi}$ but with much larger allowed Wilson coefficients.

For the fermionic DM, there are only two relevant operators \mathcal{Q}_{qX} and \mathcal{Q}_{dX} (cf. eq. (4.3)) in the DSMEFT. The experimental constraints are shown in figure 4. In the cases of $m_\chi \lesssim 0.6 \text{ GeV}$ and $m_\chi \gtrsim 2.3 \text{ GeV}$, the parameter spaces required to account for the Belle II measurement are already excluded by the $B^0 \rightarrow K^{*0} + \text{inv}$ and $B_s \rightarrow \text{inv}$ decays, respectively. In the range of $0.6 \lesssim m_\chi \lesssim 2.3 \text{ GeV}$, however, large part of the parameter space survives all the constraints. This is quite different from the case of the SMEFT operator $\mathcal{Q}_{lq}^{(1)}$ discussed in section 5.1, due to the massive fermionic DM fields in the operators \mathcal{Q}_{qX} and \mathcal{Q}_{dX} . In the massless limit, their effects on the decay width are the same as that of the operator $\mathcal{Q}_{lq}^{(1)}$.⁶

⁶Although the leptonic and DM currents in these operators have different chiralities, the total

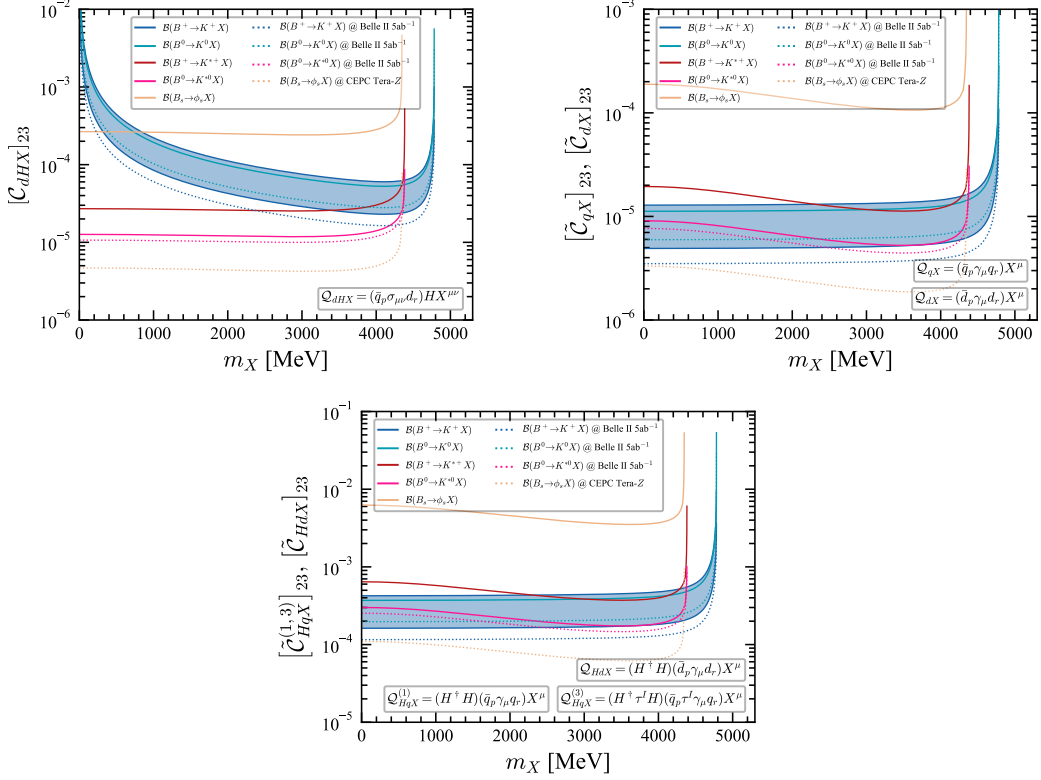


Figure 5: Same as in figure 2, but for the operators involving one vector DM.

For the vector DM, there are 8 operators (\mathcal{Q}_{dX^2} , \mathcal{Q}_{qXX} , \mathcal{Q}_{dXX} , $\mathcal{Q}_{q\tilde{X}X}$, $\mathcal{Q}_{d\tilde{X}X}$, \mathcal{Q}_{DqX^2} , \mathcal{Q}_{DdX^2} and \mathcal{Q}_{dHX^2} , cf. eq. (4.5)) contributing to the three-body $d_i \rightarrow d_j XX$ and 6 operators (\mathcal{Q}_{dHX} , \mathcal{Q}_{dX} , \mathcal{Q}_{qX} , \mathcal{Q}_{HdX} and $\mathcal{Q}_{HqX}^{(1,3)}$, cf. eqs. (4.4) and (4.5)) to the two-body $d_i \rightarrow d_j X$ decay. For the Wilson coefficient of each operator, the parameter region required to account for the Belle II measurement of the $B^+ \rightarrow K^+ + \text{inv}$ decay as well as the experimental bounds from other processes are shown in figures 5 and 6. The following observations are made:

- For the operators involving one DM field, the high-mass region of $4.3 \lesssim m_X \lesssim 4.6 \text{ GeV}$ does not suffer from any constraint, while large part of the parameter region with $m_X \lesssim 4.3 \text{ GeV}$ is excluded by the $B^0 \rightarrow K^{*0} + \text{inv}$ decay. Specifically, for the operator \mathcal{Q}_{dHX} , the unique one built from the field strength tensor $X_{\mu\nu}$, the parameter region with $m_X \lesssim 4.3 \text{ GeV}$ is excluded; for the other operators, parts of the parameter region still survive for $m_X \lesssim 2.5 \text{ GeV}$ or $4.3 \lesssim m_X < 4.6 \text{ GeV}$.
- For the operators involving two DM fields, except for \mathcal{Q}_{dHX^2} , the parameter spaces with $m_X \gtrsim 2 \text{ GeV}$ are all excluded by the $B_s \rightarrow \text{inv}$ decay. For \mathcal{Q}_{DqX^2} ,

decay width does not depend on the chirality of the currents.

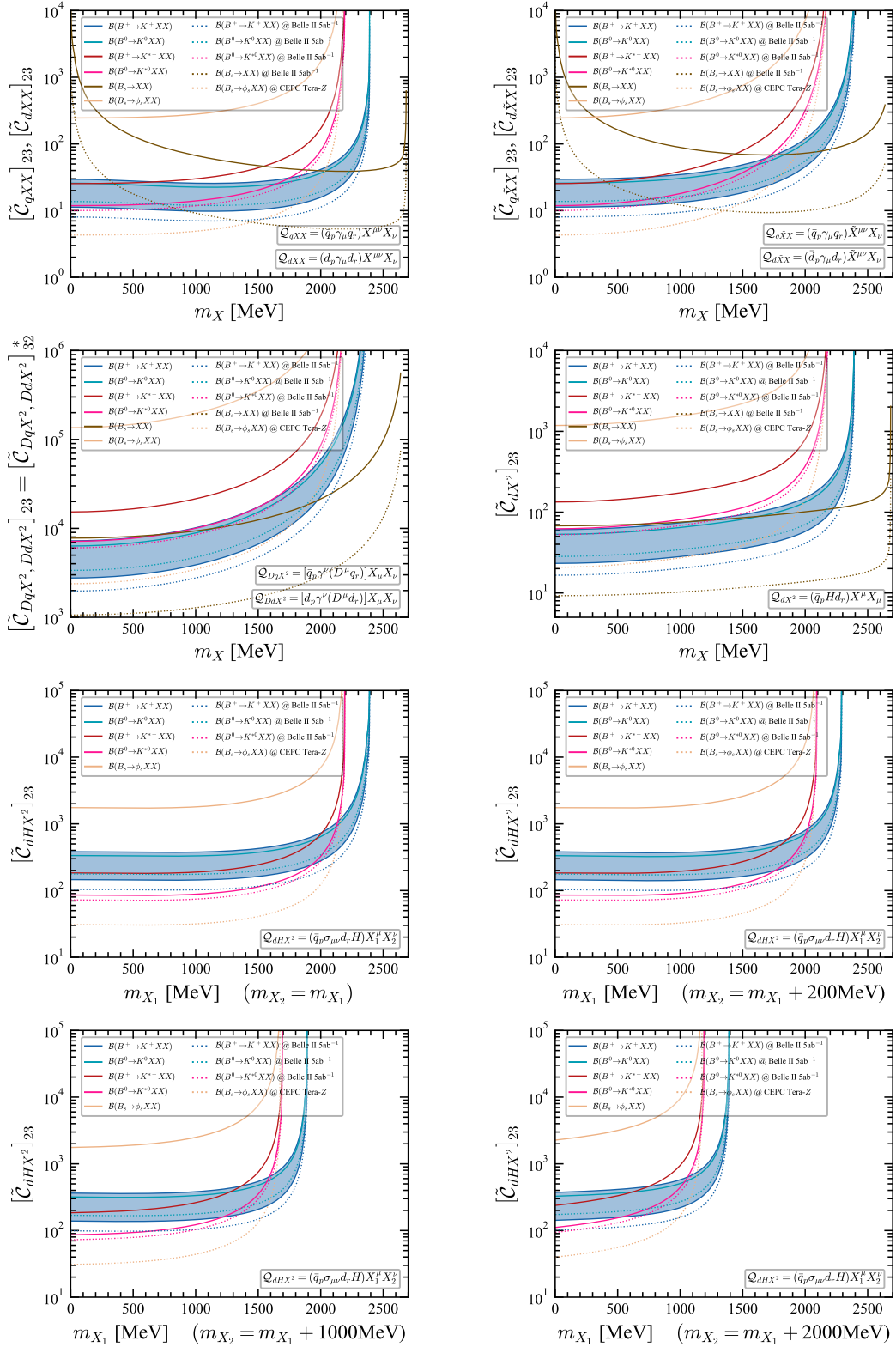


Figure 6: Same as in figure 2, but for the operators involving two vector DM fields. For the operator \mathcal{Q}_{dHX^2} , we have considered four different cases for the masses of the two DM particles, as indicated in the last four plots.

\mathcal{Q}_{DdX^2} and \mathcal{Q}_{dX^2} , the $B_s \rightarrow \text{inv}$ decay also provides almost the strongest constraints in the whole DM mass region, although the constraints in the region of $m_X \lesssim 1.7 \text{ GeV}$ are quite weak. For the other operators, the parameter regions with $m_X \lesssim 1.7 \text{ GeV}$ are highly constrained or largely excluded by the $B^0 \rightarrow K^{*0} + \text{inv}$ decay.

- Constraints on the operator \mathcal{Q}_{dHX^2} are quite different from the other ones. As the tensor hadronic matrix element $\langle 0 | \bar{b} \sigma_{\mu\nu} s | B_s \rangle$ vanishes identically, this operator does not contribute to the $B_s \rightarrow \text{inv}$ decay. Therefore, the high-mass regions do not suffer from any constraint. However, most of the low-mass regions are excluded by the $B^0 \rightarrow K^{*0} + \text{inv}$ decay, e.g., the one with $m_{X_1} \lesssim 1.8 \text{ GeV}$ is excluded in the case of $m_{X_2} - m_{X_1} = 200 \text{ MeV}$.

All the data on $b \rightarrow s$ decays discussed above will be significantly improved in the future [12, 13, 128, 132]. Considering the expected sensitivities at Belle II (5 ab^{-1}), CEPC and FCC-ee (Tera- Z phase) listed in table 2, we also show in figures 2-6 the projected 90% CL bounds on the DSMEFT operators. It is observed that

- At the Belle II with 5 ab^{-1} , the relative uncertainty of the measured $\mathcal{B}(B^+ \rightarrow K^+ \nu \bar{\nu})$ is expected to be 19%. Using the SM prediction to estimate the future experimental central value, the projected bound covers all the parameter space explaining the recent Belle II excess. If the central value of the current Belle II data remains unchanged in the future, the future experimental measurement of $\mathcal{B}(B^+ \rightarrow K^+ \nu \bar{\nu})$ is expected to be $(23 \pm 4) \times 10^{-6}$, which would deviate from the current SM prediction by about 4σ .
- For the $B^0 \rightarrow K^0 + \text{inv}$ decay, the projected bound can cover most of the parameter regions required to explain the $B^+ \rightarrow K^+ + \text{inv}$ excess. Therefore, this decay can provide an independent probe of the proposed mechanism behind the Belle II excess.
- The $B_s \rightarrow \phi + \text{inv}$ and $B_s \rightarrow \text{inv}$ decays can strongly constrain the low- and high-mass regions of the parameter space used to explain the Belle II excess, respectively. Their combination can even exclude almost all the parameter regions. It is also noted that the operators $\mathcal{Q}_{d\phi^2}$ and \mathcal{Q}_{dX^2} affect the $B_s \rightarrow \text{inv}$ decay without helicity suppression, which makes the projected bound of the $B_s \rightarrow \text{inv}$ decay cover the whole parameter space of these two operators.
- All the operators involving one DM (such as $\mathcal{Q}_{d\phi}$ and \mathcal{Q}_{da}), as well as the operator \mathcal{Q}_{dHX^2} , do not contribute to the $B_s \rightarrow \text{inv}$ decay. Therefore, the high-mass regions do not suffer from any constraint, even at the Belle II with 5 ab^{-1} or at the CEPC and FCC-ee during the Tera- Z phase.

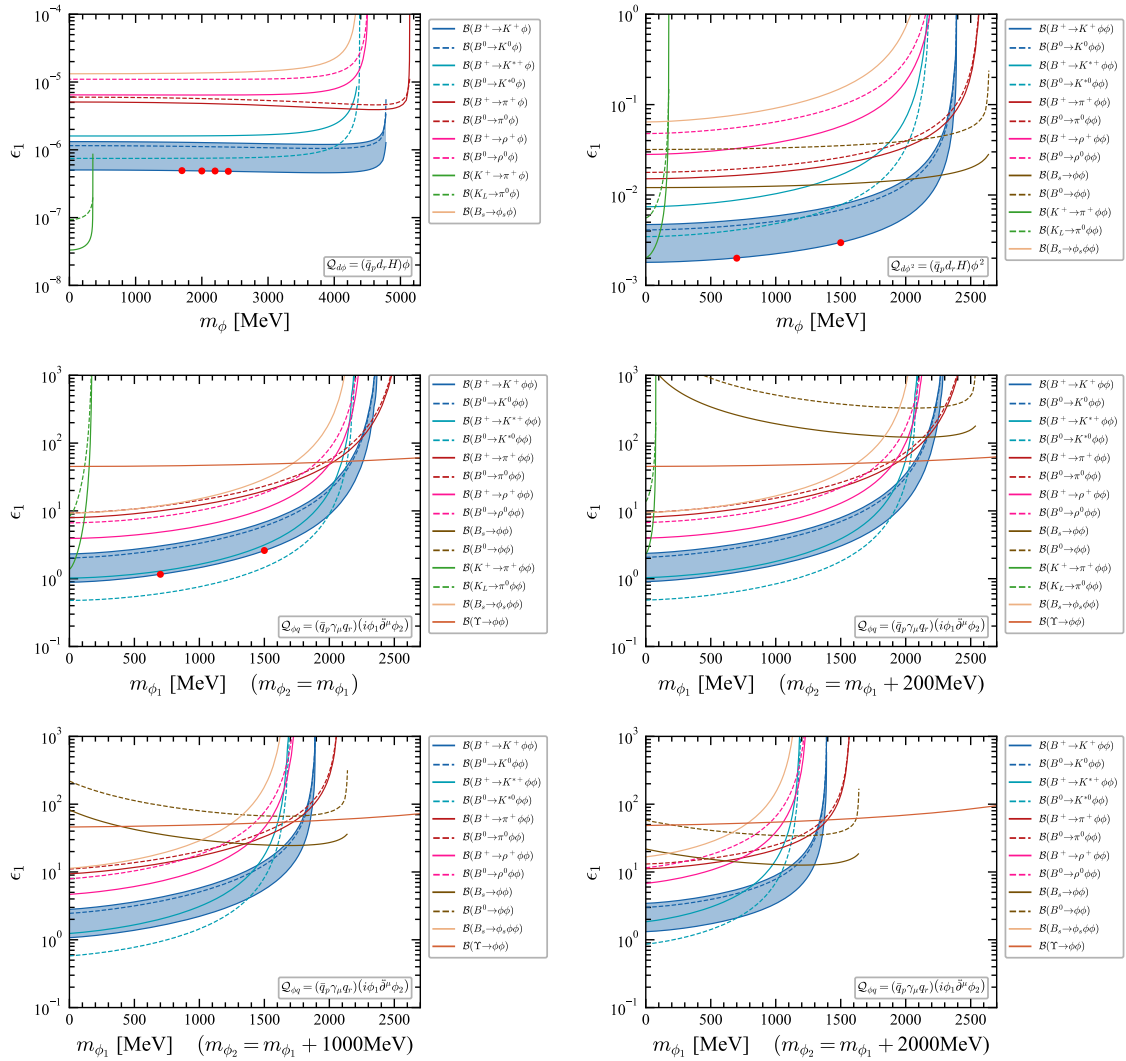


Figure 7: Constraints on the MFV parameter ϵ_1 for the operators involving scalar DM as a function of the scalar mass m_ϕ . The blue band denotes the 2σ allowed region by the recent Belle II measurement of the $B^+ \rightarrow K^+ + \text{inv}$ decay, while the upper bounds obtained from all the other processes are shown by the solid and dashed lines. The red points denote the benchmark points used to investigate the q^2 distributions in figure 12; see text for more details.

5.2.2 MFV

As demonstrated in eq. (4.8), once the MFV hypothesis is assumed, 8 out of the 22 DSMEFT operators do not induce down-type FCNC interactions. Therefore, these operators cannot account for the recent Belle II measurement of the $B^+ \rightarrow K^+ + \text{inv}$ decay. For the remaining 14 operators, their MFV couplings make the $b \rightarrow d$ and $s \rightarrow d$ processes also relevant. We consider the constraints from the experimental measurements summarized in table 2, which include the branching ratios of the

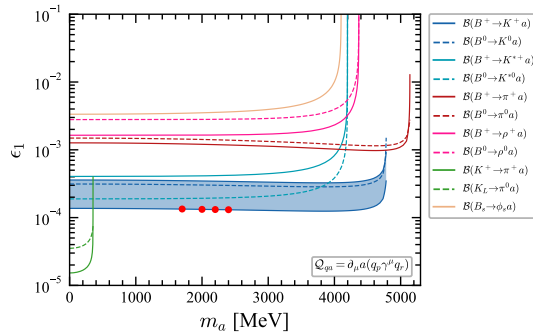


Figure 8: Same as in figure 7, but for the operator involving ALP.

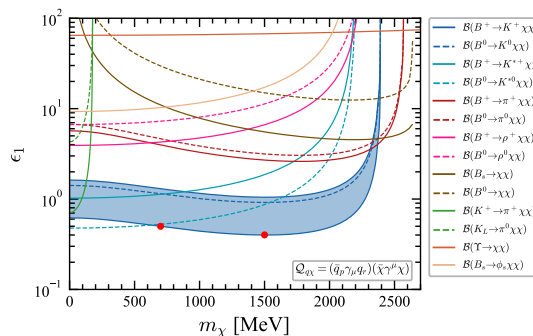


Figure 9: Same as in figure 7, but for the operator involving fermionic DM.

$B \rightarrow K^{(*)}, \pi, \rho + \text{inv}, K^+ \rightarrow \pi^+ + \text{inv}, K_L \rightarrow \pi^0 + \text{inv}, B_s \rightarrow \phi + \text{inv}$ and $B_{s,d} \rightarrow \text{inv}$ decays. It is noted that, as discussed in the last subsection, the $b \rightarrow s$ transition in the MFV hypothesis approximately depends only on one Wilson coefficient. Numerically, this situation is similar to the treatment in the general DSMEFT discussed in the last section; see footnote 5 for an example. Consequently, the relative strength of the constraints from the various $b \rightarrow s$ processes are the same between the general case and the MFV hypothesis. Therefore, in the following, we focus on whether the $s \rightarrow d$ and $b \rightarrow d$ processes can provide further constraint with respect to that from the $b \rightarrow s$ processes.

For the three operators with scalar DM (cf. eq. (4.2)), the allowed regions of the MFV parameter ϵ_1^i are shown in figure 7. In the low-mass region of $m_\phi \lesssim 200$ MeV, the $K^+ \rightarrow \pi^+ + \text{inv}$ decay puts the strongest constraint for the operators $\mathcal{Q}_{d\phi}$ and $\mathcal{Q}_{d\phi^2}$. For all the operators, the $B^+ \rightarrow \pi^+ + \text{inv}$ or the $B^+ \rightarrow \rho^+ + \text{inv}$ decay, depending on the DM mass, provides the strongest constraint among all the $b \rightarrow d$ processes. However, this decay provides no further constraint after considering the constraints from the $b \rightarrow s$ processes. The only exception is the constraint for the operator $\mathcal{Q}_{\phi q}$ in the case of $m_{\phi_1} = m_{\phi_2} \equiv m_\phi$. In the region of $m_\phi \gtrsim 2.3$ GeV, the strongest constraint is provided by the $B^+ \rightarrow \pi^+ + \text{inv}$ decay (as well as the $\Upsilon(1S) \rightarrow \text{inv}$ decay; see the later discussion), because $m_{\phi_1} = m_{\phi_2}$ makes the NP

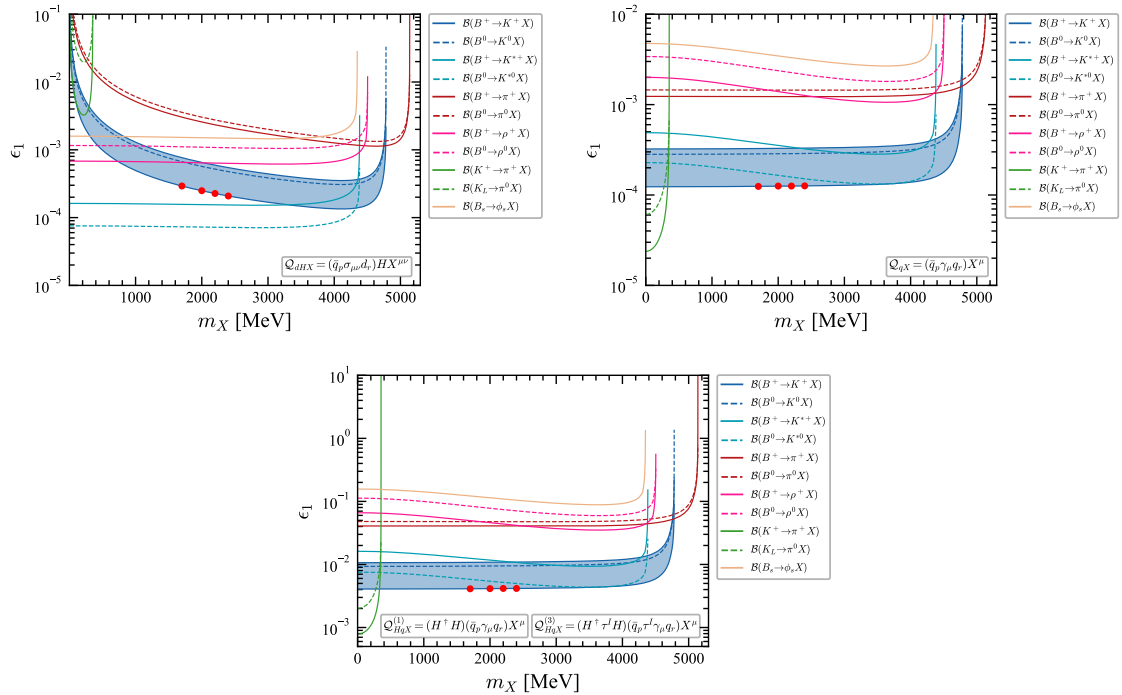


Figure 10: Same as in figure 7, but for the operators involving one vector DM.

contribution to the $B_s \rightarrow \phi_1 \phi_2$ decay vanishing. In addition, \mathcal{Q}_{qa} is the unique operator involving ALP in the MFV framework. The constraints on this operator are shown in figure 8, which are, as in the general case, very similar to the ones for $\mathcal{Q}_{d\phi}$ but with a much larger allowed Wilson coefficient.

Among the operators with fermionic DM, there is only one relevant operator (\mathcal{Q}_{qX} , cf. eq. (4.3)) in the MFV hypothesis. The experimental constraints are shown in figure 9. We can see that, after considering the constraints from the $b \rightarrow s$ processes, all the $s \rightarrow d$ and $b \rightarrow d$ decays provide no further constraints, except in a narrow window near $m_X \approx 2.3$ GeV, where the $B^+ \rightarrow \pi^+ + \text{inv}$ decay gives the strongest bound.

For the vector DM, in the MFV framework, there are five operators (\mathcal{Q}_{qXX} , $\mathcal{Q}_{q\tilde{X}X}$, \mathcal{Q}_{dX^2} , \mathcal{Q}_{DqX^2} and \mathcal{Q}_{dHX^2} , cf. eq. (4.5)) contributing to the three-body $d_i \rightarrow d_j XX$ and four operators (\mathcal{Q}_{dHX} , \mathcal{Q}_{qX} and $\mathcal{Q}_{HqX}^{(1,3)}$, cf. eqs. (4.4) and (4.5)) to the two-body $d_i \rightarrow d_j X$ decay. The relevant experimental constraints are shown in figures 10 and 11. For the operators \mathcal{Q}_{qX} and $\mathcal{Q}_{HqX}^{(1,3)}$, the $K^+ \rightarrow \pi^+ + \text{inv}$ decay provides the strongest constraint for $m_X \lesssim 0.35$ GeV and exclude the parameter region required to account for the Belle II excess. For the four operators involving one DM, the $B^+ \rightarrow \pi^+ + \text{inv}$ decay excludes the mass window around $m_X \approx 4.8$ GeV. For the five operators involving two DM, neither the $s \rightarrow d$ nor the $b \rightarrow d$ processes can put further constraints after considering those from the $b \rightarrow s$ decays. One exception is the operator \mathcal{Q}_{dHX^2} , where the decay $B^+ \rightarrow \pi^+ + \text{inv}$ excludes the tail in the

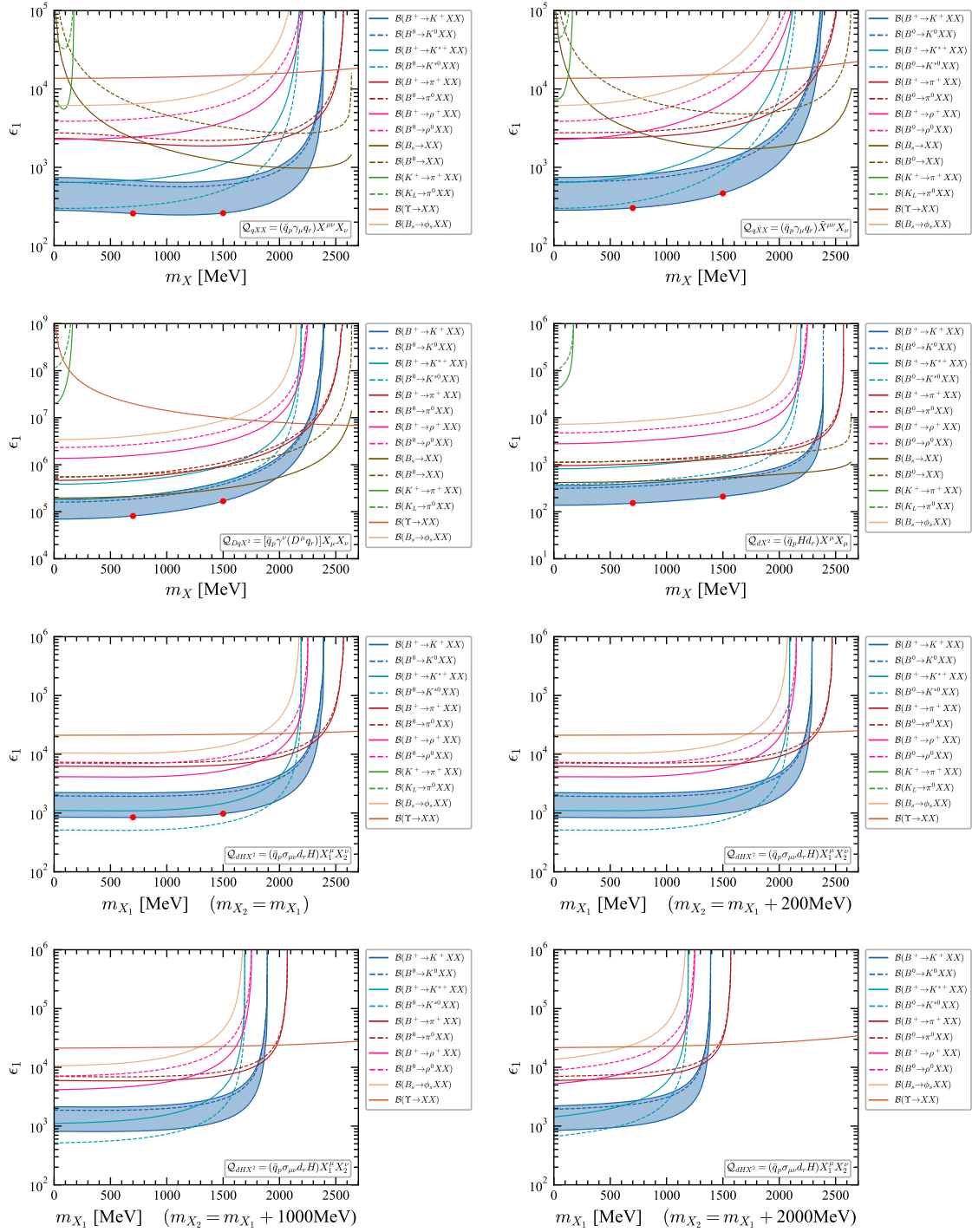


Figure 11: Same as in figure 7, but for the operators involving two vector DM fields. For the operator \mathcal{Q}_{dHX^2} , we have considered four different cases for the DM masses, as indicated in the last four plots.

high-mass region.

In the MFV hypothesis, as indicated by eqs. (2.16) and (2.17), the flavour-

conserving couplings to the third generation are much larger than all the other FCNC couplings.⁷ Therefore, the $\Upsilon \rightarrow \text{DM} + \text{DM}$ decay could be highly enhanced. However, the current experimental bounds on the invisible Υ decays are still quite weak. For the $\Upsilon(1S) \rightarrow \text{inv}$ decay, the 90% CL upper limit on its branching ratio is 3.0×10^{-4} [133], which is about one order of magnitude higher than the SM prediction 9.9×10^{-6} [134–136]. Constraints from this process are also shown in figures 7–11. For the operator $\mathcal{Q}_{\phi q}$ with $m_{\phi_2} - m_{\phi_1} \leq 200 \text{ MeV}$, we can see that the constraints from the $\Upsilon(1S) \rightarrow \text{inv}$ decay are much stronger than from all the $b \rightarrow d$ decays in the high mass region of $m_{\phi_2} \gtrsim 2 \text{ GeV}$ and, especially, exclude the regions of $m_{\phi_2} \gtrsim 2.3 \text{ GeV}$ required to explain the Belle II excess. However, the constraints for all the other operators are much weaker than from the B -meson and kaon decays in the range of $m_{\text{DM}} \lesssim m_B/2$. On the other hand, the constraints from invisible charmonium decays are totally negligible, because the NP contributions are suppressed by a factor of $\mathcal{O}(\lambda_c^4)$ in the MFV hypothesis.

The q^2 distributions of the FCNC decays can also provide useful information about the NP effects. Considering the large uncertainty of the Belle II measurement, we take a conservative estimation of the NP contributions to the q^2 distributions: For each DSMEFT operator, the minimal value of the MFV parameter allowed by all the experimental constraints is chosen as the benchmark point, which is also shown in figures 7–11. Therefore, all the benchmark points actually correspond to the same branching ratio $\mathcal{B}(B^+ \rightarrow K^+ + \text{inv}) = 4.8 \times 10^{-6}$, which is the 2σ lower bound allowed by the Belle II measurement. Furthermore, we choose two typical values of the DM masses, 700 MeV and 1500 MeV. By using these benchmark points, we show in figure 12 our predictions for the q^2 distributions of $B^+ \rightarrow K^+ + \text{inv}$ and $B^0 \rightarrow K^{*0} + \text{inv}$ decays.⁸ In the case of $m_{\text{DM}} = 700 \text{ MeV}$, we can see that, for the operators $\mathcal{Q}_{\phi q}$ and $\mathcal{Q}_{d\phi^2}$, the distributions are close to each other in the $B^+ \rightarrow K^+ + \text{inv}$, but distinguishable in the $B^0 \rightarrow K^{*0} + \text{inv}$ decay. However, for the operators \mathcal{Q}_{qXX} and $\mathcal{Q}_{q\tilde{X}X}$, the distributions are quite close in both of these two decays. In the case of $m_{\text{DM}} = 1500 \text{ MeV}$, the distributions are quite different, and hence distinguishable from each other for most operators. Therefore, all the operators are distinguishable from each other by combining the two decay spectra.

As can be seen from ref. [11], excesses of the $B^+ \rightarrow K^+ + \text{inv}$ events mostly appear

⁷As can be seen from eq. (4.8), the flavour-conserving couplings can also be altered by the MFV parameter ϵ_0 . However, this parameter does not affect the FCNC processes, e.g., the $B^+ \rightarrow K^+ + \text{inv}$ decay. For simplicity, we take $\epsilon_0 = 0$ to derive the bounds on ϵ_1 from the invisible decays of charmoniums and bottomoniums. For a non-zero ϵ_0 , it is straightforward to obtain the corresponding bounds on ϵ_1 by using eq. (4.8).

⁸The q^2 distributions of other $P \rightarrow P + \text{inv}$ and $P \rightarrow V + \text{inv}$ decays are similar to that of $B^+ \rightarrow K^+ + \text{inv}$ and $B^0 \rightarrow K^{*0} + \text{inv}$ respectively, and hence are not shown here anymore. In addition, for comparison, we show the q^2 distributions of these decays by considering the benchmark values of the Wilson coefficients of the operators $\mathcal{Q}_{\phi q}$, \mathcal{Q}_{dHX} and \mathcal{Q}_{dHX^2} , although they are already excluded by the $B^0 \rightarrow K^{*0} + \text{inv}$ bound.

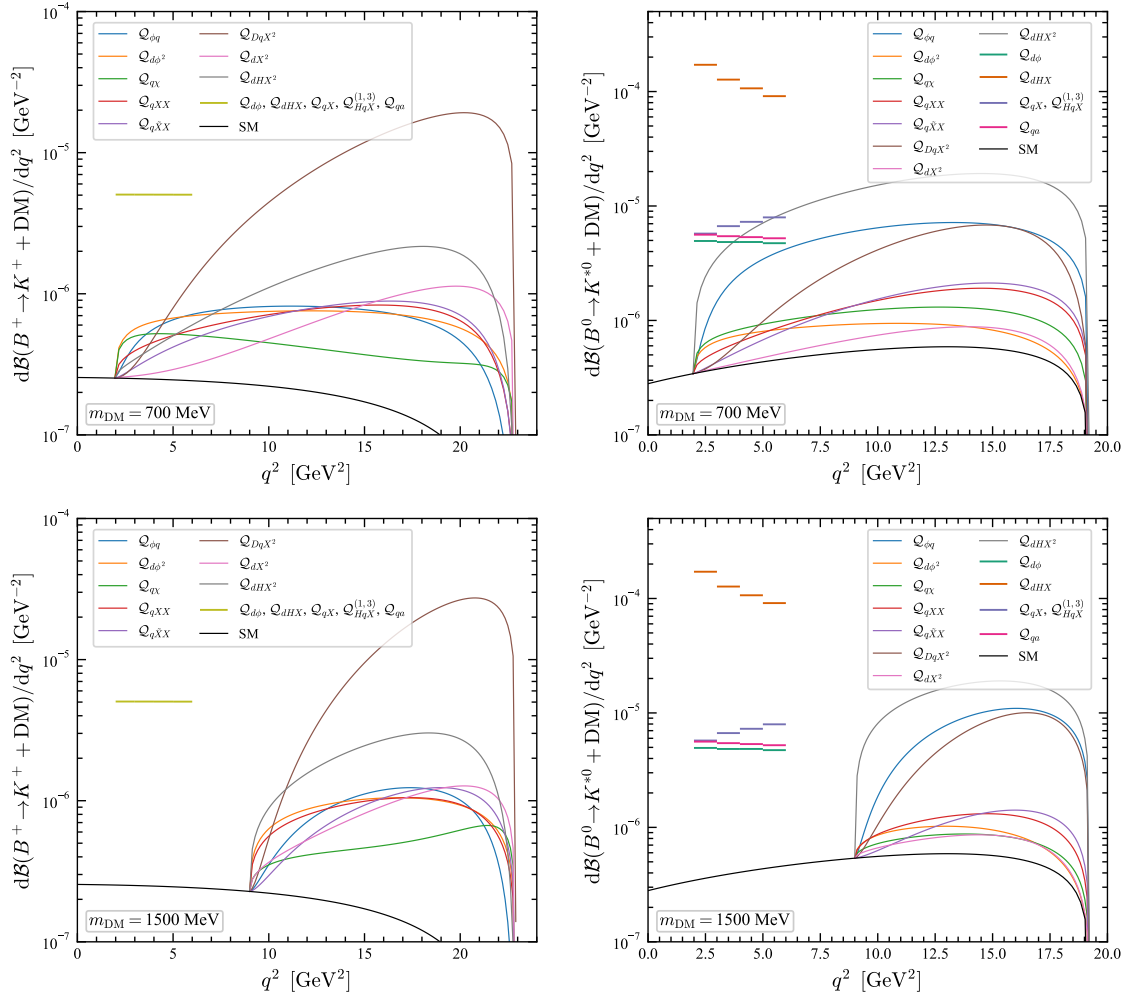


Figure 12: Differential branching ratios of the $B^+ \rightarrow K^+ + \text{inv}$ and $B^0 \rightarrow K^{*0} + \text{inv}$ decays both within the SM and in the DSMEFT with MFV hypothesis. For each effective operator, the DM mass is chosen either as 700 MeV or 1500 MeV, and the MFV parameters are fixed at the corresponding benchmark points shown in figures 7–11. For the operators involving one DM field, $m_{\text{DM}} = 1.7, 2.0, 2.2$ and 2.4 GeV are chosen and the corresponding averaged branching ratios in the $[2, 3], [3, 4], [4, 5]$ and $[5, 6]$ GeV² bins are shown, respectively.

in the bins $2 \leq q^2 \leq 7$ GeV², although the uncertainties are still quite large. From the predictions shown in figure 12, one can see that the q^2 distribution resulting from the operator $\mathcal{Q}_{q\chi}$ with $m_\chi = 700$ MeV can closely match that of the Belle II excess. As another possibility, the two-body decay with a DM mass around 2 GeV could also contribute to the observed distribution. In this case, the DSMEFT operators involving one DM field become relevant, and there are 6 such operators in the MFV hypothesis, i.e., $\mathcal{Q}_{d\phi}, \mathcal{Q}_{qa}, \mathcal{Q}_{dHX}, \mathcal{Q}_{qX}$ and $\mathcal{Q}_{HqX}^{(1,3)}$. In order to study the possible excesses in the $[2, 3], [3, 4], [4, 5]$ and $[5, 6]$ GeV² bins, we choose $m_{\text{DM}} = 1.7, 2.0,$

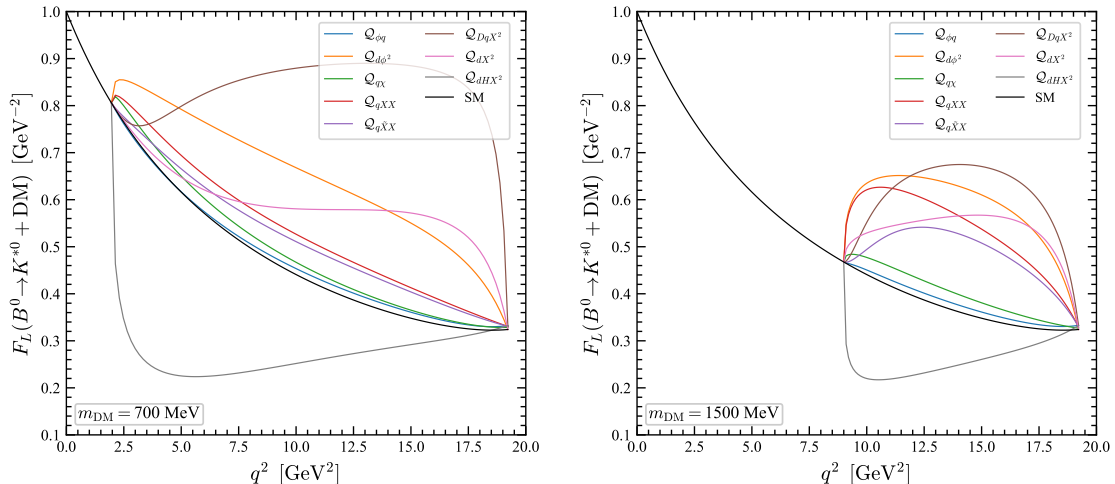


Figure 13: Longitudinal polarization fraction of the $B^0 \rightarrow K^{*0} + \text{inv}$ decay both within the SM and in the DSMEFT with MFV hypothesis. The benchmark points used in this figure are the same as the ones in figure 12.

2.2 and 2.4 GeV as benchmarks, respectively. For the MFV couplings of these 6 operators, we choose the minimal values allowed by all the experimental constraints, as done for the operators involving two DM fields. By using these benchmark points, we also show in figure 12 the bin-averaged branching ratios of the $B^+ \rightarrow K^+ + \text{inv}$ and $B^0 \rightarrow K^{*0} + \text{inv}$ decays. Since the minimal values allowed by the Belle II measurement are chosen, the distributions resulting from these operators are the same for the $B^+ \rightarrow K^+ + \text{inv}$ decay spectrum. The resulting $B^0 \rightarrow K^{*0} + \text{inv}$ decay spectra are, however, distinguishable from each other for the operators \mathcal{Q}_{dHX} , \mathcal{Q}_{qa} and $\mathcal{Q}_{d\phi}$. They can also be distinguished from that resulting from the operators \mathcal{Q}_{qX} and $\mathcal{Q}_{HqX}^{(1,3)}$, which have the same distribution. As the two-body decay kinematics is quite different from that of the three-body decay, a dedicated statistical analysis can provide more insightful information, for which we refer to ref. [23] for a recent study.

For the $B \rightarrow K^* + \text{inv}$ decays, the polarization of the K^* meson can be extracted via an angular analysis of its decay products. This virtue allows us to define an additional observable, the longitudinal polarization fraction $F_L \equiv (d\Gamma_L/dq^2)/(d\Gamma/dq^2)$, where $d\Gamma_L$ denotes the differential decay width with a longitudinally polarized K^* . By using the same benchmark points used to investigate the branching ratios in figure 12, our predictions for the longitudinal polarization fraction of the $B^0 \rightarrow K^{*0} + \text{inv}$ decay are shown in figure 13. Comparing figures 12 and 13, we can see that the longitudinal polarization fraction is complementary to the branching ratio and can, therefore, serve as an additional observable to distinguish the various DSMEFT operators. For example, in the case of $m_{\text{DM}} = 1500$ MeV, the operators \mathcal{Q}_{qX} and \mathcal{Q}_{dX^2} , while predicting quite similar $B^0 \rightarrow K^* + \text{inv}$ decay spectra, result in quite different F_L . However, in the case of $m_{\text{DM}} = 700$ MeV, the operators \mathcal{Q}_{qXX} and $\mathcal{Q}_{q\bar{X}X}$, which

are the remaining indistinguishable operators by combine the $B^+ \rightarrow K^+ + \text{inv}$ and $B^0 \rightarrow K^* + \text{inv}$ decay spectra, show at most around 5% difference in F_L .

From figures 7-11, we can see that the benchmark points actually correspond to the minimal allowed parameter values required to explain the $B^+ \rightarrow K^+ + \text{inv}$ excess. They are irrelevant to the $b \rightarrow d + \text{inv}$ and $s \rightarrow d + \text{inv}$ decays. Therefore, the predicted branching ratios and longitudinal polarization fractions of the $B^+ \rightarrow K^+ + \text{inv}$ and $B^0 \rightarrow K^{*0} + \text{inv}$ decays in figures 12 and 13 can also be applied to the general DSMEFT case discussed in the last subsection.

6 Conclusion

The recent Belle II measurement of $\mathcal{B}(B^+ \rightarrow K^+ \nu \bar{\nu})$ is about 2.7σ higher than the SM prediction. In this work, we have deciphered the data with two different NP scenarios: the underlying quark-level $b \rightarrow s \nu \bar{\nu}$ transition is, besides the SM contribution, further affected by some heavy new mediators that are much heavier than the electroweak scale, or amended by an additional decay channel with light new final states that are sufficiently long-lived to escape the detector and appear as missing-energy signals. To make our analyses model-independent as much as possible, we have studied these two scenarios in the SMEFT and the DSMEFT framework, respectively. Furthermore, the flavour structures of the resulting effective operators are taken to be either of the most generic form or satisfy the MFV hypothesis, both for the quark and lepton sectors.

In the first scenario, we have focused on the implications of the MFV hypothesis. It is found that, once the MFV hypothesis is assumed for the quark sector while without any assumption on the lepton sector, only one SM-like low-energy effective operator $\mathcal{O}_L^{\nu_i \nu_j}$ can be induced by the SMEFT dim-6 operators. As a consequence, the ratio of the branching fractions of any two $b \rightarrow s \nu \bar{\nu}$ decays remains a constant, which can be used to test the MFV hypothesis. In particular, the resulting ratio $\mathcal{B}(B^+ \rightarrow K^+ \nu \bar{\nu})_{\text{MFV}} / \mathcal{B}(B^0 \rightarrow K^{*0} \nu \bar{\nu})_{\text{MFV}} = 0.46 \pm 0.07$ is inconsistent with the current 90% CL lower limit 0.70 derived by combining the recent Belle II measurement of $\mathcal{B}(B^+ \rightarrow K^+ \nu \bar{\nu})$ and the Belle upper bound on $\mathcal{B}(B^0 \rightarrow K^{*0} \nu \bar{\nu})$. Thus, the Belle II excess cannot be explained in the SMEFT with MFV hypothesis for the quark sector. Such a conclusion is true irrespective of the flavour structure of the lepton sector. As the uncertainty of the Belle II measurement of $\mathcal{B}(B^+ \rightarrow K^+ \nu \bar{\nu})$ is still quite large, we have also used all the relevant processes but without the $B^+ \rightarrow K^+ \nu \bar{\nu}$ decay to constrain the parameter space of the MFV parameters, and then predicted that $\mathcal{B}(B^+ \rightarrow K^+ \nu \bar{\nu})_{\text{MFV}} < 10.5 \times 10^{-6}$ and $3.5 < \mathcal{B}(B^+ \rightarrow K^+ \nu \bar{\nu})_{\text{MFV}} < 5.0 \times 10^{-6}$, which correspond to the cases without and with the leptonic MFV, respectively. These predictions can be further tested at the Belle II with more statistics.

In the second scenario, it is found that the Belle II excess can be accommodated by 22 DSMEFT operators with $\text{dim} \leq 6$, which include 4 operators involving scalar,

2 operators involving fermionic, 14 operators involving vector DM, as well as 2 operators involving ALP. For each operator, the current experimental constraints on the corresponding Wilson coefficient and DM (ALP) mass are derived. For most of these operators, large parts of the parameter spaces required to account for the $B^+ \rightarrow K^+ + \text{inv}$ excess are excluded by the $B^0 \rightarrow K^{*0} + \text{inv}$ and $B_s \rightarrow \text{inv}$ decays. Nevertheless, none of the operators is fully excluded by the current data. The future Belle II (5 ab^{-1}), CEPC and FCC-ee (Tera- Z phase) data on $B_s \rightarrow \phi + \text{inv}$ and $B_s \rightarrow \text{inv}$ decays are, however, expected to cover almost all the parameter spaces needed for explaining the Belle II excess. Furthermore, the $B^0 \rightarrow K^0 + \text{inv}$ decay can provide an independent probe of the NP mechanism proposed for the Belle II excess. Once the MFV hypothesis is assumed, 8 out of the 22 viable DSMEFT operators do not induce the down-type FCNC interactions, and hence cannot account for the Belle II excess. For the remaining 14 operators, their MFV couplings make the $b \rightarrow d$ and $s \rightarrow d$ processes also relevant. For $\mathcal{Q}_{d\phi}$, \mathcal{Q}_{qa} , \mathcal{Q}_{qX} and $\mathcal{Q}_{HqX}^{(1,3)}$, which all involve one DM field, the $K^+ \rightarrow \pi^+ + \text{inv}$ decay provides the strongest constraint in the low-mass region $m_{\text{DM}} \lesssim m_K - m_\pi$. For \mathcal{Q}_{qX} , \mathcal{Q}_{dHX} , \mathcal{Q}_{qX} , $\mathcal{Q}_{HqX}^{(1,3)}$ and \mathcal{Q}_{dHX^2} , especially for the ones (e.g., \mathcal{Q}_{dHX^2}) that make no contribution to the $B_s \rightarrow \text{inv}$ decay, the $B^+ \rightarrow \pi^+ + \text{inv}$ decay puts the most stringent bound in the high-mass region. In addition, the $\Upsilon(1S) \rightarrow \text{inv}$ decay provides the strongest constraint in the high-mass region for the operator $\mathcal{Q}_{\phi q}$ with $m_{\phi_2} - m_{\phi_1} < 200 \text{ MeV}$. Within the parameter space allowed by all the current experimental data, the differential branching ratios (as well as the longitudinal polarization fractions) of the $B \rightarrow K^{(*)} + \text{inv}$ decays are then studied for each viable operator. We find that the resulting prediction of the operator $\mathcal{Q}_{qX} = (\bar{q}_p \gamma_\mu q_r)(\bar{\chi} \gamma^\mu \chi)$ with a fermionic dark matter mass $m_\chi \approx 700 \text{ MeV}$ can closely match the Belle II event distribution in the bins $2 \leq q^2 \leq 7 \text{ GeV}^2$. Our numerical results also show that the longitudinal polarization fractions are complementary to the branching ratios. By combining them, all the DSMEFT operators are distinguishable from each other, except the operators \mathcal{Q}_{qXX} and $\mathcal{Q}_{q\tilde{X}X}$ in the case of $m_X = 700 \text{ MeV}$.

At the Belle II with 5 ab^{-1} dataset, the branching ratio $\mathcal{B}(B^+ \rightarrow K^+ + \text{inv})$ is expected to be measured with an uncertainty of 19%. If the central value of the current Belle II measurement remains unchanged but the uncertainty is reduced accordingly in the future, the discrepancy from the SM prediction will increase to 4σ level. At the same time, in the future, the $B^0 \rightarrow K^0 + \text{inv}$, $B^0 \rightarrow K^{*0} + \text{inv}$, $B^+ \rightarrow \pi^+ + \text{inv}$, $B^+ \rightarrow \rho^+ + \text{inv}$ and $B_s \rightarrow \text{inv}$ decays at Belle II [12, 13], the $B_s \rightarrow \phi + \text{inv}$ at CEPC [128] and FCC-ee [132] as well as the $K \rightarrow \pi + \text{inv}$ at NA62 [137] and KOTO [138], are all expected to provide complementary information about the (D)SMEFT operators as well as the validity of the MFV hypothesis studied here.

The new singlets introduced in the DSMEFT could be the DM candidates in the universe. In this case, the parameter space derived in our work could be further

constrained by cosmological observations, such as the DM relic density and the Big Bang nucleosynthesis, as well as the DM direct detection [139–143]. For the operators involving one new particle, their couplings should also suffer from additional constraints to ensure that the particle is sufficiently long-lived to escape the detector. In addition, the DM FCNC couplings can affect the neutral-meson mixings, such as $B_s - \bar{B}_s$ mixing [120, 121]. At the LHC, the large couplings of the new singlets to the third generation in MFV can lead to the DM production associated with top and bottom quarks [144]. However, a complete and dedicated study of all these constraints should go beyond the EFT framework and specific UV completions are needed. Therefore, we leave these explorations for our future work.

Acknowledgments

This work is supported by the National Natural Science Foundation of China under Grant Nos. 12135006, 12075097 and 11805077, as well as by the Fundamental Research Funds for the Central Universities under Grant No. CCNU22LJ004. XY is also supported in part by the Startup Research Funding from CCNU.

A Hadronic matrix elements

For the B -meson and kaon decays discussed in sections 3 and 4, as well as the invisible decays of charmoniums and bottomoniums, we need the hadronic matrix elements between the vacuum and the initial hadronic states or between the initial and the final hadronic state, which can be parameterized by the decay constants or by the transition form factors. For convenience, they are recapitulated in appendices A.1 and A.2, respectively. The matrix elements of other bilinear quark currents not mentioned explicitly are zero due to parity invariance of strong interaction.

A.1 Decay constants

For the B_q meson ($q = u, d$), the non-vanishing annihilation matrix elements are defined as

$$\langle 0 | \bar{q} \gamma_\mu \gamma_5 b | \bar{B}_q(p) \rangle = i f_{B_q} p_\mu, \quad \langle 0 | \bar{q} \gamma_5 b | \bar{B}_q(p) \rangle = -i \frac{m_{B_q}^2}{\bar{m}_q(\mu) + \bar{m}_b(\mu)} f_{B_q}, \quad (\text{A.1})$$

with $\bar{m}_b(\mu)$ and $\bar{m}_q(\mu)$ denoting the b - and q -quark running masses at the scale μ defined in the $\overline{\text{MS}}$ scheme. Here f_{B_q} denote the B_q -meson decay constants, and their up-to-date Lattice QCD values can be found in ref. [145] and references therein. For the vector quarkonium V (such as Υ and J/ψ), the relevant hadronic matrix elements are given by [146, 147]

$$\langle 0 | \bar{q} \gamma^\mu q | V(p, \varepsilon) \rangle = f_V m_V \varepsilon^\mu,$$

$$\langle 0 | \bar{q} \sigma^{\mu\nu} q | V(p, \varepsilon) \rangle = i f_V^T(\mu) (\varepsilon^\mu p^\nu - \varepsilon^\nu p^\mu), \quad (\text{A.2})$$

where ε^μ denotes the polarization vector of the vector quarkonium, and $f_V^{(T)}$ is the decay constant. The matrix element of the axial-tensor current can be related to that of the tensor current, while the ones of all the other currents are zero. In the numerical analysis, we use the values of f_Υ in ref. [147], $f_{J/\psi}$ in ref. [148], and $f_V^T(2 \text{ GeV})/f_V$ in ref. [149].

A.2 Transition form factors

The transition form factors for a B meson decaying into a pseudoscalar meson P (e.g., $B \rightarrow K$) are defined by [150, 151]

$$\begin{aligned} c_P \langle P(p') | \bar{q} \gamma^\mu b | \bar{B}(p) \rangle &= f_+(q^2) \left(P^\mu - \frac{m_B^2 - m_P^2}{q^2} q^\mu \right) + f_0(q^2) \frac{m_B^2 - m_P^2}{q^2} q^\mu, \\ c_P \langle P(p') | \bar{q} b | \bar{B}(p) \rangle &= \frac{m_B^2 - m_P^2}{\bar{m}_b(\mu) - \bar{m}_q(\mu)} f_0(q^2), \\ c_P \langle P(p') | \bar{q} \sigma^{\mu\nu} b(p) | \bar{B}(p) \rangle &= i \frac{P^\mu q^\nu - P^\nu q^\mu}{m_B + m_P} f_T(q^2), \end{aligned} \quad (\text{A.3})$$

where $q = p - p'$, $P = p + p'$, and $c_P = -\sqrt{2}$ for π^0 and $c_P = 1$ otherwise. For a B meson decaying into a vector meson V , the relevant transition form factors are introduced by the following Lorentz decompositions of the bilinear quark current matrix elements [150, 152]:

$$\begin{aligned} c_V \langle V(p', \varepsilon^*) | \bar{q} \gamma_\mu b | \bar{B}(p) \rangle &= -\epsilon_{\mu\nu\rho\sigma} \varepsilon^{*\nu} P^\rho q^\sigma \frac{V(q^2)}{m_B + m_V}, \\ c_V \langle V(p', \varepsilon^*) | \bar{q} \gamma^\mu \gamma^5 b | \bar{B}(p) \rangle &= i \varepsilon^{*\mu} (m_B + m_V) A_1(q^2) - i P^\mu \frac{\varepsilon^* \cdot q}{m_B + m_V} A_2(q^2) \\ &\quad - i q^\mu (\varepsilon^* \cdot q) \frac{2m_V}{q^2} [A_3(q^2) - A_0(q^2)], \\ c_V \langle V(p', \varepsilon^*) | \bar{q} \gamma^5 b | \bar{B}(p) \rangle &= -2i \frac{m_V}{\bar{m}_b(\mu) + \bar{m}_q(\mu)} (\varepsilon^* \cdot q) A_0(q^2), \\ c_V \langle V(p', \varepsilon^*) | \bar{q} \sigma_{\mu\nu} q^\nu b | \bar{B}(p) \rangle &= -i \epsilon_{\mu\nu\rho\sigma} \varepsilon^{*\nu} P^\rho q^\sigma T_1(q^2), \\ c_V \langle V(p', \varepsilon^*) | \bar{q} \sigma_{\mu\nu} q^\nu \gamma^5 b | \bar{B}(p) \rangle &= [(m_B^2 - m_V^2) \varepsilon_\mu^* - (\varepsilon^* \cdot q) P_\mu] T_2(q^2) \\ &\quad + (\varepsilon^* \cdot q) \left(q_\mu - \frac{q^2}{m_B^2 - m_V^2} P_\mu \right) T_3(q^2), \end{aligned} \quad (\text{A.4})$$

where ε denotes the polarization vector of the vector meson, and $c_V = -\sqrt{2}$ for ρ^0 and $c_V = 1$ otherwise. We adopt the convention $\epsilon^{0123} = +1$ and $\sigma_{\mu\nu} = i/2 [\gamma_\mu, \gamma_\nu]$. With the above parameterizations, the absence of dynamical singularities at $q^2 = 0$ implies that $f_+(0) = f_0(0)$ and $A_0(0) = A_3(0)$. In addition, the algebraic relation

between $\sigma_{\mu\nu}$ and $\sigma_{\mu\nu}\gamma_5$, $\sigma_{\mu\nu}\gamma_5 = i/2\epsilon_{\mu\nu\alpha\beta}\sigma^{\alpha\beta}$, gives rise to the identity $T_1(0) = T_2(0)$. It is also noted that the form factor A_3 is redundant and can be written as a linear combination of A_1 and A_2 [152]

$$A_3(q^2) = \frac{(m_B + m_V)}{2m_V}A_1(q^2) - \frac{m_B - m_V}{2m_V}A_2(q^2). \quad (\text{A.5})$$

The hadronic matrix elements of the tensor and axial-tensor currents can also be decomposed as [153]

$$\begin{aligned} c_V \langle V(p', \varepsilon^*) | \bar{q} \sigma^{\mu\nu} b | \bar{B}(p) \rangle &= i\epsilon_{\mu\nu\rho\sigma} \left[P^\rho \varepsilon^{*\sigma} - \frac{m_B^2 - m_V^2}{q^2} q^\rho \varepsilon^{*\sigma} + \frac{\varepsilon^* \cdot q}{q^2} q^\rho P^\sigma \right] T_1(q^2) \\ &\quad + i\epsilon_{\mu\nu\rho\sigma} \left[\frac{m_B^2 - m_V^2}{q^2} q^\rho \varepsilon^{*\sigma} + \frac{\varepsilon^* \cdot q}{q^2} P^\rho q^\sigma \right] T_2(q^2) \\ &\quad + i\epsilon_{\mu\nu\rho\sigma} \frac{\varepsilon^* \cdot q}{m_B^2 - m_V^2} P^\rho q^\sigma T_3(q^2), \\ c_V \langle V(p', \varepsilon^*) | \bar{q} \sigma^{\mu\nu} \gamma_5 b | \bar{B}(p) \rangle &= \left[(\varepsilon^{*\mu} P^\nu - P^\mu \varepsilon^{*\nu}) + \frac{m_B^2 - m_V^2}{q^2} (q^\mu \varepsilon^{*\nu} - \varepsilon^{*\mu} q^\nu) \right. \\ &\quad \left. + \frac{\varepsilon^* \cdot q}{q^2} (P^\mu q^\nu - q^\mu P^\nu) \right] T_1(q^2) \\ &\quad + \left[\frac{m_B^2 - m_V^2}{q^2} (\varepsilon^{*\mu} q^\nu - q^\mu \varepsilon^{*\nu}) + \frac{\varepsilon^* \cdot q}{q^2} (q^\mu P^\nu - P^\mu q^\nu) \right] T_2(q^2) \\ &\quad + \frac{\varepsilon^* \cdot q}{m_B^2 - m_V^2} (q^\mu P^\nu - P^\mu q^\nu) T_3(q^2), \end{aligned} \quad (\text{A.6})$$

from which the forms given in eq. (A.4) can be obtained by multiplying both sides by q_ν . All the $B_s \rightarrow P$ (V) and $K \rightarrow \pi$ form factors can be defined similarly.

Numerically, we use the values obtained in ref. [151] for the $B \rightarrow P$ and in ref. [152] for the $B \rightarrow V$ transition form factors. As the Lattice QCD results are still not available for all of these form factors, especially for the tensor ones (see ref. [145] and references therein), we use instead the calculations based on the light-cone sum rule approach [151, 152]. For the $K \rightarrow \pi$ vector and scalar form factors, the results obtained in refs. [154, 155] are adopted, while the value in ref. [156] is used for the $K \rightarrow \pi$ tensor form factor.

For the operator \mathcal{Q}_{DdX^2} defined in eq. (4.5), the relevant form factors are not available in the literature so far. However, when the Wilson coefficient \mathcal{C}_{DdX^2} is assumed to be hermitian, they can be derived from the above form factors. Taking the $\bar{B} \rightarrow \bar{K}^0$ transition as an example, we have the relation $\langle \bar{K}^0(p') | (\partial^\mu \bar{s}) \gamma^\nu P_L b + \bar{s} \gamma^\nu P_L (\partial^\mu b) | \bar{B}(p) \rangle = -iq^\mu \langle \bar{K}^0(p') | \bar{s} \gamma^\nu P_L b | \bar{B}(p) \rangle$.

References

- [1] S. L. Glashow, J. Iliopoulos, and L. Maiani, *Weak Interactions with Lepton-Hadron Symmetry*, *Phys. Rev. D* **2** (1970) 1285–1292.

- [2] W. Altmannshofer, A. J. Buras, D. M. Straub, and M. Wick, *New strategies for New Physics search in $B \rightarrow K^{*\nu\bar{\nu}}$, $B \rightarrow K\nu\bar{\nu}$ and $B \rightarrow X_s\nu\bar{\nu}$ decays*, *JHEP* **04** (2009) 022, [[arXiv:0902.0160](#)].
- [3] A. J. Buras, J. Girrbach-Noe, C. Niehoff, and D. M. Straub, *$B \rightarrow K^{(*)}\nu\bar{\nu}$ decays in the Standard Model and beyond*, *JHEP* **02** (2015) 184, [[arXiv:1409.4557](#)].
- [4] D. Bećirević, G. Piazza, and O. Sumensari, *Revisiting $B \rightarrow K^{(*)}\nu\bar{\nu}$ decays in the Standard Model and beyond*, *Eur. Phys. J. C* **83** (2023), no. 3 252, [[arXiv:2301.06990](#)].
- [5] T. Felkl, S. L. Li, and M. A. Schmidt, *A tale of invisibility: constraints on new physics in $b \rightarrow s\nu\nu$* , *JHEP* **12** (2021) 118, [[arXiv:2111.04327](#)].
- [6] R. Bause, H. Gisbert, M. Golz, and G. Hiller, *Interplay of dineutrino modes with semileptonic rare B -decays*, *JHEP* **12** (2021) 061, [[arXiv:2109.01675](#)].
- [7] X. G. He and G. Valencia, *$R_{K^{(*)}}^\nu$ and non-standard neutrino interactions*, *Phys. Lett. B* **821** (2021) 136607, [[arXiv:2108.05033](#)].
- [8] T. E. Browder, N. G. Deshpande, R. Mandal, and R. Sinha, *Impact of $B \rightarrow K\nu\bar{\nu}$ measurements on beyond the Standard Model theories*, *Phys. Rev. D* **104** (2021), no. 5 053007, [[arXiv:2107.01080](#)].
- [9] C.-H. Chen, C.-W. Chiang, and C.-W. Su, *Compatibility of $CE\nu NS$ with muon $g-2$, W mass, and $R(D^{(*)})$ in a gauged $L_\mu - L_\tau$ with a scalar LQ* , [[arXiv:2305.09256](#)].
- [10] C.-H. Chen and C.-W. Chiang, *Flavor anomalies in leptoquark model with gauged $U(1)_{L_\mu - L_\tau}$* , [[arXiv:2309.12904](#)].
- [11] **Belle-II** Collaboration, I. Adachi et al., *Evidence for $B^+ \rightarrow K^+\nu\bar{\nu}$ Decays*, [[arXiv:2311.14647](#)].
- [12] **Belle-II** Collaboration, W. Altmannshofer et al., *The Belle II Physics Book*, *PTEP* **2019** (2019), no. 12 123C01, [[arXiv:1808.10567](#)]. [Erratum: *PTEP* 2020, 029201 (2020)].
- [13] **Belle-II** Collaboration, L. Aggarwal et al., *Snowmass White Paper: Belle II physics reach and plans for the next decade and beyond*, [[arXiv:2207.06307](#)].
- [14] P. Athron, R. Martinez, and C. Sierra, *B meson anomalies and large $B^+ \rightarrow K^+\nu\bar{\nu}$ in non-universal $U(1)'$ models*, [[arXiv:2308.13426](#)].
- [15] R. Bause, H. Gisbert, and G. Hiller, *Implications of an enhanced $B \rightarrow K\nu\bar{\nu}$ branching ratio*, *Phys. Rev. D* **109** (2024), no. 1 015006, [[arXiv:2309.00075](#)].
- [16] L. Allwicher, D. Bećirevic, G. Piazza, S. Rosauero-Alcaraz, and O. Sumensari, *Understanding the first measurement of $\mathcal{B}(B \rightarrow K\nu\bar{\nu})$* , *Phys. Lett. B* **848** (2024) 138411, [[arXiv:2309.02246](#)].
- [17] T. Felkl, A. Giri, R. Mohanta, and M. A. Schmidt, *When energy goes missing: new*

- physics in $b \rightarrow s\nu\nu$ with sterile neutrinos, *Eur. Phys. J. C* **83** (2023), no. 12 1135, [[arXiv:2309.02940](#)].
- [18] M. Abdughani and Y. Reyimuaji, *Constraining light dark matter and mediator with $B^+ \rightarrow K^+\nu\bar{\nu}$ data*, [arXiv:2309.03706](#).
- [19] H. K. Dreiner, J. Y. Günther, and Z. S. Wang, *The Decay $B \rightarrow K\nu\bar{\nu}$ at Belle II and a Massless Bino in R-parity-violating Supersymmetry*, [arXiv:2309.03727](#).
- [20] X.-G. He, X.-D. Ma, and G. Valencia, *Revisiting models that enhance $B^+ \rightarrow K^+\nu\bar{\nu}$ in light of the new Belle II measurement*, [arXiv:2309.12741](#).
- [21] A. Berezhnoy and D. Melikhov, *$B \rightarrow K^*M_X$ vs $B \rightarrow KM_X$ as a probe of a scalar-mediator dark matter scenario*, *EPL* **145** (2024), no. 1 14001, [[arXiv:2309.17191](#)].
- [22] A. Datta, D. Marfatia, and L. Mukherjee, *$B \rightarrow K\nu\bar{\nu}$, MiniBooNE and muon $g-2$ anomalies from a dark sector*, *Phys. Rev. D* **109** (2024), no. 3 L031701, [[arXiv:2310.15136](#)].
- [23] W. Altmannshofer, A. Crivellin, H. Haigh, G. Inguglia, and J. Martin Camalich, *Light New Physics in $B \rightarrow K^{(*)}\nu\bar{\nu}$?*, [arXiv:2311.14629](#).
- [24] D. McKeen, J. N. Ng, and D. Tuckler, *Higgs Portal Interpretation of the Belle II $B^+ \rightarrow K^+\nu\nu$ Measurement*, [arXiv:2312.00982](#).
- [25] K. Fridell, M. Ghosh, T. Okui, and K. Tobioka, *Decoding the $B \rightarrow K\nu\nu$ excess at Belle II: kinematics, operators, and masses*, [arXiv:2312.12507](#).
- [26] S.-Y. Ho, J. Kim, and P. Ko, *Recent $B^+ \rightarrow K^+\nu\bar{\nu}$ Excess and Muon $g-2$ Illuminating Light Dark Sector with Higgs Portal*, [arXiv:2401.10112](#).
- [27] F.-Z. Chen, Q. Wen, and F. Xu, *Correlating $B \rightarrow K^{(*)}\nu\bar{\nu}$ and flavor anomalies in SMEFT*, [arXiv:2401.11552](#).
- [28] E. Gabrielli, L. Marzola, K. Müirsepp, and M. Raidal, *Explaining the $B^+ \rightarrow K^+\nu\bar{\nu}$ excess via a massless dark photon*, [arXiv:2402.05901](#).
- [29] T. Li, Z. Qian, M. A. Schmidt, and M. Yuan, *The quark flavor-violating ALPs in light of B mesons and hadron colliders*, [arXiv:2402.14232](#).
- [30] C.-H. Chen and C.-W. Chiang, *Rare B and K decays in a scotogenic model*, [arXiv:2403.02897](#).
- [31] **Particle Data Group** Collaboration, R. L. Workman et al., *Review of Particle Physics*, *PTEP* **2022** (2022) 083C01. and 2023 update.
- [32] G. Alonso-Álvarez and M. Escudero, *The first limit on invisible decays of B_s mesons comes from LEP*, [arXiv:2310.13043](#).
- [33] I. Brivio and M. Trott, *The Standard Model as an Effective Field Theory*, *Phys. Rept.* **793** (2019) 1–98, [[arXiv:1706.08945](#)].
- [34] G. Isidori, F. Wilsch, and D. Wyler, *The Standard Model effective field theory at work*, [arXiv:2303.16922](#).

- [35] G. Buchalla, A. J. Buras, and M. E. Lautenbacher, *Weak decays beyond leading logarithms*, *Rev. Mod. Phys.* **68** (1996) 1125–1144, [[hep-ph/9512380](#)].
- [36] E. E. Jenkins, A. V. Manohar, and P. Stoffer, *Low-Energy Effective Field Theory below the Electroweak Scale: Operators and Matching*, *JHEP* **03** (2018) 016, [[arXiv:1709.04486](#)].
- [37] W. Dekens and P. Stoffer, *Low-energy effective field theory below the electroweak scale: matching at one loop*, *JHEP* **10** (2019) 197, [[arXiv:1908.05295](#)]. [Erratum: *JHEP* **11**, 148 (2022)].
- [38] J. Aebischer, A. Crivellin, M. Fael, and C. Greub, *Matching of gauge invariant dimension-six operators for $b \rightarrow s$ and $b \rightarrow c$ transitions*, *JHEP* **05** (2016) 037, [[arXiv:1512.02830](#)].
- [39] E. Del Nobile and F. Sannino, *Dark Matter Effective Theory*, *Int. J. Mod. Phys. A* **27** (2012) 1250065, [[arXiv:1102.3116](#)].
- [40] M. Baumgart et al., *Snowmass White Paper: Effective Field Theories for Dark Matter Phenomenology*, [arXiv:2203.08204](#).
- [41] M. Duch, B. Grzadkowski, and J. Wudka, *Classification of effective operators for interactions between the Standard Model and dark matter*, *JHEP* **05** (2015) 116, [[arXiv:1412.0520](#)].
- [42] J. F. Kamenik and C. Smith, *FCNC portals to the dark sector*, *JHEP* **03** (2012) 090, [[arXiv:1111.6402](#)].
- [43] J. Brod, A. Gootjes-Dreesbach, M. Tamaro, and J. Zupan, *Effective Field Theory for Dark Matter Direct Detection up to Dimension Seven*, *JHEP* **10** (2018) 065, [[arXiv:1710.10218](#)]. [Erratum: *JHEP* **07**, 012 (2023)].
- [44] J. C. Criado, A. Djouadi, M. Perez-Victoria, and J. Santiago, *A complete effective field theory for dark matter*, *JHEP* **07** (2021) 081, [[arXiv:2104.14443](#)].
- [45] J. Aebischer, W. Altmannshofer, E. E. Jenkins, and A. V. Manohar, *Dark matter effective field theory and an application to vector dark matter*, *JHEP* **06** (2022) 086, [[arXiv:2202.06968](#)].
- [46] H. Song, H. Sun, and J.-H. Yu, *Complete EFT Operator Bases for Dark Matter and Weakly-Interacting Light Particle*, [arXiv:2306.05999](#).
- [47] X.-G. He, X.-D. Ma, and G. Valencia, *FCNC B and K meson decays with light bosonic Dark Matter*, *JHEP* **03** (2023) 037, [[arXiv:2209.05223](#)].
- [48] J.-H. Liang, Y. Liao, X.-D. Ma, and H.-L. Wang, *Dark sector effective field theory*, *JHEP* **12** (2023) 172, [[arXiv:2309.12166](#)].
- [49] R. D. Peccei and H. R. Quinn, *CP Conservation in the Presence of Instantons*, *Phys. Rev. Lett.* **38** (1977) 1440–1443.
- [50] R. D. Peccei and H. R. Quinn, *Constraints Imposed by CP Conservation in the Presence of Instantons*, *Phys. Rev. D* **16** (1977) 1791–1797.

- [51] S. Weinberg, *A New Light Boson?*, *Phys. Rev. Lett.* **40** (1978) 223–226.
- [52] F. Wilczek, *Problem of Strong P and T Invariance in the Presence of Instantons*, *Phys. Rev. Lett.* **40** (1978) 279–282.
- [53] H. Georgi, D. B. Kaplan, and L. Randall, *Manifesting the Invisible Axion at Low-energies*, *Phys. Lett. B* **169** (1986) 73–78.
- [54] I. Brivio, M. B. Gavela, L. Merlo, K. Mimasu, J. M. No, R. del Rey, and V. Sanz, *ALPs Effective Field Theory and Collider Signatures*, *Eur. Phys. J. C* **77** (2017), no. 8 572, [[arXiv:1701.05379](#)].
- [55] M. Chala, G. Guedes, M. Ramos, and J. Santiago, *Running in the ALPs*, *Eur. Phys. J. C* **81** (2021), no. 2 181, [[arXiv:2012.09017](#)].
- [56] M. Bauer, M. Neubert, S. Renner, M. Schnubel, and A. Thamm, *The Low-Energy Effective Theory of Axions and ALPs*, *JHEP* **04** (2021) 063, [[arXiv:2012.12272](#)].
- [57] A. M. Galda, M. Neubert, and S. Renner, *ALP — SMEFT interference*, *JHEP* **06** (2021) 135, [[arXiv:2105.01078](#)].
- [58] H. Song, H. Sun, and J.-H. Yu, *Effective Field Theories of Axion, ALP and Dark Photon*, [arXiv:2305.16770](#).
- [59] G. Isidori, Y. Nir, and G. Perez, *Flavor Physics Constraints for Physics Beyond the Standard Model*, *Ann. Rev. Nucl. Part. Sci.* **60** (2010) 355, [[arXiv:1002.0900](#)].
- [60] W. Altmannshofer and J. Zupan, *Snowmass White Paper: Flavor Model Building*, in *Snowmass 2021*, 3, 2022. [arXiv:2203.07726](#).
- [61] R. S. Chivukula and H. Georgi, *Composite Technicolor Standard Model*, *Phys. Lett. B* **188** (1987) 99–104.
- [62] A. J. Buras, P. Gambino, M. Gorbahn, S. Jager, and L. Silvestrini, *Universal unitarity triangle and physics beyond the standard model*, *Phys. Lett. B* **500** (2001) 161–167, [[hep-ph/0007085](#)].
- [63] G. D’Ambrosio, G. F. Giudice, G. Isidori, and A. Strumia, *Minimal flavor violation: An Effective field theory approach*, *Nucl. Phys. B* **645** (2002) 155–187, [[hep-ph/0207036](#)].
- [64] J. M. Gerard, *FERMION MASS SPECTRUM IN $SU(2)_L \times U(1)$* , *Z. Phys. C* **18** (1983) 145.
- [65] G. Colangelo, E. Nikolidakis, and C. Smith, *Supersymmetric models with minimal flavour violation and their running*, *Eur. Phys. J. C* **59** (2009) 75–98, [[arXiv:0807.0801](#)].
- [66] L. Mercolli and C. Smith, *EDM constraints on flavored CP-violating phases*, *Nucl. Phys. B* **817** (2009) 1–24, [[arXiv:0902.1949](#)].
- [67] B. Grinstein, X. Lu, L. Merlo, and P. Quilez, *Hilbert series for covariants and their applications to Minimal Flavor Violation*, [arXiv:2312.13349](#).

- [68] X.-G. He, C.-J. Lee, S.-F. Li, and J. Tandean, *Fermion EDMs with Minimal Flavor Violation*, *JHEP* **08** (2014) 019, [[arXiv:1404.4436](#)].
- [69] X.-G. He, C.-J. Lee, S.-F. Li, and J. Tandean, *Large electron electric dipole moment in minimal flavor violation framework with Majorana neutrinos*, *Phys. Rev. D* **89** (2014), no. 9 091901, [[arXiv:1401.2615](#)].
- [70] X.-G. He, C.-J. Lee, J. Tandean, and Y.-J. Zheng, *Seesaw Models with Minimal Flavor Violation*, *Phys. Rev. D* **91** (2015), no. 7 076008, [[arXiv:1411.6612](#)].
- [71] C.-W. Chiang, X.-G. He, J. Tandean, and X.-B. Yuan, *$R_{K^{(*)}}$ and related $b \rightarrow s\ell\bar{\ell}$ anomalies in minimal flavor violation framework with Z' boson*, *Phys. Rev. D* **96** (2017), no. 11 115022, [[arXiv:1706.02696](#)].
- [72] J.-J. Zhang, M. He, X.-G. He, and X.-B. Yuan, *Flavor Violating Higgs Couplings in Minimal Flavor Violation*, *JHEP* **02** (2019) 007, [[arXiv:1807.00921](#)].
- [73] V. Cirigliano, B. Grinstein, G. Isidori, and M. B. Wise, *Minimal flavor violation in the lepton sector*, *Nucl. Phys. B* **728** (2005) 121–134, [[hep-ph/0507001](#)].
- [74] V. Cirigliano and B. Grinstein, *Phenomenology of minimal lepton flavor violation*, *Nucl. Phys. B* **752** (2006) 18–39, [[hep-ph/0601111](#)].
- [75] S. Davidson and F. Palorini, *Various definitions of Minimal Flavour Violation for Leptons*, *Phys. Lett. B* **642** (2006) 72–80, [[hep-ph/0607329](#)].
- [76] G. C. Branco, A. J. Buras, S. Jager, S. Uhlig, and A. Weiler, *Another look at minimal lepton flavour violation, $l_i \rightarrow l_j\gamma$, leptogenesis, and the ratio M_ν/Λ_{LFV}* , *JHEP* **09** (2007) 004, [[hep-ph/0609067](#)].
- [77] M. B. Gavela, T. Hambye, D. Hernandez, and P. Hernandez, *Minimal Flavour Seesaw Models*, *JHEP* **09** (2009) 038, [[arXiv:0906.1461](#)].
- [78] R. Alonso, G. Isidori, L. Merlo, L. A. Munoz, and E. Nardi, *Minimal flavour violation extensions of the seesaw*, *JHEP* **06** (2011) 037, [[arXiv:1103.5461](#)].
- [79] D. Aristizabal Sierra, A. Degee, and J. F. Kamenik, *Minimal Lepton Flavor Violating Realizations of Minimal Seesaw Models*, *JHEP* **07** (2012) 135, [[arXiv:1205.5547](#)].
- [80] B. Batell, J. Pradler, and M. Spannowsky, *Dark Matter from Minimal Flavor Violation*, *JHEP* **08** (2011) 038, [[arXiv:1105.1781](#)].
- [81] L. Lopez-Honorez and L. Merlo, *Dark matter within the minimal flavour violation ansatz*, *Phys. Lett. B* **722** (2013) 135–143, [[arXiv:1303.1087](#)].
- [82] P. Agrawal, M. Blanke, and K. Gemmler, *Flavored dark matter beyond Minimal Flavor Violation*, *JHEP* **10** (2014) 072, [[arXiv:1405.6709](#)].
- [83] M.-C. Chen, J. Huang, and V. Takhistov, *Beyond Minimal Lepton Flavored Dark Matter*, *JHEP* **02** (2016) 060, [[arXiv:1510.04694](#)].
- [84] H. Acaroğlu and M. Blanke, *Tasting flavoured Majorana dark matter*, *JHEP* **05** (2022) 086, [[arXiv:2109.10357](#)].

- [85] W. Buchmuller and D. Wyler, *Effective Lagrangian Analysis of New Interactions and Flavor Conservation*, *Nucl. Phys. B* **268** (1986) 621–653.
- [86] B. Grzadkowski, M. Iskrzynski, M. Misiak, and J. Rosiek, *Dimension-Six Terms in the Standard Model Lagrangian*, *JHEP* **10** (2010) 085, [[arXiv:1008.4884](#)].
- [87] G. Buchalla and A. J. Buras, *QCD corrections to rare K and B decays for arbitrary top quark mass*, *Nucl. Phys. B* **400** (1993) 225–239.
- [88] M. Misiak and J. Urban, *QCD corrections to FCNC decays mediated by Z penguins and W boxes*, *Phys. Lett. B* **451** (1999) 161–169, [[hep-ph/9901278](#)].
- [89] G. Buchalla and A. J. Buras, *The rare decays $K \rightarrow \pi\nu\bar{\nu}$, $B \rightarrow X\nu\bar{\nu}$ and $B \rightarrow l^+l^-$: An Update*, *Nucl. Phys. B* **548** (1999) 309–327, [[hep-ph/9901288](#)].
- [90] J. Brod, M. Gorbahn, and E. Stamou, *Two-Loop Electroweak Corrections for the $K \rightarrow \pi\nu\bar{\nu}$ Decays*, *Phys. Rev. D* **83** (2011) 034030, [[arXiv:1009.0947](#)].
- [91] P. Colangelo, F. De Fazio, P. Santorelli, and E. Scrimieri, *Rare $B \rightarrow K^{(*)}\nu\bar{\nu}$ decays at B factories*, *Phys. Lett. B* **395** (1997) 339–344, [[hep-ph/9610297](#)].
- [92] J. F. Kamenik and C. Smith, *Tree-level contributions to the rare decays $B^+ \rightarrow \pi^+\nu\bar{\nu}$, $B^+ \rightarrow K^+\nu\bar{\nu}$, and $B^+ \rightarrow K^{*+}\nu\bar{\nu}$ in the Standard Model*, *Phys. Lett. B* **680** (2009) 471–475, [[arXiv:0908.1174](#)].
- [93] D. London and J. Matias, *B Flavour Anomalies: 2021 Theoretical Status Report*, *Ann. Rev. Nucl. Part. Sci.* **72** (2022) 37–68, [[arXiv:2110.13270](#)].
- [94] B. Capdevila, A. Crivellin, and J. Matias, *Review of Semileptonic B Anomalies*, *Eur. Phys. J. ST* **1** (2023) 20, [[arXiv:2309.01311](#)].
- [95] S. S. Gershtein and M. Y. Khlopov, *SU(4) Symmetry Breaking and Lepton Decays of Heavy Pseudoscalar Mesons*, *JETP Lett.* **23** (1976) 338.
- [96] M. Y. Khlopov, *Effects of Symmetry Violation in Semileptonic Meson Decays*, *Sov. J. Nucl. Phys.* **28** (1978) 583.
- [97] A. Crivellin, L. Hofer, J. Matias, U. Nierste, S. Pokorski, and J. Rosiek, *Lepton-flavour violating B decays in generic Z' models*, *Phys. Rev. D* **92** (2015), no. 5 054013, [[arXiv:1504.07928](#)].
- [98] C.-J. Lee and J. Tandean, *Minimal lepton flavor violation implications of the $b \rightarrow s$ anomalies*, *JHEP* **08** (2015) 123, [[arXiv:1505.04692](#)].
- [99] A. J. Buras, F. Schwab, and S. Uhlig, *Waiting for precise measurements of $K^+ \rightarrow \pi^+\nu\bar{\nu}$ and $K_L \rightarrow \pi^0\nu\bar{\nu}$* , *Rev. Mod. Phys.* **80** (2008) 965–1007, [[hep-ph/0405132](#)].
- [100] F. Mescia and C. Smith, *Improved estimates of rare K decay matrix-elements from $K_{\ell 3}$ decays*, *Phys. Rev. D* **76** (2007) 034017, [[arXiv:0705.2025](#)].
- [101] V. Cirigliano, G. Ecker, H. Neufeld, A. Pich, and J. Portoles, *Kaon Decays in the Standard Model*, *Rev. Mod. Phys.* **84** (2012) 399, [[arXiv:1107.6001](#)].

- [102] A. J. Buras, D. Buttazzo, J. Girrbach-Noe, and R. Knegjens, $K^+ \rightarrow \pi^+ \nu \bar{\nu}$ and $K_L \rightarrow \pi^0 \nu \bar{\nu}$ in the Standard Model: status and perspectives, *JHEP* **11** (2015) 033, [[arXiv:1503.02693](#)].
- [103] A. J. Buras, M. Gorbahn, U. Haisch, and U. Nierste, Charm quark contribution to $K^+ \rightarrow \pi^+ \nu \bar{\nu}$ at next-to-next-to-leading order, *JHEP* **11** (2006) 002, [[hep-ph/0603079](#)]. [Erratum: *JHEP* **11**, 167 (2012)].
- [104] J. Brod and M. Gorbahn, Electroweak Corrections to the Charm Quark Contribution to $K^+ \rightarrow \pi^+ \nu \bar{\nu}$, *Phys. Rev. D* **78** (2008) 034006, [[arXiv:0805.4119](#)].
- [105] G. Isidori, F. Mescia, and C. Smith, Light-quark loops in $K \rightarrow \pi \nu \bar{\nu}$, *Nucl. Phys. B* **718** (2005) 319–338, [[hep-ph/0503107](#)].
- [106] L. S. Littenberg, The CP Violating Decay $K_L^0 \rightarrow \pi^0 \nu \bar{\nu}$, *Phys. Rev. D* **39** (1989) 3322–3324.
- [107] G. Buchalla and G. Isidori, The CP conserving contribution to $K_L \rightarrow \pi^0 \nu \bar{\nu}$ neutrino anti-neutrino in the standard model, *Phys. Lett. B* **440** (1998) 170–178, [[hep-ph/9806501](#)].
- [108] G. Buchalla and A. J. Buras, $K_L \rightarrow \pi \nu \bar{\nu}$ and high precision determinations of the CKM matrix, *Phys. Rev. D* **54** (1996) 6782–6789, [[hep-ph/9607447](#)].
- [109] W. J. Marciano and Z. Parsa, Rare kaon decays with “missing energy”, *Phys. Rev. D* **53** (1996), no. 1 R1.
- [110] M. Williams, C. P. Burgess, A. Maharana, and F. Quevedo, New Constraints (and Motivations) for Abelian Gauge Bosons in the MeV-TeV Mass Range, *JHEP* **08** (2011) 106, [[arXiv:1103.4556](#)].
- [111] E. E. Jenkins, A. V. Manohar, and P. Stoffer, Low-Energy Effective Field Theory below the Electroweak Scale: Anomalous Dimensions, *JHEP* **01** (2018) 084, [[arXiv:1711.05270](#)].
- [112] C. Bird, P. Jackson, R. V. Kowalewski, and M. Pospelov, Search for dark matter in $b \rightarrow s$ transitions with missing energy, *Phys. Rev. Lett.* **93** (2004) 201803, [[hep-ph/0401195](#)].
- [113] G. Li, J.-Y. Su, and J. Tandean, Flavor-changing hyperon decays with light invisible bosons, *Phys. Rev. D* **100** (2019), no. 7 075003, [[arXiv:1905.08759](#)].
- [114] X.-G. He, X.-D. Ma, J. Tandean, and G. Valencia, Evading the Grossman-Nir bound with $\Delta I = 3/2$ new physics, *JHEP* **08** (2020), no. 08 034, [[arXiv:2005.02942](#)].
- [115] C.-Q. Geng and J. Tandean, Probing new physics with the kaon decays $K \rightarrow \pi \pi \cancel{E}$, *Phys. Rev. D* **102** (2020) 115021, [[arXiv:2009.00608](#)].
- [116] G. Li, T. Wang, J.-B. Zhang, and G.-L. Wang, The light invisible boson in FCNC decays of B and B_c mesons, *Eur. Phys. J. C* **81** (2021), no. 6 564, [[arXiv:2103.12921](#)].

- [117] F. Kling, S. Li, H. Song, S. Su, and W. Su, *Light Scalars at FASER*, *JHEP* **08** (2023) 001, [[arXiv:2212.06186](#)].
- [118] J.-Y. Su and J. Tandean, *Exploring leptoquark effects in hyperon and kaon decays with missing energy*, *Phys. Rev. D* **102** (2020), no. 7 075032, [[arXiv:1912.13507](#)].
- [119] G. Li, T. Wang, Y. Jiang, J.-B. Zhang, and G.-L. Wang, *Spin-1/2 invisible particles in heavy meson decays*, *Phys. Rev. D* **102** (2020), no. 9 095019, [[arXiv:2004.10942](#)].
- [120] J. Martin Camalich, M. Pospelov, P. N. H. Vuong, R. Ziegler, and J. Zupan, *Quark Flavor Phenomenology of the QCD Axion*, *Phys. Rev. D* **102** (2020), no. 1 015023, [[arXiv:2002.04623](#)].
- [121] M. Bauer, M. Neubert, S. Renner, M. Schnubel, and A. Thamm, *Flavor probes of axion-like particles*, *JHEP* **09** (2022) 056, [[arXiv:2110.10698](#)].
- [122] A. W. M. Guerrero and S. Rigolin, *ALP Production in Weak Mesonic Decays*, *Fortsch. Phys.* **71** (2023), no. 2-3 2200192, [[arXiv:2211.08343](#)].
- [123] B.-F. Hou, X.-Q. Li, H. Yan, Y.-D. Yang, and X.-B. Yuan, “HadronToNP: a package to calculate decay of hadron to new particles.” in preparation.
- [124] **CKMfitter Group** Collaboration, J. Charles, A. Hocker, H. Lacker, S. Laplace, F. R. Le Diberder, J. Malcles, J. Ocariz, M. Pivk, and L. Roos, *CP violation and the CKM matrix: Assessing the impact of the asymmetric B factories*, *Eur. Phys. J. C* **41** (2005), no. 1 1–131, [[hep-ph/0406184](#)]. Updated results and plots available at: <http://ckmfitter.in2p3.fr>.
- [125] A. Glazov, “Belle II physics highlights.” plenary talk given at the EPS-HEP2023 Conference in Hamburg (Germany), 2023.
- [126] **Belle** Collaboration, J. Grygier et al., *Search for $B \rightarrow h\nu\bar{\nu}$ decays with semileptonic tagging at Belle*, *Phys. Rev. D* **96** (2017), no. 9 091101, [[arXiv:1702.03224](#)]. [Addendum: *Phys.Rev.D* 97, 099902 (2018)].
- [127] **DELPHI** Collaboration, W. Adam et al., *Study of rare b decays with the DELPHI detector at LEP*, *Z. Phys. C* **72** (1996) 207–220.
- [128] L. Li, M. Ruan, Y. Wang, and Y. Wang, *Analysis of $B_s \rightarrow \phi\nu\bar{\nu}$ at CEPC*, *Phys. Rev. D* **105** (2022), no. 11 114036, [[arXiv:2201.07374](#)].
- [129] **NA62** Collaboration, E. Cortina Gil et al., *Measurement of the very rare $K^+ \rightarrow \pi^+\nu\bar{\nu}$ decay*, *JHEP* **06** (2021) 093, [[arXiv:2103.15389](#)].
- [130] **KOTO** Collaboration, J. K. Ahn et al., *Search for the $K_L \rightarrow \pi^0\nu\bar{\nu}$ and $K_L \rightarrow \pi^0 X^0$ decays at the J-PARC KOTO experiment*, *Phys. Rev. Lett.* **122** (2019), no. 2 021802, [[arXiv:1810.09655](#)].
- [131] L. Calibbi, A. Crivellin, and T. Ota, *Effective Field Theory Approach to $b \rightarrow s\ell\ell^{(\prime)}$, $B \rightarrow K^{(*)}\nu\bar{\nu}$ and $B \rightarrow D^{(*)}\tau\nu$ with Third Generation Couplings*, *Phys. Rev. Lett.* **115** (2015) 181801, [[arXiv:1506.02661](#)].

- [132] Y. Amhis, M. Kenzie, M. Reboud, and A. R. Wiederhold, *Prospects for searches of $b \rightarrow s\nu\bar{\nu}$ decays at FCC-ee*, *JHEP* **01** (2024) 144, [[arXiv:2309.11353](#)].
- [133] **BaBar** Collaboration, B. Aubert et al., *A Search for Invisible Decays of the Upsilon(1S)*, *Phys. Rev. Lett.* **103** (2009) 251801, [[arXiv:0908.2840](#)].
- [134] L. N. Chang, O. Lebedev, and J. N. Ng, *On the invisible decays of the Upsilon and J/Ψ resonances*, *Phys. Lett. B* **441** (1998) 419–424, [[hep-ph/9806487](#)].
- [135] N. Fernandez, J. Kumar, I. Seong, and P. Stengel, *Complementary Constraints on Light Dark Matter from Heavy Quarkonium Decays*, *Phys. Rev. D* **90** (2014), no. 1 015029, [[arXiv:1404.6599](#)].
- [136] E. Bertuzzo, C. J. Caniu Barros, and G. Grilli di Cortona, *MeV Dark Matter: Model Independent Bounds*, *JHEP* **09** (2017) 116, [[arXiv:1707.00725](#)].
- [137] **NA62** Collaboration, E. Cortina Gil et al., *The Beam and detector of the NA62 experiment at CERN*, *JINST* **12** (2017), no. 05 P05025, [[arXiv:1703.08501](#)].
- [138] **KOTO** Collaboration, T. Yamanaka, *The J-PARC KOTO experiment*, *PTEP* **2012** (2012) 02B006.
- [139] K. M. Nollett and G. Steigman, *BBN And The CMB Constrain Light, Electromagnetically Coupled WIMPs*, *Phys. Rev. D* **89** (2014), no. 8 083508, [[arXiv:1312.5725](#)].
- [140] K. Cheung, P.-Y. Tseng, Y.-L. S. Tsai, and T.-C. Yuan, *Global Constraints on Effective Dark Matter Interactions: Relic Density, Direct Detection, Indirect Detection, and Collider*, *JCAP* **05** (2012) 001, [[arXiv:1201.3402](#)].
- [141] C. Balázs, T. Li, and J. L. Newstead, *Thermal dark matter implies new physics not far above the weak scale*, *JHEP* **08** (2014) 061, [[arXiv:1403.5829](#)].
- [142] S. Liem, G. Bertone, F. Calore, R. Ruiz de Austri, T. M. P. Tait, R. Trotta, and C. Weniger, *Effective field theory of dark matter: a global analysis*, *JHEP* **09** (2016) 077, [[arXiv:1603.05994](#)].
- [143] **GAMBIT** Collaboration, P. Athron et al., *Thermal WIMPs and the scale of new physics: global fits of Dirac dark matter effective field theories*, *Eur. Phys. J. C* **81** (2021), no. 11 992, [[arXiv:2106.02056](#)].
- [144] T. Lin, E. W. Kolb, and L.-T. Wang, *Probing dark matter couplings to top and bottom quarks at the LHC*, *Phys. Rev. D* **88** (2013), no. 6 063510, [[arXiv:1303.6638](#)].
- [145] **Flavour Lattice Averaging Group (FLAG)** Collaboration, Y. Aoki et al., *FLAG Review 2021*, *Eur. Phys. J. C* **82** (2022), no. 10 869, [[arXiv:2111.09849](#)]. Updated results and plots available at: <http://flag.unibe.ch/>.
- [146] D. Aloni, A. Efrati, Y. Grossman, and Y. Nir, *Υ and ψ leptonic decays as probes of solutions to the $R_D^{(*)}$ puzzle*, *JHEP* **06** (2017) 019, [[arXiv:1702.07356](#)].
- [147] D. Hatton, C. T. H. Davies, J. Koponen, G. P. Lepage, and A. T. Lytle,

- Bottomonium precision tests from full lattice QCD: Hyperfine splitting, Υ leptonic width, and b quark contribution to $e^+e^- \rightarrow$ hadrons*, *Phys. Rev. D* **103** (2021), no. 5 054512, [[arXiv:2101.08103](#)].
- [148] **HPQCD** Collaboration, D. Hatton, C. T. H. Davies, B. Galloway, J. Koponen, G. P. Lepage, and A. T. Lytle, *Charmonium properties from lattice QCD + QED: Hyperfine splitting, J/ψ leptonic width, charm quark mass, and a_μ^c* , *Phys. Rev. D* **102** (2020), no. 5 054511, [[arXiv:2005.01845](#)].
- [149] M. König and M. Neubert, *Exclusive Radiative Higgs Decays as Probes of Light-Quark Yukawa Couplings*, *JHEP* **08** (2015) 012, [[arXiv:1505.03870](#)].
- [150] M. Beneke and T. Feldmann, *Symmetry breaking corrections to heavy to light B meson form-factors at large recoil*, *Nucl. Phys. B* **592** (2001) 3–34, [[hep-ph/0008255](#)].
- [151] P. Ball and R. Zwicky, *New results on $B \rightarrow \pi, K, \eta$ decay formfactors from light-cone sum rules*, *Phys. Rev. D* **71** (2005) 014015, [[hep-ph/0406232](#)].
- [152] P. Ball and R. Zwicky, *$B_{d,s} \rightarrow \rho, \omega, K^*, \phi$ decay form-factors from light-cone sum rules revisited*, *Phys. Rev. D* **71** (2005) 014029, [[hep-ph/0412079](#)].
- [153] A. Khodjamirian, *Hadron Form Factors: From Basic Phenomenology to QCD Sum Rules*. CRC Press, Taylor & Francis Group, Boca Raton, FL, USA, 2020.
- [154] V. Bernard, M. Oertel, E. Passemar, and J. Stern, *$K_{\mu 3}^L$ decay: A Stringent test of right-handed quark currents*, *Phys. Lett. B* **638** (2006) 480–486, [[hep-ph/0603202](#)].
- [155] V. Bernard, M. Oertel, E. Passemar, and J. Stern, *Dispersive representation and shape of the $K(l3)$ form factors: Robustness*, *Phys. Rev. D* **80** (2009) 034034, [[arXiv:0903.1654](#)].
- [156] I. Baum, V. Lubicz, G. Martinelli, L. Orifici, and S. Simula, *Matrix elements of the electromagnetic operator between kaon and pion states*, *Phys. Rev. D* **84** (2011) 074503, [[arXiv:1108.1021](#)].